2002

A neural networks-based in-process adaptive surface roughness control (NN-IASRC) system in end-milling operations

Po-Tsang Bernie Huang
Iowa State University

A neural networks-based in-process adaptive surface roughness control (NN-IASRC) system in end-milling operations

by

Po-Tsang Bernie Huang

A dissertation submitted to the graduate faculty

in partial fulfillment of the requirements for the degree of

DOCTOR OF PHILOSOPHY

Major: Industrial Education and Technology

Program of Study Committee:
Joseph C. Chen (Major Professor)
Larry L. Bradshaw
Tao Chang
Shana S-F Smith
Robert W. Stephenson

Iowa State University

Ames, Iowa

2002

Graduate College
Iowa State University

This is to certify that the doctoral dissertation of

Po-Tsang Bernie Huang

has met the dissertation requirements of Iowa State University

Signature was redacted for privacy.

Major Professor

Signature was redacted for privacy.

For the Major Program

TABLE OF CONTENTS

LIST OF FIGURES vi

LIST OF TABLES viii

ABSTRACT x

CHAPTER 1 – INTRODUCTION 1
- Problem of Study 1
- Purpose of Study 4
- Signification of Study 5
- Research Questions 6
- Procedures of Study 6
- Limitation of Study 7

CHAPTER 2 – LITERATURE REVIEW 8
- Machine Control Unit of CNC Machine 8
- Machining Dynamic 10
- Surface Characteristics 13
- Sensing Technology 15
- Cutting Force and Surface Roughness in Milling Operations 18
- In-process Decision-making Techniques 20
  - Multiple regression model 21
  - Neural networks 22
    - Backpropagation (BP) 25
  - Neural-fuzzy modeling 28
- Adaptive Control System 29
  - Model-reference adaptive system (MRAS) 30
- Summary of Literature Review 31

CHAPTER 3 – METHODOLOGY 33
- Experimental Setup 33
  - Hardware setup 34
    - The principles of the dynamometer sensor 35
    - The principles of the dual mode amplifier 38
    - The principles of the proximity sensor 39
  - Software setup 42
- Statistics Analysis for Surface Roughness and Cutting Force 44
  - Experimental design 44
  - The property of cutting force 46
  - Statistical inference 50
- PCN Training Procedure for BP 52
- Adaptive Control System 53

Summary of Methodologies 55

CHAPTER 4 - THE IN-PROCESS SURFACE ROUGHNESS PREDICTION SYSTEM 56
Statistical Analysis for Cutting Force Selection 56
In-process NN-based Surface Roughness Prediction (INN-SRP) Subsystem 64
Step 1. Construct an experimental design to collect data for training 65
Step 2. Determine the input and output factors 67
Step 3. Scale the data set 68
Step 4. Training the data to obtain the weight between each neuron 69
Step 5. Build the INN-SRP subsystem 74
Step 6. Test the INN-SRP subsystem 75
Summary of the INN-SRP Subsystem 77

CHAPTER 5 – NEURAL NETWORK BASED IN PROCESS ADAPTIVE SURFACE ROUGHNESS CONTROL SYSTEM 79
Neural Network-based Adaptive Machining Parameter Control Subsystem 79
Step 1. Pre-process the experimental data 79
Step 2. Determine the input and output factors 83
Step 3. Scale the data set 84
Step 4. Training the data to obtain the weight between each neuron 84
Step 5. Build the NN-AMPC subsystem 85
The Integration and Testing of the NN-IASRC System 88
Summary of the NN-IASRC System 94

CHAPTER 6 – CONCLUSIONS 96
Recommendations for Further Research 99

APPENDIX A - NC PROGRAM FOR DATA COLLECTION 102

APPENDIX B - A/D CONVERTING PROGRAM 103

APPENDIX C - CUTTING FORCE ANALYTICAL PROGRAM 106

APPENDIX D - EXPERIMENTAL DATA FOR INN-SRP SYSTEM 109

APPENDIX E - THE PROGRAM OF THE INN-SRP SYSTEM 117

APPENDIX F - SAMPLES FOR THE DEVELOPMENT OF NN-AMPC SYSTEM 122

APPENDIX G - PCN TRAINING AND TESTING DATA FOR THE NN-AMPC SYSTEM 129

APPENDIX H - THE PROGRAM OF THE NN-IASRC SYSTEM 136

APPENDIX I - NC PROGRAM FOR THE NN-IASRC SYSTEM 142

REFERENCES 143

ACKNOWLEDGMENTS 147

LIST OF FIGURES

Figure 2.1 Peripheral milling 11

Figure 2.2 End milling 12

Figure 2.3 Profile of surface texture 14

Figure 2.4 Trochoidal path for milling operation 18

Figure 2.5 Surface generation in a milling operation 19

Figure 2.6 Structure of a feedforward 2-3-2 neural networks 23

Figure 2.7 Logistic function 26

Figure 2.8 Key operation of BP 26

Figure 2.9 Architecture of Sugeno-fuzzy model 29

Figure 2.10 Block diagram of a MRAS 31

Figure 3.1 Architecture of NN-IASRC system 33

Figure 3.2 Experimental setup of hardware 34

Figure 3.3 Structure of force sensor 36

Figure 3.4 Geometry of a dynamometer 37

Figure 3.5 Block diagram 38

Figure 3.6 Structure of proximity sensor 40

Figure 3.7 Diagram of an open-collector transistor circuit 41

Figure 3.8 Conventional milling (left), with cutting force diagram (right) in cutting process 46

Figure 3.9 Actual resultant force diagram of four-tooth milling tool 48

Figure 3.10 Cutting force diagram in the Z direction 49

Figure 3.11 Block diagram of an MRAS for adjustment 54

Figure 4.1 Scatter plot matrix 63

Figure 4.2 Architecture of the INN-SRP system 64

Figure 4.3 Architecture of the 4-5-5-1 INN-SRP system 73

Figure 5.1 Architecture of the NN-AMPC system 80

Figure 5.2 Architecture of the 5-8-7-1 NN-AMPC system 87

Figure 5.3 Detailed architecture of the NN-IASRC system 89

Figure 5.4 The material of testing for NN-IASRC system 89

Figure 5.5 Feed rate override device 91

LIST OF TABLES

Table 2.1 Summary of learning methods for neural networks 24

Table 3.1 Tool one (T_1) with first replication 45

Table 3.2 Tool one (T_1) with second replication 45

Table 3.3 Tool two (T_2) with first replication 45

Table 3.4 Tool two (T_2) with second replication 45

Table 4.1 ANOVA table for cutting tool one (T_1) 58

Table 4.2 ANOVA table for cutting tool two (T_2) 58

Table 4.3 ANOVA table for surface roughness 59

Table 4.4 ANOVA table for average resultant peak force (F_{ap}) 59

Table 4.5 ANOVA table for average resultant force (F_{avg}) 60

Table 4.6 ANOVA table for absolute average force (F_{az}) 60

Table 4.7 Pearson correlation value 62

Table 4.8 Tool one (T_1) with first replication 66

Table 4.9 Tool one (T_1) with second replication 66

Table 4.10 Tool two (T_2) with first replication 66

Table 4.11 Tool two (T_2) with second replication 67

Table 4.12 Comparison of *RMS* error for different sample size 70

Table 4.13 Comparison of *RMS* error for different hidden neurons and layers 71

Table 4.14 Comparison of *RMS* error of learning rate in the 4-5-5-1 INN-SRP subsystem 72

Table 4.15 Comparison of *RMS* error of momentum factor in the 4-5-5-1 INN-SRP subsystem 73

Table 4.16 The weight between each neuron and bias of each neuron for the INN-SRP subsystem 74

Table 4.17 Results of testing data for the INN-SRP subsystem 77

Table 5.1 Samples of group one for data pre-processing 81

Table 5.2 Optimal combination of the NN-AMPC subsystem 85

Table 5.3 The weight between each neuron and bias of each neuron for the NN-AMPC subsystem 86

Table 5.4 Testing machining parameters and R_a^d for the NN-IASRC system 92

Table 5.5 Result of the testing for the NN-IASRC system 93

ABSTRACT

In this research, the neural networks-based in-process adaptive surface roughness control (NN-IASRC) system employing multiple cutting tools was successfully developed for end-milling operations. The dynamometer sensor was used to monitor the uncontrolled cutting tool conditions to increase the accuracy of the surface roughness control. An empirical approach was applied to discover the proper cutting force signals, the average resultant peak force in XY plane (F_{ap}) and the absolute average force in the Z direction (F_{az}). These two forces were employed to represent the uncontrollable cutting tool conditions for surface roughness control. A statistical method was employed to verify that the cutting tools could influence the surface roughness, and obtain the correlation between surface roughness and the cutting force signals for the preparation of constructing the NN-IASRC system.

A neural networks theorem was successfully applied to build the NN-IASRC system. The neural networks associated with sensing technology were applied as a decision-making technique to control the surface roughness for a wide range of machining parameters. The NN-IASRC system consisted of two subsystems. One was the in-process neural networks based surface roughness prediction (INN-SRP) system, which was employed to predict the surface roughness. The other was the neural networks based adaptive machining parameters control (NN-APMC) system, which was utilized to adjust the adaptive degree of feed rate when the quality of predicted surface roughness did not fit the desired one. The accuracy of the INN-SRP system was 93 %, and 100% for the NN-IASRC system. The high accuracy of results within a wide range of machining parameters indicates that the system can be practically applied in industry.

CHAPTER 1 - INTRODUCTION

Problem of Study

In recent years, the intense competition among companies in the industrial or business field has made customer satisfaction the most important factor for these companies. Business behaviors have changed from a production trend to a customer trend. Customers are looking for the product with the highest quality and best service. Therefore, companies must produce a product that satisfies the needs of the customer and increases productivity in order to share in a proportion of the market. To achieve these objectives, the structure of the manufacturing system has been simplified as systems have become more automated. Several system improvement methods, including flexible manufacturing systems (FMS), just in time (JIT), integrated manufacturing production systems (IMPS), and linked-cell manufacturing systems (L-CMS), were developed and implemented. The implementation of these manufacturing systems improved both the productivity and quality of the product. To successfully execute these systems, the correct use of facilities and/or technologies for these systems became a critical factor. Several new technologies or facilities were developed or designed to assist these systems. For example, the implementation of a computer numerical control (CNC) machine was one of the new equipments and technologies.

In manufacturing systems, machines are the fundamental equipment. CNC machines are widely used and play an important role in modern factories. CNC machines have been widely implemented to not only increase productivity but also to improve the accuracy of the product (Lin, 1994). However, since the dynamic cutting process in the CNC machines is difficult to control because of tool conditions and chatter, defects still occasionally occur in production. To prevent the defects from reaching the market, the idea of quality control was

proposed to remove the defect from the customer. Quality control assists the whole manufacturing system in every company. However, the implementing of quality control always takes time, which reduces the productivity and increases the cost. Therefore, designing a smart system for CNC machines, that cannot only maintain the productivity but also reduce the time of quality control, becomes a profitable issue for each company.

To reduce the quality control time for products manufactured by the CNC machines, several technologies were applied such as pokayoke. Pokayoke is a Japanese word for defect prevention. It is an idea to develop a method, mechanism, or device, which can prevent the defect from occurring rather than to find the defect after it has occurred (Black, 1991). However, the pokayoke is still a method of off-line quality control. It still takes time for the operation by human beings. To eliminate the quality control time of a CNC machining product, the best idea is to build the CNC machine that is capable of inspecting the quality of a product by itself. Therefore, the idea for the development of an in-process monitoring system for CNC machines was proposed.

An in-process monitoring system uses a mathematical algorithm or expert system to analyze data within each machining process. Since analytical activities are made by the computer within the machining process, this system responds to the quality characteristic immediately. Therefore, the time of quality inspection typically taken by operators or quality engineers has been decreased. Eventually, an in-process monitoring system would be able to both ensure the quality and maintain the normal productivity.

The idea of an in-process monitoring system has been widely studied and applied recently. For example, the detection of tool breakage (Chen & Black, 1997; Li & Elbestawi, 1996; Zhang, Han & Chen, 1995) and the monitoring of tool wear (Elanayar & Shin, 1995;

Gong, Obikawa & Shirakashi, 1997) have been studied to reduce the time of tool monitoring. These two monitoring systems were designed to determine the tool condition in the cutting process. When the cutting tool was monitored to show breakage or wear, the machine stopped, and humans changed the tool. Another application of the in-process monitoring system was to predict the surface roughness within a cutting process (Chen & Lou, 2000; Shin, Oh & Coker, 1995; Coker & Shin, 1996; Chang & Lin, 1999). The study of in-process surface roughness monitoring has been used to predict not only the surface roughness, but also to diagnose the tool conditions (Elbestawi et al, 1994). Therefore, successfully developing an in-process surface roughness monitoring system would be more useful and efficient among in-process monitoring systems since the cutting surface roughness can also respond to the tool conditions.

Surface finish is a key factor in evaluating the quality of a product. Surface roughness (R_a) is the most common index used to determine the surface finish. Since surface roughness affects several functional attributes of products, such as contact causing surface friction, wearing, light reflection, the ability to distribute and hold a lubricant, accept a coating, and to resist fatigue, it is very important to understand how well the surface finish is produced and to specify the desired surface roughness. Therefore, the desired surface roughness value is usually specified for a product and the pertinent processes are selected to achieve the desired quality (Kalpakjian, 1995).

Surface roughness is not only a parameter of quality control but also a factor in monitoring machining processes. Surface finish specifications are useful for determining the stability of a manufacturing process, where a deteriorating surface finish may be interpreted as a signal of material non-homogeneity, progressive tool wear, or even tool breakage

(Jansson, Rourke & Bell, 1984). Surface finish is also an important consideration in determining the machinability of materials. Therefore, the estimation of the magnitude of surface roughness under given machining conditions resulting from metal removal operations is one of the major goals in this area.

However, the problem of studying the in-process surface roughness monitoring is that the monitoring system can only predict the value of surface roughness, and the system does not have the capability to adjust the machining cutting parameters to produce a desired surface roughness required for the customers when a defect has been detected on-line. Theoretically, to perform the in-process adaptive surface roughness control, the system must have the adaptive control function to adjust the machining parameters in order to produce a product with desired surface roughness required by customers. Therefore, there is a need to develop an adaptive surface roughness control system to ensure that a CNC machine can produce the product with zero defect of the surface roughness.

Purpose of Study

The purpose of this research is to develop an in-process adaptive surface roughness control (IASRC) system. This system is designed to provide the real-time, in-process surface roughness monitoring, which cannot only recognize the surface roughness but also adjust the machining parameters to produce a product with desired surface roughness in end milling operations.

To construct this system, the sensor used to monitor the cutting condition should be discussed in order to decide upon the proper sensor for surface roughness recognition. Two subsystems should be developed for the IASRC system. One is the in-process surface roughness prediction (ISRP) system used to generate the predicted surface roughness. The

predicted surface roughness will be compared to the desired surface roughness. If the predicted value is larger than the desired one, the product is defective. Under the circumstances, the other subsystem, the adaptive machining parameter control (AMPC) system, is applied. The AMPC system is used to generate the adaptive cutting conditions and result in a new surface roughness to satisfy the needs of the customers. The details of constructing these systems will be discussed in chapter four and five.

Significance of Study

The in-process surface roughness control system in this research provides the adaptive control function to control the surface roughness in milling operations. Many studies for the in-process surface roughness recognition system only focused on the measurement of surface roughness. These studies can only decrease the time of measurement and response. From the aspect of quality control, it is not enough to monitor the surface roughness without comparing the specified surface roughness to the predictive surface roughness. It is important to make the surface roughness satisfy the needs of the customer. The IASRC system not only supports the prediction function to predict the surface roughness but also prepares the adaptive control function of the machining parameter to generate the surface roughness for customer needs. This research provides a system of assuring that the quality of the surface roughness for a product can satisfy the customer. Furthermore, quality control will no longer be controlled by an off-line quality control room but by the accurate smart CNC machining control system.

Research Questions

The following questions are discussed in this research:

1. What is the relationship between the explanatory variables, such as feed rate, depth of cut, spindle speed, and the response variable surface roughness?
2. What is the correlation between surface roughness and cutting force, such as peak force and average force, in different directions?
3. Will different tools manufactured by the same company with the same patterns affect the surface roughness?
4. Can the neural networks approach develop a prediction model to recognize the surface roughness accurately?
5. Can the adaptive control system adjust the machining parameters successfully to make the predictive surface roughness smaller than the desired surface roughness?
6. Can the prediction and adaptive control system be integrated as an in-process surface roughness control system?

Procedures of Study

To develop the in-process surface roughness control system, the procedures of this study consisted of the following:

1. Indicate the importance of surface roughness in the aspect of quality control and industrial field.
2. Review related literature concerning the relationship between the dynamic cutting process and surface roughness in milling operations.
3. Review related literature concerning the sensors of monitoring the dynamic cutting process and the methods of predicting the surface roughness.

4. Develop the experimental set-up consisting of hardware and software setup, and experimental design to collect data.
5. Apply the statistical approach to analyze these data, which could illustrate the relationship among cutting force, surface roughness, and machining parameters.
6. Use the machining parameters and cutting force signals to develop a neural networks based prediction system to predict the surface roughness.
7. Develop a neural networks based adaptive control system to adjust the machining parameters and to achieve the desired surface roughness.
8. Integrate the neural networks based prediction system and adaptive control system to become a neural networks based in-process adaptive surface roughness control system.
9. Write the summaries, conclusions, and recommendations based on the findings.

Limitation of Study

The research goal is to develop an in-process adaptive surface roughness control system. This system adjusts the machining parameters within the cutting process to achieve the desired surface roughness. However, due to the limitation of hardware, it is difficult to transmit the results of adaptive control to the machine control unit of the CNC machine in order to adjust the machining parameters within the cutting process. Therefore, the off-line method will be applied to evaluate the performance of the IASRC system.

CHAPTER 2 - LITERATURE REVIEW

The in-process adaptive surface roughness control (IASRC) system will be used to control the surface roughness within a cutting process in an end-milling operation. To develop the IASRC system, there are some aspects related to this system that should be reviewed in this chapter. These aspects are the machine control unit (MCU) of the CNC machine, the influence of machining dynamic in surface roughness, the surface characteristics, the sensing technologies of surface roughness recognition, the in-process decision-making techniques, and the adaptive control systems.

Machine Control Unit of the CNC Machine

Related to the definition of the Electronic Industries Association (EIA), the computer numerical control (CNC) is a technology in which actions are controlled by the direct insertion of numerical data and a computer. The CNC machine could be considered as a versatile form of programmable automation in which the machine tool and table are controlled by a series of coded instructions. These coded instructions are converted into pulses of electric output signals and on/off control signals. The pulses of electric output signals implement the positioning and speed of the machine table and spindle tool, and the on/off signals control the direction of spindle rotation, coolant supply, and tool selection. The CNC machine offers many features not found in the conventional engineered machine. These features make the CNC machine more flexible and functional in the application of manufacturing. One of the features is the communication ability. CNC control units have the capability of communicating with other microprocessor-based devices such as computers and robotic controllers. The communication ability enables the CNC machine to be linked with other computer devices. Another feature of a CNC machine is the controller memory.

The controller memory provides the capacity of data entry and program storage (Lin, 1994). To execute an in-process monitoring system, the machine must have the ability to collect data for analysis or to connect with another computer that can execute the data collecting and analyzing. Therefore, a CNC machine is needed for any in-process monitoring system.

The CNC machine contains six major components, which are the NC program, program input device, machine control unit (MCU), drive system, machine tool, and feedback system. Among these components, MCU is the key component for each CNC machine. MCU is used to read and interpret the NC program for machining processes and then generate electric output signals. These signals are fed into a servo drive amplifier for driving the axis control motors, which could be a hydraulic or stepping motor. Since these signals are controlled by numerical data, the volume of these signals could be continuous. Therefore, the feed rate, spindle speed, or depth of cut could be set at any value. This feature allows the in-process control system to change the machining parameters to any value to achieve the desired quality. Due to the advantages of communication ability, memory storage, and adjustable machining parameters, the CNC machine is necessary for the IASRC system to perform.

In a CNC machine, the feed rate, spindle speed, and depth of cut can be controlled by an MCU within the cutting process. However, the cutting process is dynamic, and there are some factors that are difficult to control within the cutting process. Therefore, the machining dynamic will be discussed to identify the uncontrolled factors within the cutting process.

Machining Dynamic

Metal cutting processes removing material from the surface of workpiece are the most fundamental methods of shaping a product in an industrial field. Metal cutting processes include milling, turning, grinding, and drilling operations (Kalpakjian, 1995). Since most of the metal cutting processes are the final procedure of machining a product, it is very important to control the quality of these processes. The application of a CNC machine increases the accuracy of cutting processes to enhance the quality of product. However, since these processes are dynamic and are affected by many uncontrolled factors, such as tool wear, tool run-out, tool deflection, chatter, and material properties, it is difficult to control the quality of product by only using the machining parameters, such as spindle speed, feed rate, and depth of cut. To successfully develop an accurate in-process monitoring system, the decision-making algorithm of this system should have the ability to analyze the information obtained by both controllable and uncontrolled factors. Therefore, it is very important to monitor the uncontrolled messages within these cutting processes for an in-process monitoring system.

To monitor the uncontrolled factors within cutting processes, sensing technology is applied. Sensing technology is the application of sensors to monitor the signal of force, vibration, or sound. These signals should represent the uncontrolled factors. Several mechanistic models have been developed to express the dynamic conditions to ensure the quality of the product. Basically, these models monitoring the sensing signal could express the tool conditions, such as tool breakage (Tarng & Lee, 1993), wear (Elbestawi et al., 1991), deflection, run-out (Ismail et al. 1993), or rake angle (Melkote & Thangaraj, 1994). Furthermore, these models indicated that the tool conditions significantly influenced the

quality of the product, such as surface roughness. Theoretically, the sensing technology is a very important technique for indicating the uncontrolled tool conditions.

In these cutting processes, the milling operation is a very important process in making slots, pockets, molds, and dies (Melkote & Thangaraj, 1994). Milling operations are widely used in the automotive and aerospace areas of manufacturing. Milling is an interrupted cutting process by which a surface is generated progressively as chips are removed from a workpiece and fed into a rotating cutter in a direction perpendicular to the axis of the cutter (DeGarmo, Black & Kohser, 1997). A milling operation can be classified into two types. One is the peripheral milling, as shown in Figure 2.1, used to generate the surface of the workpiece, which is rendered by a tooth in the periphery of the cutter body.

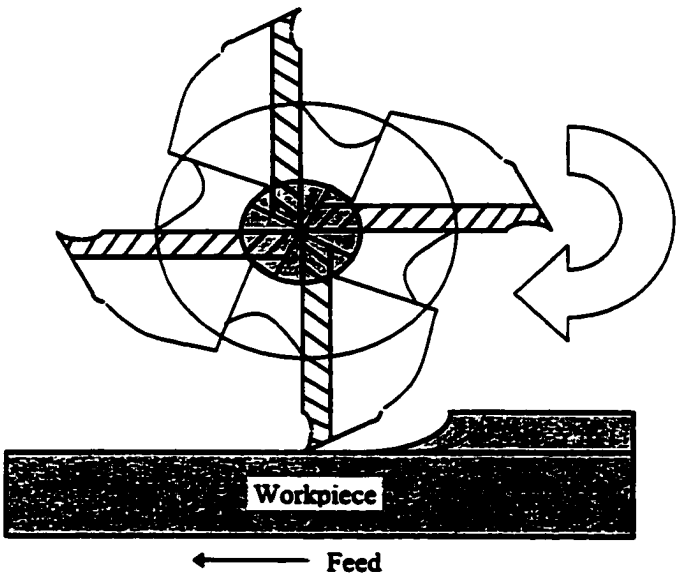

Figure 2.1. Peripheral milling (DeGarmo, Black & Kohser, 1997)

The other is the end milling, as shown in Figure 2.2, which is employed to generate a smooth surface vertical to the axis of rotation. Most milling is implemented by peripheral milling while end milling provides the profiling and finishing actions. End milling is the most common operation used for the finishing process (Sutherland & Devor, 1986). An end milling operation will be used to test the surface roughness in this research because it is the most common machining process in industrial manufacturing for machining and finishing complex contours.

Since surface roughness will be applied to develop the IASRC system in end the milling operation, it is important to understand the surface characteristics involved in end milling operations.

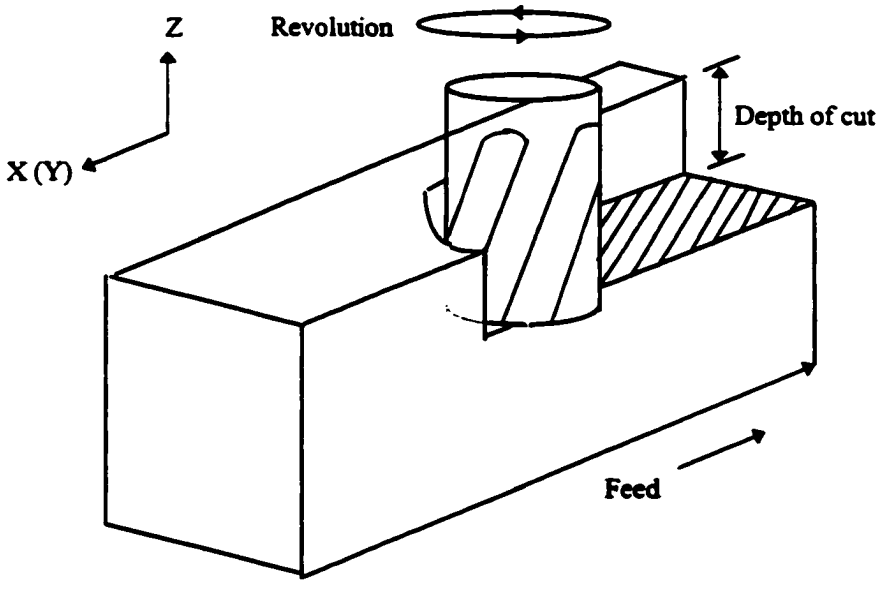

Figure 2.2. End milling

Surface Characteristics

The term surface finish is used very widely in industry and is generally used to quantify the smoothness of a surface. Surface finish can be specified in many different parameters. Early surface finish configurations measured only arithmetic mean roughness (R_a) values because of computational restrictions. However, this situation has been changed in past decades. A large number of newly developed surface roughness parameters were conceived and instruments to measure them were developed due to the need for different parameters in a wide variety of machining operations. Some of the most popular parameters of surface finish specification are described in the following paragraphs:

Roughness average (R_a): This parameter is also known as the arithmetic mean roughness value, arithmetic average (AA), or center line average (CLA). R_a is universally recognized and the most used international parameter of roughness. It can be expressed as:

$$R_a = \frac{1}{L}\int_0^L |Y(x)|dx, \tag{2.1}$$

where R_a is the arithmetic average deviation from the mean line, L is sampling length, and y is ordinate of the curve of the profile (Lou, 1997).

Roughness average is the arithmetic mean of the departure of the roughness profile from the mean line. An example of the surface profile is shown in Figure 2.3. An approximation of the average roughness R_a may be obtained by adding the y increments without regard to sign and dividing the sum by the number of increments. Therefore:

$$R_a(approx.) = \frac{y_1 + y_2 + y_3 + \ldots + y_n}{n}. \tag{2.2}$$

Root-mean-square (rms) roughness (R_q): R_q is the root-mean-square parameter corresponding to R_a :

$$R_q = \sqrt{[\frac{1}{L}\int_0^L (Y(x))^2 dx]}, \tag{2.3}$$

or approximately:

$$R_q = \sqrt{\frac{y_1^2 + y_2^2 + y_3^2 + \ldots + y_n^2}{n}}. \tag{2.4}$$

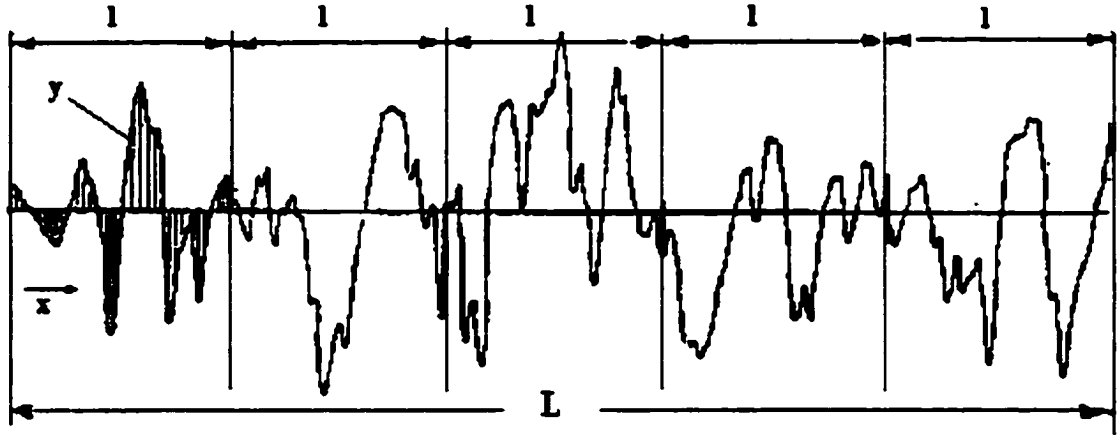

Figure 2.3. Profile of surface texture (Kalpakjian, 1995)

Maximum peak-to-valley roughness height (R_y or R_{max}): This is the distance between two lines parallel to the mean line that contacts the extreme upper and lower points on the profile within the roughness sampling length.

Basically, the roughness average (R_a) is the most common parameter used in the industrial field to decide the quality of product. Therefore, the IASRC system will be developed to recognize the R_a in an end milling operation.

Sensing Technology

To detect the uncontrolled factors within cutting processes, sensing technology is needed to monitor the uncontrolled signals. The correct use of sensing technology leads to the development of successful in-process monitoring systems for surface roughness.

Sensing technology can be separated into two categories. One is the direct method, which measures and evaluates volumetric changes on the surface. The stylus profiler or surface print is always used to measure the surface roughness in this approach. This method, however, tends to be an off-line technique and is not suitable to the in-process surface roughness recognition because measurements are usually taken only as the tool completes the cutting process and the workpiece is removed from the machine. The other method is the indirect method. This method measures the cutting parameters, including the cutting force, sound, acoustic emission, vibration, and optical fiber employed during the cutting process (Tarng & Lee, 1993). The indirect method is always considered to be an on-line technique and can be implemented in the in-process surface roughness recognition because it can predict the surface roughness without removing the tool or workpiece during the cutting process. Therefore, the indirect sensing method would be best applied to the IASRC system.

Several kinds of sensors are mainly used to detect surface roughness in the indirect method:

1. Dynamometer sensor: A dynamometer sensor makes a dynamic measurement of the magnitude of cutting force and torque generated from any direction to the top plate of the sensor. Martelloti (1941) was the earliest to represent a major contribution to the understanding of mechanism of surface generation in milling. Jung and Oh (1991) proposed the mathematical model to indicate that tool deflection influences the

generation of surface roughness. Melkote and Thangaraj (1994) presented the radial rake and relief angles of tools that affect the surface roughness. Fuh and Wu (1995) stated the effect of tool nose radius on surface roughness. Baek et al. (1997) created a model to prove the effect of tool run-out on the cutting surface. These models used the cutting force signal to describe the uncontrolled and dynamical tool conditions. Theoretically, the force signal is a good tool to predict the surface roughness.

2. Acoustic emission sensor: An acoustic sensor measures the sound caused by air-vibration in the form of an alternating compression incurred during the cutting process. The changes in the air stress distribution around the cutting surface were measured to predict the surface roughness. Susic and Grabec (1995) used the AE sensor to predict surface roughness in grinding operations. The model between air vibration and surface roughness is too complex to generate. Therefore, an empirical modeling method should be applied to create the prediction model.
3. Accelerometer sensor: An accelerometer is a sensor used to measure the surface vibration during the cutting process. Ismail et al. (1993) developed a model to indicate the relationship among surface roughness, cutting force, and moving acceleration. You and Ehmann (1991), Lou and Chen (1999), and Tsai et al. (1999) used an accelerometer sensor to monitor the vibration signal to develop a surface prediction model.
4. Ultrasonic sensor: A spherically focused ultrasonic sensor is positioned with a non-normal incidence angle above the surface. The sensor sends out an ultrasonic pulse to the cutting surface and measures the amplitude of the returned signal (Coker & Shin, 1996). The acoustic wavelengths are much greater than the electromagnetic wavelengths of an optic sensor. The ultrasonic sensor can be used to monitor the wet surface (Blessing et

al., 1993). However, due to the limitation range of the reflection angle, the ultrasonic sensor is always applied to predict the surface roughness in the grinding operation, which could process a fine surface ranging from 10 to 50 μ in.

5. Optical sensor: With a range of surface roughness for common finish machining being 20 to 70 μ in, the present optical systems are mostly applied in nature. The fiber-optic bundle that measured the intensity of a beam of light reflected from the machined surface in the specular direction was applied to predict the surface roughness (Inasaki, 1985; Dornfield & Fei, 1986). The diffuseness of the reflected light from the surface was also applied to generate a model to predict the surface roughness (Takeyama et al., 1976)

In milling operations, the surface roughness always ranges from 30 to 250 μ in (Lin, 1994). The AE sensor, ultrasonic sensor, and optical sensor are limited by the reflection angle from the surface. They are suitable to be applied for monitoring the cutting process, which can generate a fine surface, such as grinding. To predict the surface roughness in milling operations, which have wide ranges of surface roughness, the dynamometer or accelerometer sensor can be applied. Furthermore, the IASRC system must have the adaptive function to adjust the machining parameters to achieve the desired R_a. The AE, ultrasonic and optical sensors, which could be categorized as a non-contact sensing technology, can only monitor the surface of the cutting area. These sensors cannot detect the uncontrolled factors that result from the cutting tool. It would be difficult to provide enough information, including both controllable and uncontrolled factors, for the adaptive control system to adjust the machining parameters.

Cutting Force and Surface Roughness in Milling Operations

Martellotti (1941) was the pioneer who created the mathematical model of surface generation of milling operations. Ideally, the milling path is a trochoidal path of one tooth (shown in Figure 2.4). In Martellotti's work (1941), the trochoidal path of the tool tip could be expressed as:

$$x' = -R\sin\theta + \frac{fr \times \theta}{2\pi}, \tag{2.5}$$

$$y' = -R\cos\theta, \tag{2.6}$$

where fr is the feed per revolution, R is the tool radius, and θ is the rotating angle of the tool tip.

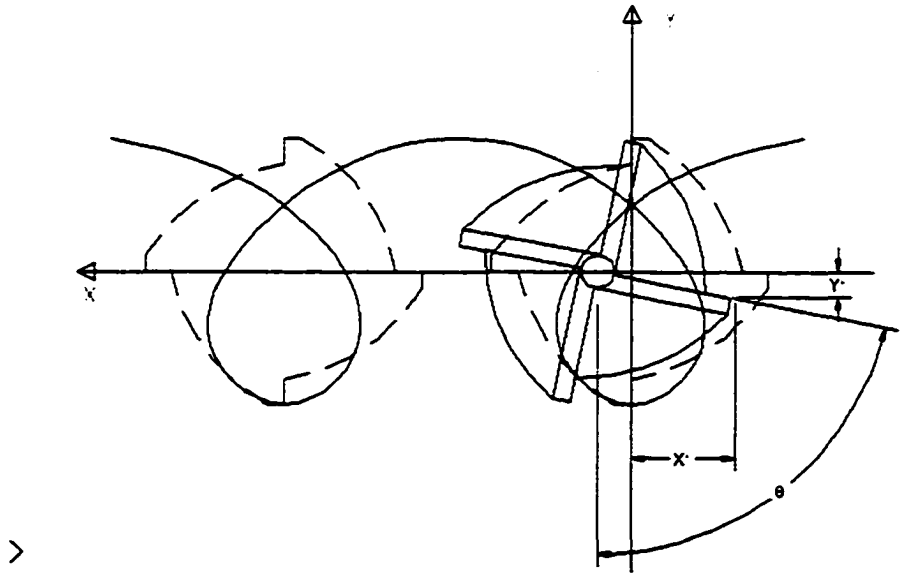

Figure 2.4. Trochoidal path for milling operation (Elbestawi el al, 1994)

These two equations represent the dynamic displacements of the trochoidal path in the cutting plane. In peripheral milling operations, according to the principle of the trochoidal path, the cutting surface should look like waves (shown in Figure 2.5). Therefore, if the feed rate and tool diameter were given, the approximate analytic expression for the peak to valley could be calculated and determine the surface roughness. Furthermore, these two equations also indicated that the surface roughness could be influenced by the feed rate and tool diameter in peripheral milling operations.

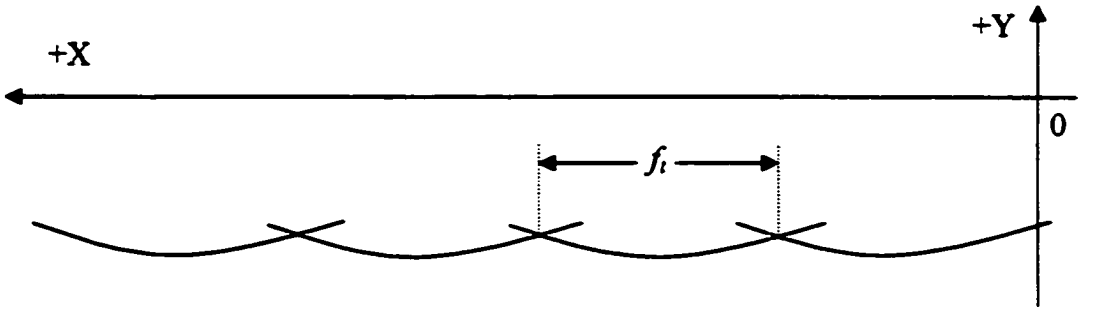

Figure 2.5. Surface generation in a milling operation (Elbestawi et al., 1994)

Smith and Tlusty (1991) developed a force model in a milling operation. In this model, the relationship between cutting force and displacements in a cutting plan were discussed. The cutting force in both the X and Y directions, F_x and F_y, could be expressed as a dynamic model comprising two degrees of freedom along each direction, which is:

$$F_x = m_x \ddot{x} + C_x \dot{x} + K_x x, \tag{2.7}$$

$$F_y = m_y \ddot{y} + C_y \dot{y} + K_y y, \tag{2.8}$$

where m_x, C_x, and K_x represent the mass, damping , and stiffness coefficients in the X direction, $\dot{x}$ and $\ddot{x}$ are the velocity and acceleration for the mass moving in the X direction. Similar notations apply to the Y direction.

The cutting force could also be expressed as:

$$F_x = F_t \cos\theta + F_r \sin\theta, \tag{2.9}$$

$$F_y = -F_t \sin\theta + F_r \cos\theta, \tag{2.10}$$

where F_t and F_r are the tangential and radial force of the tool tip.

The displacement in the X and Y directions can be applied to link these equations to explain the relationship between cutting force and surface roughness. Theoretically, the cutting force is a useful tool in predicting surface roughness. However, these equations could only be applied in peripheral milling operations. They cannot be directly applied in the end milling operations. The relationship between cutting force and surface roughness in end milling operations will be discussed first. The empirical analysis using a statistical method will be applied to determine the relationship between surface roughness and cutting force in different directions and machining parameters. These will be discussed in Chapters 3 and 4.

In-process Decision-making Techniques

To successfully perform an IASRC system, the most important part is to develop an in-process decision-making technique, which can analyze the input information and give a correct surface roughness. There are many different factors for the IASRC system, such as machining parameters and force signals, which need to be considered at the same time. It is difficult to develop the decision-making technique by only using human experience. Under the circumstance, the learning ability becomes a key factor for developing the decision-

making technology. In this section, the decision-making techniques with learning ability will be discussed.

Multiple regression model

The multiple regression model is used to investigate the relationships among a group of variables and to create a model for some variables that can predict its value in the future. The process of finding a mathematical model that best fits the data is regression analysis. Regression analysis is a statistical method, which is concerned with the relationship between a dependent variable, y, and a set of explanatory variables, $x_1, x_2,\ldots,x_k$. It is a very powerful statistical tool, which provides a technique for building a statistical predictor of an explanatory variable and places an approximate limit on the error of prediction. The objective of regression analysis is to build a good model to predict y for given values of x_i, and to do so with a small error of prediction. A multiple regression model was developed to solve the problems of complex applications. Fuh and Wu (1995) developed a regression model that used the feed rate and tool nose radius as explanatory variables to predict the surface roughness. Lou and Chen (1999) developed a multiple regression model to predict the surface roughness. The explanatory variables in this model included the spindle speed, feed rate, depth of cut, and vibration signal.

A multiple regression model includes more than one independent variable. It is also called a linear statistical model. The general form of a multiple regression model can be expressed as (Mendenhall & Sincich, 1996):

$$y = \beta_0 + \beta_1 x_1 + \beta_2 x_2 + \cdots + \beta_k x_k + \varepsilon, \qquad (2.11)$$

where y is the dependent variable, $x_1, x_2,\ldots,x_k$ are the explanatory variables, ε is called the random error term with mean = 0 and variance $=\sigma^2$, β_0 is the y-intercept of the model, and β_1 to β_k are the regression coefficients.

The dependent variable is a function of k explanatory variables, $x_1, x_2,\ldots,x_k$. The random error term is added to make the model probabilistic rather than deterministic. The coefficients β_i determine the contribution of the explanatory variable x_i. The coefficients $\beta_0, \beta_1,\cdots,\beta_k$ are usually unknown since they represent population parameters. Therefore, the method of least squares is applied to estimate the coefficients and to fit the multiple regression model. The estimated model can be expressed as:

$$\hat{y} = \hat{\beta}_0 + \hat{\beta}_1 x_1 + \cdots + \hat{\beta}_k x_k . \tag{2.12}$$

Then, minimize the estimated model by:

$$\text{SSE} = \sum_{i=1}^{n} (y_i - \hat{y}_i)^2 , \tag{2.13}$$

where SSE represents the sum of squares of the errors, $\hat{y}$ is the estimator of the mean value of y, n is the number of sample size, and $\hat{\beta}_0, \hat{\beta}_1 \cdots, \hat{\beta}_k$ are estimators of $\beta_0, \beta_1,\cdots,\beta_k$.

Neural networks

A neural networks (NN) is a network structure in which input-output behavior is determined by a collection of modifiable parameters. A set of nodes connected by directed links constitutes a neural networks structure. Each node performs a node function on its input data to form a single node output, and each link specifies the direction of data flow from one node to another. The NN model aids in solving some nonlinear relationships between input and output. The NN model aims to construct a network for achieving a

nonlinear mapping that is regulated by a training data set and to use the learning rules or adaptation algorithms to adjust the parameters, improving the network's performance. Susic and Grabec (1995) proposed a neural networks model to estimate the surface roughness. Figure 2.6 provides a sample structure of a neural networks.

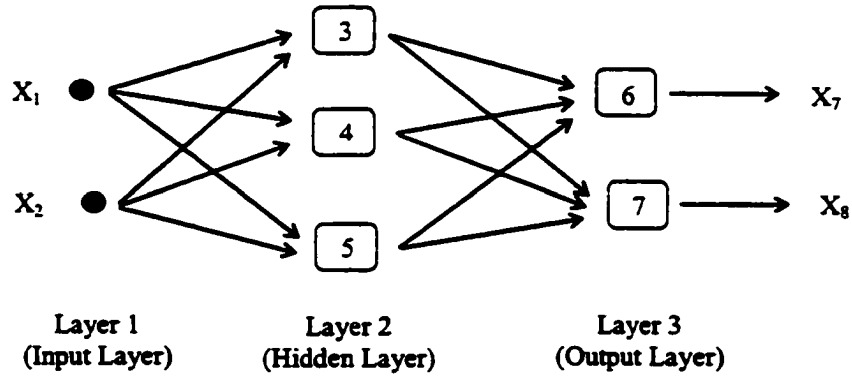

Figure 2.6. Structure of a feedforward 2-3-2 neural networks (Jang et al., 1996)

NN can compute any computable function. Especially the function that can be represented as a mapping between vector spaces can be approximated to arbitrary precision by feedforward NN. NN is useful for mapping problems that are tolerant of some error and have lots of example data available, to which hard and fast rules cannot easily be applied. However, NN has its limitation in being successfully applied to problems that concern manipulation of symbols and memory.

The learning ability is the most powerful function of NN. The basic learning principle of the network is the steepest descent method, in which the gradient vector is derived by successive invocations of the chain rule. There are many learning methods for NN now. Table 2.1 shows the summary of learning methods for NN. Many of these

learning methods are closely connected with a certain network topology. The main categorization of these methods is the distinction between supervised from unsupervised learning.

Table 2.1 Summary of learning methods for neural networks

Supervised Learning	Unsupervised Learning
Perceptron	Binary Adaptive Resonance Theory (ART1)
Backpropagation (BP)	Analog Adaptive Resonance Theory (ART2)
Adaptive Heuristic Critic (AHC)	Discrete Hopfield (DH)
Adaptive Logic Network (ALN)	Continuous Hopfield (CH)
Associative Reward Penalty (ARP)	Additive Grossberg (AG)
Extended Kalman Filter (EKF)	Competitive Learning (CL)
Artmap	Self-Organizing Map (SOM)
Learning Vectors Quantization (LVQ)	Learning Matrix (LM)
Recurrent Cascade Correlation (RCC)	Counterpropagation (CP)
Real-time Recurrent Learning (RTRL)	

In supervised learning, there is an "instructor", who in the learning phase, teaches the network how well to perform or what the correct behavior should be. Due to the property of the external instructor, the supervised learning contains both input and output vectors in each data set for learning. In unsupervised learning, the network is autonomous. It simply looks at the data it is presented with, determines some of the properties of the data set, and learns to reflect these properties in its output. What exactly these properties are that the network can learn to recognize depends on the particular network model and learning methods. Since no external instructor or critic's instruction is available, the unsupervised learning only contains input vectors in each data set. Since it is difficult to construct the decision-making system with human experience for the IASRC system, an experimental design must be conducted

first to obtain the desired input-output data set for learning. The resulting networks must have adjustable parameters that are updated by a supervised learning method. Therefore, the supervised learning method is recommended in this research.

Backpropagation (BP)

Among the various existing supervised learning methods, backpropagation (BP) is the most representative and commonly used algorithm and is relatively easy to apply (Jang et al., 1997). BP has been proven to be effective in dealing with the problems of surface roughness recognition (Susic & Grabec, 1995; Stark & Moon, 1999; Tasi et al., 1999). Furthermore, it is successful on practical applications in adaptive control, such as the control of servo controllers (Cui & Shin, 1993; Hemerly & Nascimento, 1999) and cutting tool error estimation (Mou, 1997). The backpropagation was reformulated from multiplayer perceptrons (MLPs) in the mid-1980s by Rumelhart et al (1986). Being a supervised learner, BP needs an instructor that knows the correct output for any input and uses gradient descent on the error provided by the instructor to train the weights between each node. In the training process, the transfer function, also known as the activation function, is applied to convert the sum of inputs to the range [0,1]. The transfer function is usually a logistic function of a weighted sum of the node inputs (shown in Figure 2.7). The logistic function can be expressed as:

$$f(x) = \frac{1}{1+e^{-x}}. \tag{2.14}$$

In the BP learning method, the output of *j*th neuron in the *k*th layer (A_j^k) is the non-linear function of the output of the (*k-1*)th layer (shown in Figure 2.8). It can be expressed as:

$$A_j^k = f(S_j^k), \tag{2.15}$$

$$S_j^k = \sum_i W_{ij} A_i^{k-1} - \theta_j^k, \tag{2.16}$$

where S_j^k is the sum of jth neuron in the kth layer, θ_j^k is the bias of jth neuron, W_{ij} is the weight between ith neuron in $(k-1)$th layer, and jth neuron in the kth layer.

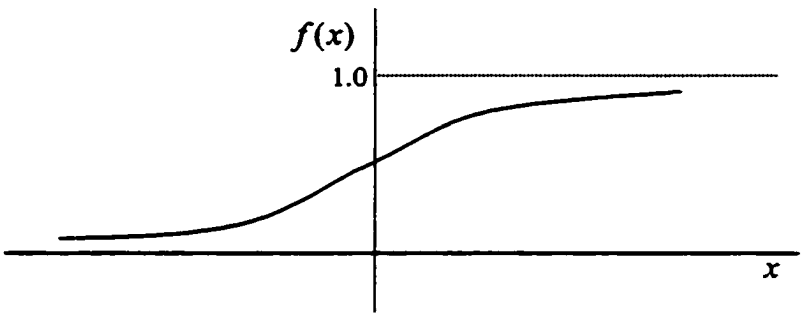

Figure 2.7. Logistic function

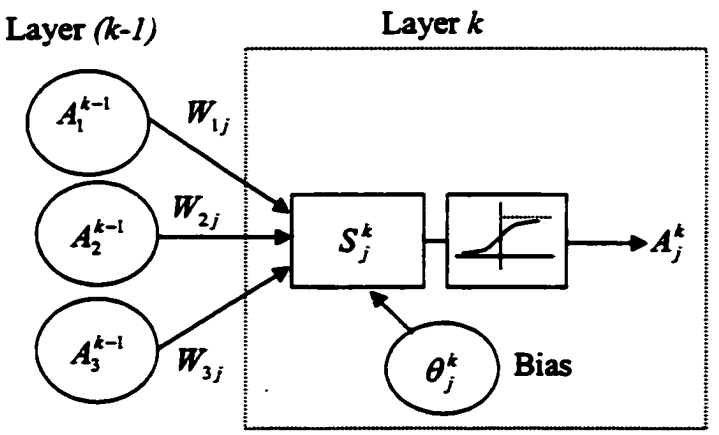

Figure 2.8. Key operation of BP

Since the goal of BP supervised learning is to minimize the error between the desired output (D_l^k) and calculated output (A_l^k) in the *l*th neuron, an error function is applied to represent the efficiency of the learning process. The error function in the *k*th layer can be expressed as:

$$e_l^k = (D_l^k - A_l^k) \times f'(S_l^k), \tag{2.17}$$

where D_l is the desired output of the *l*th neuron and $f'(x)$ is the differential of transfer function.

The learning process of BP becomes a procedure to minimize equation (2.17) by means of the gradient steepest descent method. Furthermore, when a training example is put in the BP model, the network adjusts a little amounts of the weight. This amount is a direct proportion of the sensitivity of the error function to the weights and is expressed as:

$$\Delta W_{jl}^k = -\eta \times e_l^k \times f(S_j^k), \tag{2.18}$$

$$\Delta \theta_l^k = -\eta \times e_l^k, \tag{2.19}$$

where W_{jl}^k is the connection weight between the *j*th neuron in the (*k-1*)th layer and the *l*th neuron in the *k*th layer, θ_l^k is the bias of the *l*th neuron in the *k*th layer, and η is the learning rate, which is used to control the magnitude of every adjustment during the process of minimization of the error function by the gradient steepest descent method.

The learning process always trains one example per time to adjust the weight and bias. The learning cycle is identified as the learning process of all training examples. The learning cycle of BP can be set to a range from 1,000 to 10,000. The purpose of the learning process is to minimize the error function. The root mean squared (RMS) error could be

applied to indicate if the learning process had a convergent property. The RMS error can be expressed as:

$$RMSe = \sqrt{\sum_{i=1}^{n} \sum_{l=1}^{m} (D_{il} - A_{il})^2 / (n \times m)}, \tag{2.20}$$

where n is the number of training examples and m is the number of output neurons.

Fuzzy-neural modeling

The performance of the neural networks has its disadvantages. The main disadvantage is that a neural networks has the probability to be trapped into a local minimum. It is difficult to diagnose when the training process traps into a local minimum. To solve this problem, it is necessary to train the data several times without changing any training parameters. The result of each training process provides the information to analyze and compare. The other disadvantage is that it is difficult for the neural networks to decide the number of the hidden neuron and layers, the number of the learning rate, and the momentum constant. "Learn and error" is the way to solve this problem. Therefore, it always takes time to do the training process.

To solve the disadvantages of the neural networks, fuzzy-neural modeling has been proposed. Fuzzy-neural modeling integrates the learning ability of the neural networks and the inference method of fuzzy logic. Several neural-fuzzy models have been developed. For example, Sugeno and Kang (1988) proposed the Sugeno-fuzzy model, and Chen (1996) proposed a fuzzy-net model. Basically, neural-fuzzy modeling uses the principles of fuzzy logic to deal with the input-output data set and the layer structure of the neural networks to train the weight for connection. Figure 2.9 shows the architecture of Sugeno-fuzzy model with two inputs and four fuzzy-rules. The use of the neural-fuzzy model can fix the number

of layers and the neurons in each layer. This property saves time in the "learn and error" training processes. Furthermore, the fuzzy inference in each layer prevents the result from trapping local minimum.

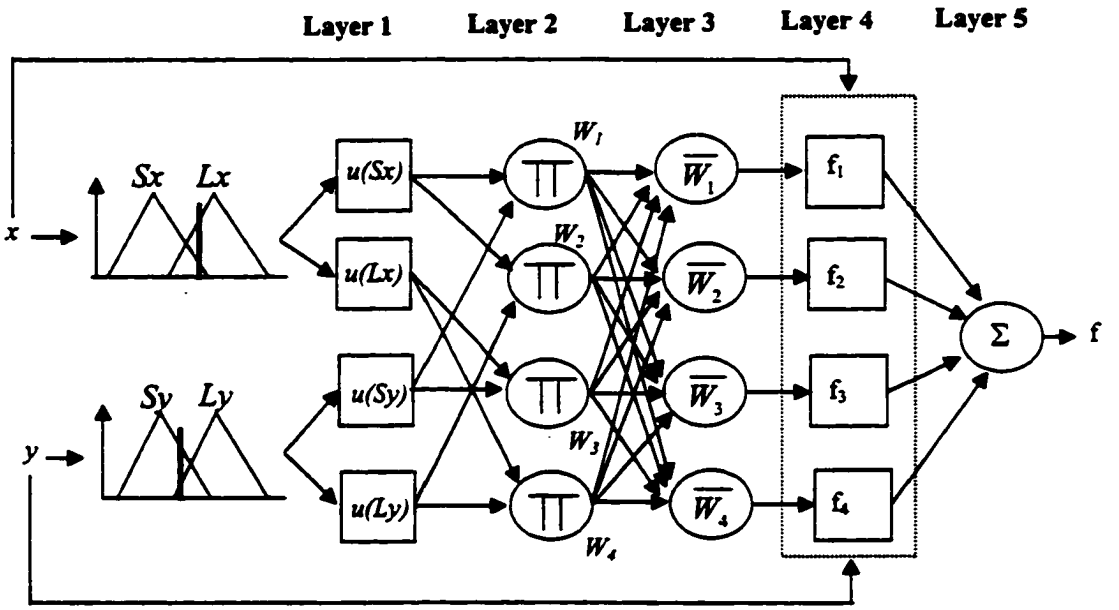

Figure 2.9. Architecture of Sugeno-fuzzy model (Sugeno & Kang, 1988)

Adaptive Control System

The adaptive control means to change a behavior to conform to new circumstances (Astrom & Wittenmark, 1989). This system is designed with an adaptive viewpoint to check the current conditions, and a feedback function to change the current conditions. Therefore, to pursue an adaptive control system, the system must have a background in conventional feedback control and also sampled dada systems. Basically, the adaptive control system is a special type of nonlinear and dynamic feedback system since the states of the process can be separated into categories, which change at different rates (Landau & M'Saad, 1998)). The

adaptive control system has been applied in many different fields, such as stochastic control, stability theory, estimation and optimization. In this research, adaptive control was applied to predict the surface roughness and feedback the estimation of adaptive machining parameters to generate a desired surface roughness within the cutting process.

In the adaptive control system, the regulator is the key component in this system. Theoretically, an adaptive regulator is a regulator that can adjust the current conditions in response to changes in the dynamics of the process. The regulator was applied in many different adaptive control schemes for different purposes, such as self-oscillating adaptive systems, model-reference adaptive systems, gain scheduling, and self-tuning regulators (Astrom & Wittenmark, 1989). In this research, the theory of adaptive control system is focused on the use of the model-reference adaptive system since this system can ideally achieve the need of the adaptive surface roughness control system.

Model-reference adaptive system (MRAS)

Figure 2.10 shows the block diagram of a model-reference adaptive system. The MRAS was design to solve a problem in which the specifications are given by the model (y_m) that tells how the process output (y) ideally should be responding to the command signal (Uc). The MRAS consists of two loops. One is the inner loop, which is an ordinary feedback loop. The inner loop composed of the process and the regulator. The parameter of the regulator is adjusted by the outer loop to make the error between the process output and the model output become small. The other loop is the output loop. The output loop is to determine the adjustment mechanism so that a stable system can be obtained. The theory of the MRAS will be further discussed in Chapter Three.

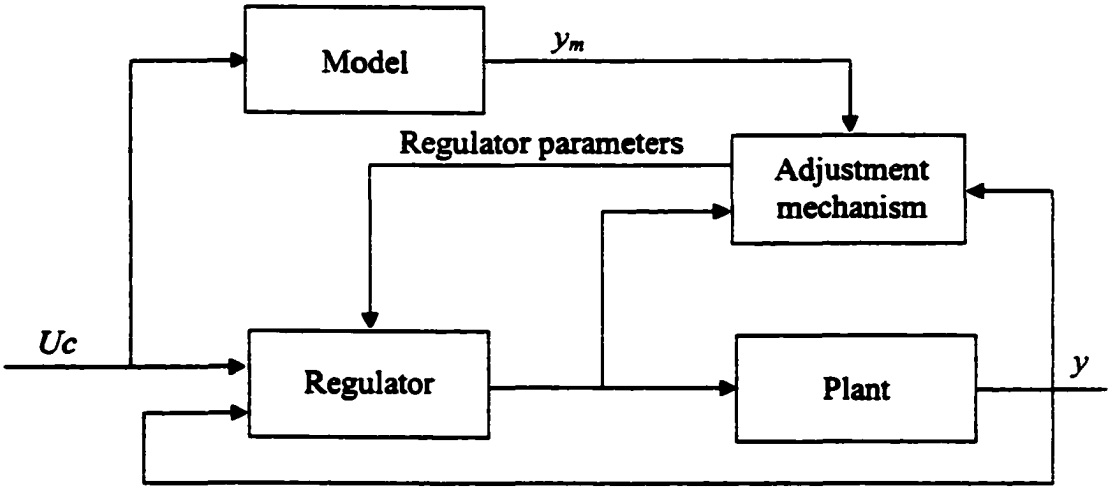

Figure 2.10. Block diagram of a MRAS (Astrom & Wittenmark, 1989)

Summary of Literature Review

To develop an in-process adaptive surface roughness control (IASRC) system, a sensing technology must be applied to monitor the dynamic cutting condition. The force signal has been proven as a useful tool in milling operations. Therefore, in this research, the dynamometer sensor will be used to monitor the force signal within the cutting process. A statistical analysis will be applied to discover the relationship between cutting force and surface roughness. Neural networks technology will be developed as decision-making algorithms to analyze the input-output data set and then predict the surface roughness.

Most of the in-process surface roughness recognition systems have focused on the prediction of surface roughness. From the aspect of quality control, to reduce the time of quality inspection, the in-process surface roughness monitoring system is used not only to predict the surface roughness but also to control the surface roughness. To achieve the goal of quality control, an adaptive control system must be developed. Therefore, a neural

networks based model will also be developed to control the surface roughness in this research. In this model, the feed rate is adjusted to achieve the desired surface roughness. To achieve the goal of the NN-IASRC system, the experimental setup, sensor principles, experimental design, statistical analysis of the relationship between surface roughness and cutting force, and the principles of a neural-networks-based surface roughness prediction and adaptive machining parameter control system is discussed in the next chapter.

CHAPTER 3 – METHODOLOGY

In this chapter, the methodology of developing a neural network-based in-process adaptive surface roughness control (NN-IASRC) system in an end milling operation is discussed. Figure 3.1 shows the architecture of the NN-IASRC system. To successfully construct this system, the experimental setup, principles of sensors, statistics analysis of surface roughness and cutting force, PCN training procedure for BP, and the principles of adaptive control system are discussed in this chapter.

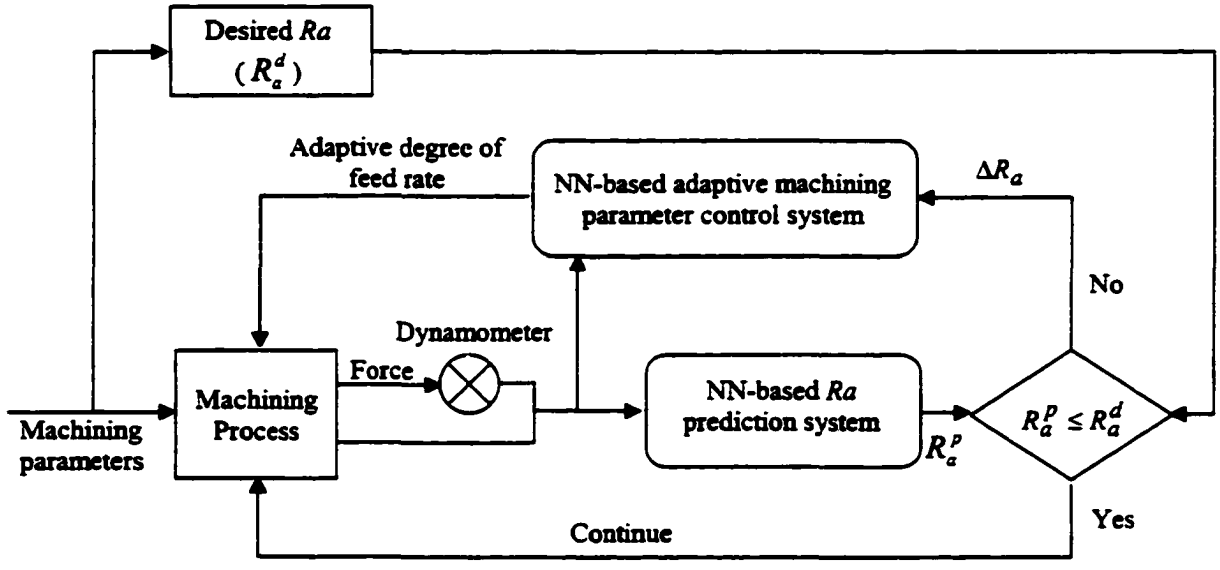

Figure 3.1. Architecture of NN-IASRC system

Experimental Setup

To develop the NN-IASRC system, the data collection is requisite for constructing the in-process decision-making algorithms. The experimental setup is used to collect data for analysis; it includes the hardware setup and software setup.

Hardware setup

The hardware setup consists of the equipment shown in Figure 3.2. The equipment is used to perform the cutting process and collect data. They include:

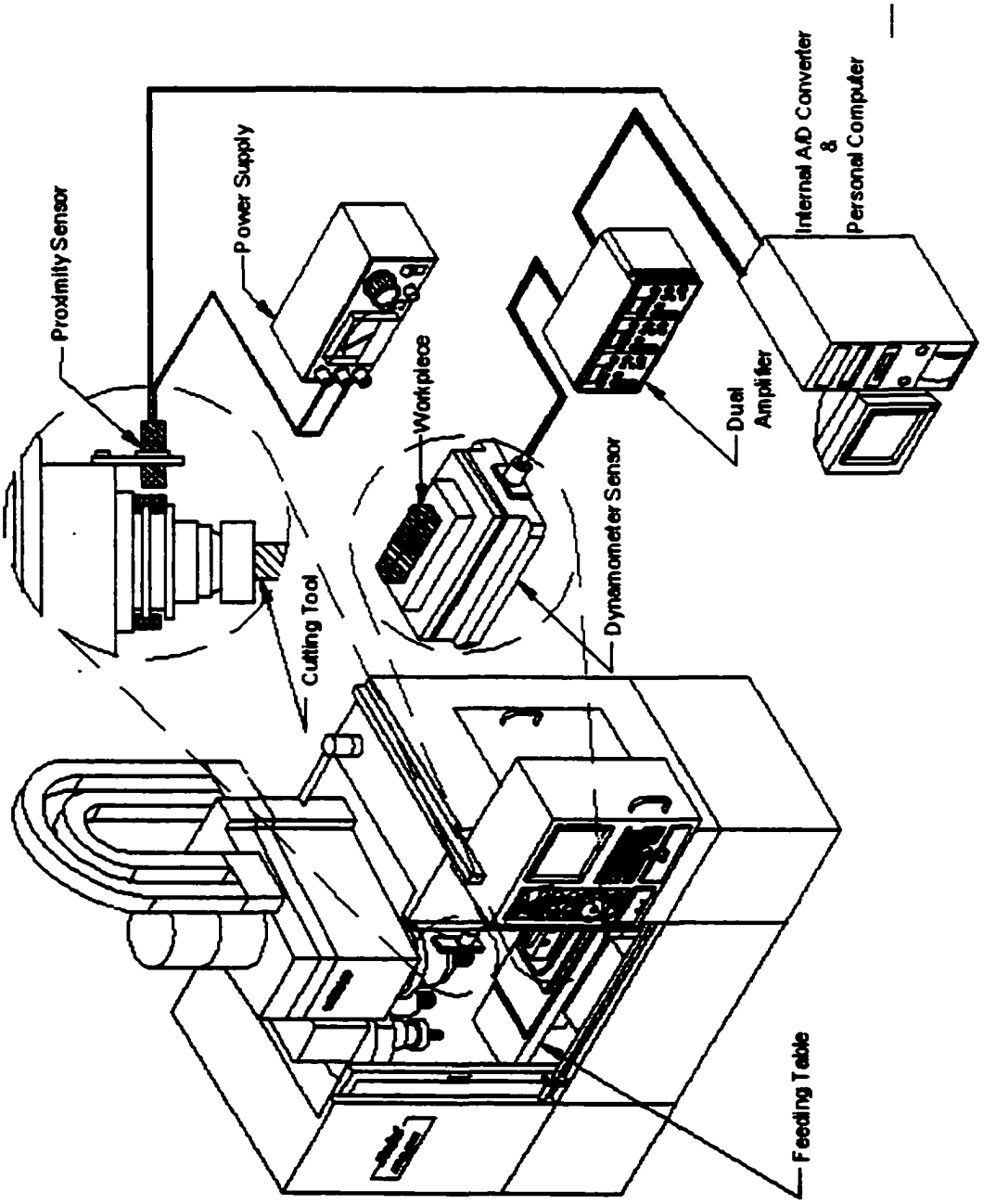

Figure 3.2. Experimental setup of hardware

1. CNC vertical machining center (Fadal VMC-40): The Fadal CNC machine was used to execute the end-milling cutting process and control the machine tool and machining parameters, such as feed rate, spindle speed, and depth of cut.
2. Milling cutters (Morse 1/2" High Speed Steel): Two center-hole type doubt-end high-speed steel milling cutters with 0.5" diameter, with four flutes numbered as 1 and 2.
3. Workpiece: The 6061 aluminum with $0.75" \times 1.2" \times 2"$ cube was selected as a workpiece. The workpiece was mounted on the dynamometer.
4. Dynamometer sensor (Kistles 9257B): The 3-component dynamometer sensor was mounted on the base table of the CNC machine. It was used to measure the cutting force in X, Y and Z directions.

The principles of the dynamometer sensor

The multi-component dynamometer provides dynamic and quasi-static measurements of the three orthogonal components of force (F_X, F_Y, and F_Z) acting from any direction onto the top plate. The dynamometer has high rigidity and high frequency. The high resolution enables very small dynamic changes to be measured in large forces. The dynamometer can measure the active cutting force regardless of its application point. It is always applied on the cutting force measurements in milling, turning, grinding, and other machining operations (Kistler Instrument, 1994).

The cutting force generated on the top plate was measured by four three-component force sensors arranged symmetrically inside the dynamometer. Each sensor had three pairs of quartz plates to sense the pressure in the X, Y and Z directions. Figure 3.3 shows the structure of the force sensor. The quartz plate was a piezo-electric material in which an

electric potential appeared across a certain surface of a crystal when the dimensions of the crystal were changed by the application of a mechanical force. The effect is known as the piezoelectric effect. The magnitude and polarity of the induced surface charges were proportional to the magnitude and direction of the applied force F and can be expressed as:

$$Q = dF \text{ Coulomb,} \tag{3.1}$$

where d is the charge sensitivity of the quartz plate in coulomb/Newton(Mansfield, 1973).

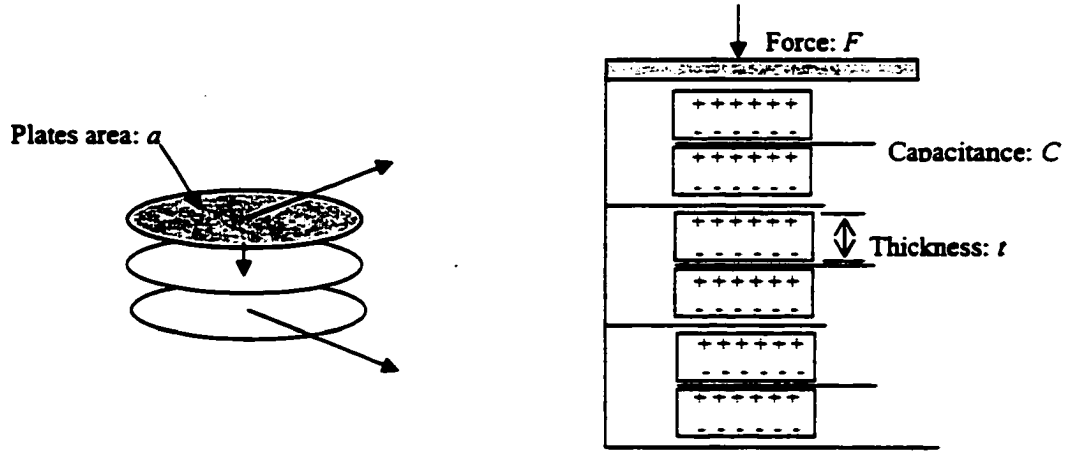

Figure 3.3. Structure of force sensor

Furthermore, the equation (3.1) can apply the Young's modulus and be expressed as:

$$Q = d\frac{aY}{t}\Delta t \text{ Coulomb,} \tag{3.2}$$

where a is the area of the quartz plate, t is the thickness of the quartz plate, Δt is the thickness variation caused by force, and Y is the proportion of stress and strain.

The charge at the electrodes gives rise to a voltage V, and it can be expressed as:

$$V = \frac{Q}{C} = d\frac{aY}{Ct}\Delta t \ , \tag{3.3}$$

where C is capacitance in farads between electrodes.

The force components are measured virtually without displacement. The unit of cutting force is the Newton (N), and it was transformed to voltage as output. In these four force sensors, the force was broken down into three components, and the collected analog signals were then led together in the connecting cable and transmitted to the amplifier. Depending on the direction of the force, the collected signals could be generated as positive or negative. However, the positive and negative force are the same if the magnitude of force is equal. Figure 3.4 shows the geometry of the dynamometer.

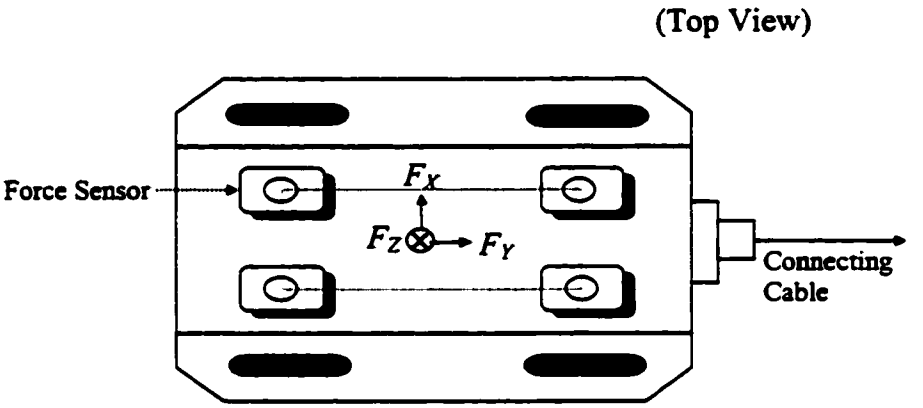

Figure 3.4. Geometry of a dynamometer

5. Dual mode amplifier (Kistler 5814A10): The amplifier was connected to the dynamometer by a cable. It was designed to adjust the charge sensitivity, d, to fit the dynamometer and the scale selected by the user. The sensitivity-values of the dynamometer in the X, Y and Z directions were set as 7.93, 7.94 and 3.71 pC/MU, respectively. The scale was set as 50 MU/V in the X, Y and Z directions.

The principles of dual mode amplifier

The amplifier was a channels charge amplifier that supplied a constant current. It converted a piezoelectric transducer signal into a proportional output voltage. This high performance analog instrument was controlled by an internal digital microcontroller which, if poorly designed, generates high frequency leading to interference and noise (Kistler Instrument, 1994). Figure 3.5 shows a block diagram of the amplifier. The device provided the necessary constant current excitation to the low impedance transducer for the voltage input, and an input capacitor C_1 decoupled the DC power from the input voltage. The decoupling capacitor also served to convert the voltage signal into a charge signal, which was fed into the charge amplifier input. The charge signal was routed through the charge amplifier, then to an adjustable gain stage, reset adjust, zero adjust, offset adjust, low pass filter, output buffer, and finally obtained the output analog voltage signal, which had a range up to ± 10 volts.

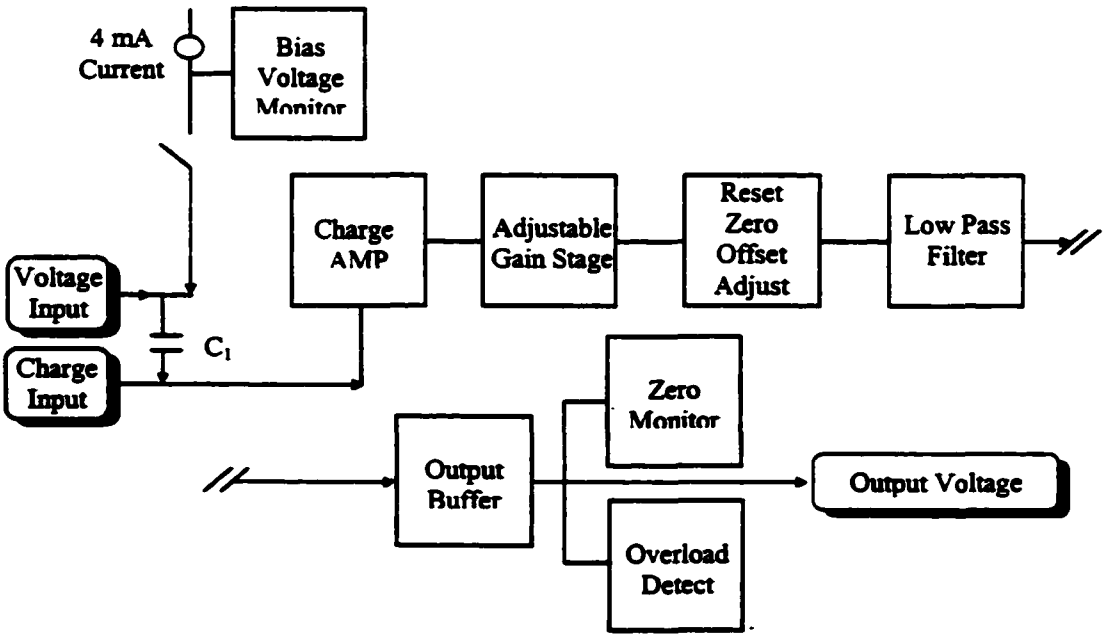

Figure 3.5. Block diagram (Kistler Instrument, 1994).

Some control buttons were provided on the front panel for user control of the amplifier. Three are pertinent to this research:

(a) Transducer sensitivity button: This button was offered to adjust the sensitive value of the amplifier, which can match different types of sensors. The unit of transducer sensitivity is pC (pico-Coulomb)/MU (Mechanical Unit).

(b) Scale button: This button was used to adjust the proportion of the Mechanical Unit (MU) selected by the user and Voltage (V). The unit of scale is MU/V. For example, the scale was set for 50 MU/V and the mechanical unit was selected as the Newton. Therefore, one volt equals 50 Newtons.

(c) Operate/Reset button: This button was designed to control the device. The microcontroller starts to work when the "Operate" light is on. The "Reset" function is utilized when the device becomes offset.

6. Proximity sensor (Micro-Switch 3-wire DC proximity sensor 992 series): The proximity sensor was located close to the spindle to indicate the data of each revolution. Since there were two protuberances on the spindle, the proximity sensor detected signals from the protuberance positions. Therefore, two specific signals could be collected in each revolution.

The principles of the proximity sensor

Proximity sensors are traditionally utilized to detect the approaching object without actually touching it. A proximity sensor was applied to generate a specific signal when an object passed nearby. The appearance of a transversal voltage difference on a conductor carrying a current perpendicular to a magnetic field, known as the Hall-effect, was the basis of a proximity sensor because the magnetic field varied with the position of a nearby object

(Honeywell Microswitch, 1997). This voltage is directly proportional to the strength of the magnetic field. The Hall-effect is present in any conductor carrying a current in a magnetic field. Therefore, a permanent magnet was installed inside the proximity sensor to provide the necessary magnetic field. If a passing object, such as a ferrous metal, approaches the sensor, it alters the magnetic field, and the Hall-effect voltage is changed at the output of the sensor. Figure 3.6 shows the structure of the proximity sensor.

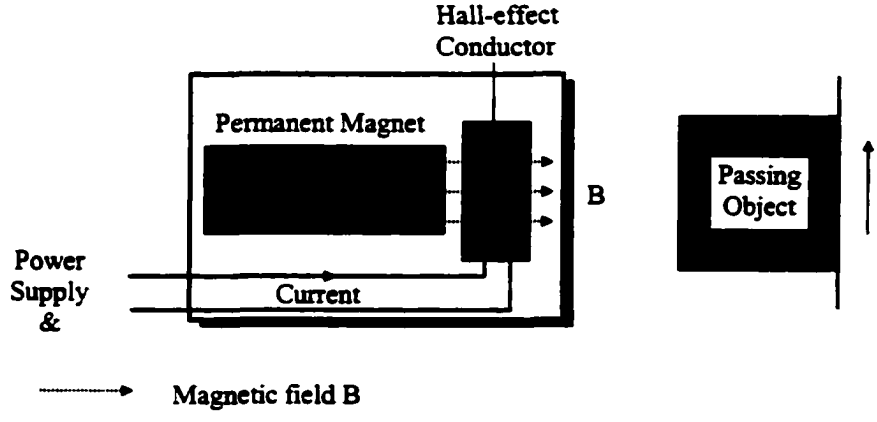

Figure 3.6. Structure of proximity sensor (Honeywell Microswitch, 1997)

To apply the proximity sensor, an open collector transistor circuit and a power supply were both necessary. The power supply provided the current and voltage to the proximity sensor to vary the voltage when an object passed by. The output of the proximity sensor was connected to the base of a transistor. The Hall-effect voltage altered and the base current changed when a metal object came near the proximity sensor. If the base current was high, the transistor turns "ON" and the collector current flows through the collector resistor and the transistor. Therefore, the voltage drop for the collector resistor is nearly the same as the

source voltage, which originated from the power supply, if the saturation voltage of transistor was zero. Otherwise, the transistor was "OFF" and the voltage of the collector resistor was zero when the metal object left from the sensor at certain distance, and thus, the base current of the transistor was zero. Figure 3.7 shows the diagram of an open-collector transistor circuit.

7. DC power supply (RCA WP-307A): The DC power supply provided constant current and reference voltage to the proximity sensor. Current was provided to generate the Hall-effect, and the reference voltage was used to compare the input voltage. The reference voltage in this experiment was set as 5 V.

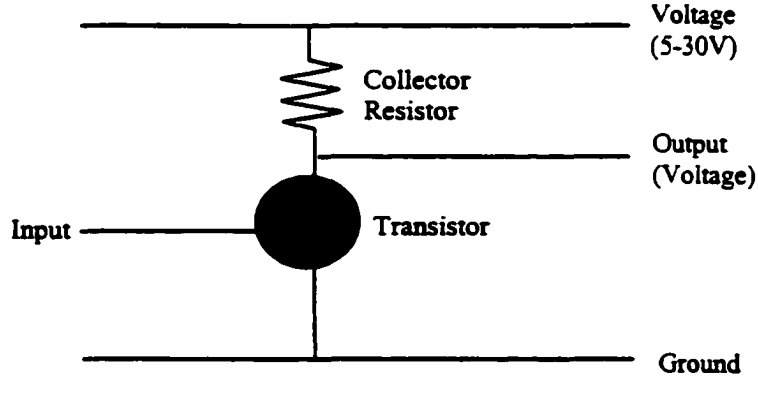

Figure 3.7. Diagram of an open-collector transistor circuit

8. Analog-to-Digital (A/D) converter (Omega DAS-1602/12): The function of this device was to convert analog signals to digital data for analysis by the microcomputer. In this multiple channels A/D converter, channel 1 was set to collect the signals from the proximity sensor. Channels 2, 3, and 4 were set to collect the analog signals from the dynamometer sensor in the X, Y and Z directions, respectively.

9. Microcomputer (Gateway Pentium): The microcomputer was used to record the digital data after the A/D conversion. Furthermore, after the decision-making algorithms were developed, the microcomputer was also applied to analyze the data and then generated a predictive surface roughness and desired adaptive feed rate.
10. Stylus profiler (Federal PocketSurf): The surface roughness of each workpiece was measured off-line by a stylus profiler to obtain the R_a value. The Federal PocketSurf was used as profiler to measure the R_a in this research. The travel length of the stylus was 0.1 inch. This length needed about seventeen revolutions for the cutting tool to travel when the feed rate was set as 12 in/min, and spindle speed was set as 2000RPM.

Software setup

The software setup consisted of several programs to collect, analyze or integrate the data for the IASRC system. These programs could be listed as follows:

1. NC program: The NC program was written to control the spindle speeds, feed rates and depth of cuts for the Fadal machine in the cutting process (see Appendix A).
2. A/D converting program: The A/D converting program developed in the C++ programming language (see Appendix B). It was used to convert the analog signal to digital data collected from the dynamometer sensor and proximate sensor and recorded the data into files.
3. Cutting force analytical program: The cutting force analytical program was developed in the C++ programming language (see Appendix C). It was applied to analyze the raw data and then to discover and calculate the average peak force and average force in the XY plane and also the average force in the Z direction within twenty revolutions.

4. JMP statistical analysis software: The JMP statistical analysis software was applied to perform the basic statistical analysis and analyze the relationship among machining parameters, surface roughness, and cutting force.
5. In-process NN-based surface roughness prediction program: The in-process NN-based surface roughness prediction (INN-SRP) program was developed by the C++ programming language to predict the surface roughness in end milling operations.
6. NN-based in-process adaptive surface roughness control program: The NN-based in-process adaptive surface roughness control (NN-IASRC) program was developed by the C++ programming language to both predict the surface roughness and adaptive degree of feed rate.
7. PC Neural (PCN) training software: The PCN neural network training software was applied to train data and obtain the weight between each neuron for both systems.

As the experimental setup for hardware and the software setup have been completed, the NN-IASRC system was ready to be constructed. To construct the NN-IASRC system, the whole system could be separated into three stages. The first stage was to discover the relationship between cutting force and surface roughness. Then, selecting the proper cutting force to monitor the uncontrollable factor within the cutting process. The second stage was to develop an in-process surface roughness prediction system. The third stage was to develop an adaptive machining parameter control system. The methodology of developing these stages is discussed in the following sections.

Statistics Analysis for Surface Roughness and Cutting Force

In the IASRC system, a dynamometer sensor would be used to monitor the cutting force within the cutting process to indicate the uncontrollable factors. However, the dynamometer sensor can only provide us the raw information of cutting force in the X, Y, or Z direction. The raw information of cutting force is difficult to directly apply in the IASRC system. Therefore, it is important to discover what kinds of cutting force could be applied in the IASRC system. To analyze the force principles in an end milling operation, the experimental design was applied to collect data.

Experimental design

To discover the force principles in an end milling operation and the correlation between surface roughness and cutting force, a factorial experimental design was applied to collect the cutting force signal during an end milling operation. Then, the surface roughness was measured by a stylus profilometer off-line.

Three controllable factors, spindle speed, feed rate, and depth of cut, were used to develop this factorial design. Three levels of spindle speed (1750, 2000, and 2250 revolution per minute (RPM)), three levels of feed rate (6, 12, and 18 in/min) and three levels of depth of cut (0.04, 0.06, and 0.08 inch) were used as the explanatory variables. Two cutting tools (T_1 and T_2) with the same geometry were selected to cut the aluminum. Each tool executed two replications. Therefore, four replications were conducted, and there were a total of 108 specimens in this experiment. Table 3.1 to Table 3.4 shows the experimental design and sequence for each replication.

Table 3.1. Tool one (T_1) with first replication

Speed / Depth / Seq. / Feed	1750			2000			2250		
	.04	.06	.08	.04	.06	.08	.04	.06	.08
6	*13*	*3*	*9*	*7*	*20*	*16*	*6*	*21*	*5*
12	*17*	*15*	*27*	*14*	*25*	*2*	*26*	*18*	*22*
18	*8*	*24*	*1*	*19*	*10*	*23*	*11*	*4*	*12*

Table 3.2. Tool one (T_1) with second replication

Speed / Depth / Seq. / Feed	1750			2000			2250		
	.04	.06	.08	.04	.06	.08	.04	.06	.08
6	*10*	*25*	*3*	*11*	*26*	*5*	*1*	*22*	*14*
12	*27*	*9*	*24*	*16*	*2*	*23*	*20*	*15*	*12*
18	*8*	*18*	*17*	*4*	*19*	*13*	*6*	*7*	*21*

Table 3.3. Tool two (T_2) with first replication

Speed / Depth / Seq. / Feed	1750			2000			2250		
	.04	.06	.08	.04	.06	.08	.04	.06	.08
6	*12*	*3*	*7*	*23*	*15*	*10*	*25*	*16*	*21*
12	*27*	*19*	*11*	*2*	*5*	*18*	*4*	*26*	*9*
18	*1*	*24*	*6*	*14*	*20*	*13*	*22*	*17*	*8*

Table 3.4. Tool two (T_2) with second replication

Speed / Depth / Seq. / Feed	1750			2000			2250		
	.04	.06	.08	.04	.06	.08	.04	.06	.08
6	*16*	*15*	*8*	*4*	*21*	*6*	*18*	*1*	*13*
12	*26*	*5*	*19*	*24*	*3*	*20*	*22*	*11*	*27*
18	*14*	*25*	*7*	*12*	*23*	*9*	*2*	*10*	*17*

After the data was collected, it was important to understand which force should be applied to compare to the surface roughness. To distinguish the types of cutting force, the property of cutting force in a milling operation were realized first.

The property of cutting force

In a milling operation, the cutting force can be categorized into two parts. One is the cutting force along the cutting plane, which is the XY plane in this research (F_X or F_Y). The other is the cutting force normal to the cutting plane, which is the Z direction in this research. In the XY plane of a milling process, when a tooth enters and leaves the cutting material, it generates a cyclic cutting force, F_X or F_Y, from zero to a maximum force, and then it returns to zero in the X or Y direction for each tooth. The cyclic force resembles a peak. Figure 3.8 shows the force diagram of one tooth. The principle of cutting force can be expanded to the resultant force, F_R, generated by the X and Y directions. The resultant force could be expressed as:

$$F_R = \sqrt{F_X^{\,2} + F_Y^{\,2}}\,. \tag{3.4}$$

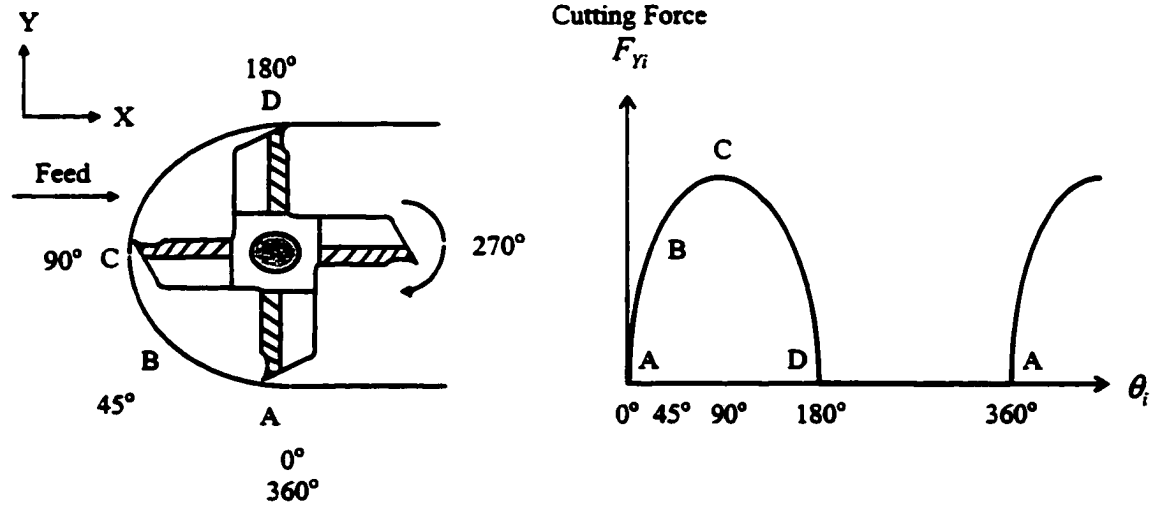

Figure 3.8. Conventional milling (left), with cutting force diagram (right) in cutting process (Huang, 1998)

The magnitude of the resultant force was affected by the tool conditions and the machining parameters, such as spindle speed, feed rate, and depth of cut. The number of peaks in each revolution was the same as the number of teeth in the milling tool. For example, a four-flute milling tool can generate four peaks in each revolution. Therefore, if the tool is in normal condition, the resultant peak force of each tooth should be the same for each revolution in the cutting process. However, because of the deflection in the cutting process and the run-out of each tooth, a normal tool still generates little variance peak force between adjacent peaks. The actual resultant peak force diagram for the four-tooth milling tool is shown in Figure 3.9. Since the peak force is the property of cutting force in the XY plane, the average resultant peak force (F_{ap}) within a certain revolution would be selected to analyze. The number of revolutions is decided by the length of the surface roughness measurement. Ideally, the in-process surface roughness prediction system can continuously predict the surface roughness in any position within the cutting process. The number of revolutions can be used to determine the responding time of predicted surface roughness. The larger the number of revolutions is, the longer the time to respond to the surface roughness. Therefore, the F_{ap} could be expressed as:

$$F_{ap} = \sum_{i=1}^{n} F_p(i)/n, \tag{3.5}$$

$$n = r \times t, \tag{3.6}$$

where F_p is the resultant peak force of each tooth, r is the number of revolutions, which is 17 in this research, and t is the number of teeth of each tool, which is 4 in this research.

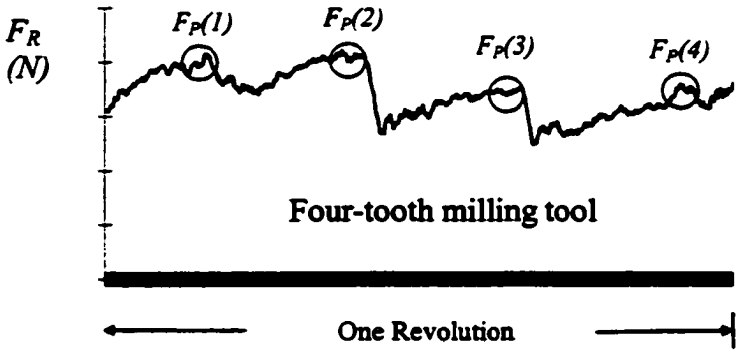

Figure 3.9. Actual resultant force diagram of four-tooth milling tool

The travel distance of the stylus profiler was around 0.1 inch when it was used to measure the surface roughness off-line. To ensure the surface roughness was measured in the same condition in both the in-process and off-line method, the measurement length of predicted surface roughness was set the same as the travel distance of the stylus profiler. The measurement length of the predicted surface roughness could be expressed as:

$$d_{Ra} = \frac{fm}{N} \times m, \tag{3.7}$$

where fm is the feed rate, N is the spindle speed and m is the number of revolutions.

In this research, the average feed rate, 12 in/min, and the average spindle speed, 2000 RPM, was utilized to decide the number of revolutions in this research. The d_{Ra} was set as 0.1 to fit the travel distance of the stylus profiler. Applying equation (3.7), the number of revolutions was set at seventeen.

The average resultant force within a certain revolution in the XY plane (F_{avg})was also used to analyze in this research. This force could be expressed as:

$$F_{avg} = \sum_{j=1}^{k} F_R(j)/k \ , \tag{3.8}$$

where k is the total number of data within 17 revolutions in this research.

For the cutting force in the Z direction (F_Z), the magnitude of the cutting force was affected by the depth of cut and vibration between the cutting tool and workpiece. Due to the vibration property between the cutting tool and workpiece, the force signal does not have any regular pattern within each revolution (shown in Figure 3.10). Intuitively, the signal pattern should relate to the profile of the cutting surface. According to the equation (2.2), the absolute average force in the Z direction within certain revolutions (F_{az}) would be expressed as:

$$F_{az} = \sum_{j=1}^{k} |F_z(j)|/k \ , \tag{3.9}$$

where k is the total number of data within 17 revolutions in this research.

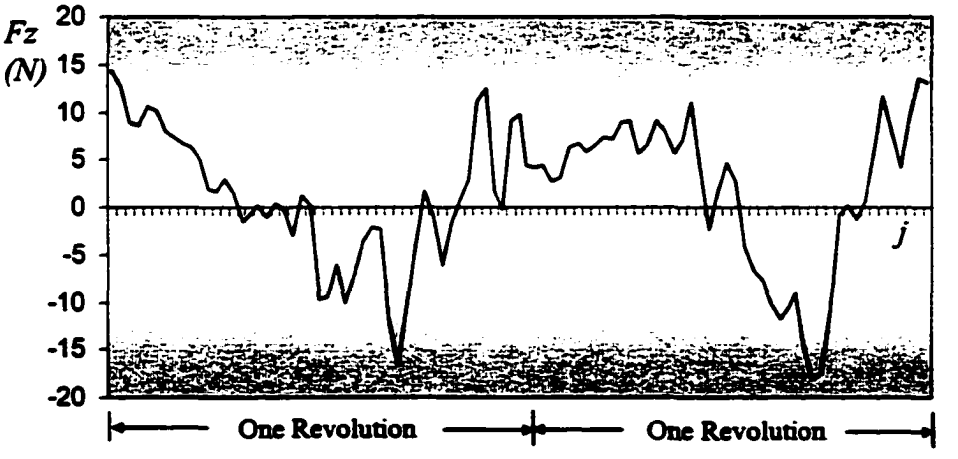

Figure 3.10. Cutting force diagram in the Z direction

The average resultant peak force (F_{ap}), the average resultant force (F_{avg}) and the absolute average force (F_{az}) were analyzed in this research to discover which force or forces have a higher correlation with surface roughness. After the data were collected and the types of cutting force for analysis were decided, the statistical analysis was applied to discover the results.

Statistical Inference

In the experimental design, two cutting tools with the same geometry were used to cut the workpiece. Intuitively, if the tool condition didn't affect the surface roughness, no matter which tool was used to cut the workpiece, the surface roughness should be the same or close to the same when the machining parameters are the same. To understand this property, it was important to understand whether the average surface roughness of one tool was the same as the other. The average surface roughness of each tool could be expressed as:

$$avgR_{a,T_j} = \sum_{i=1}^{m} R_{a,i,T_j} / m, \tag{3.10}$$

where m is the sample size of each tool, which is 54 in this research, and j represents the numbered cutting tool, which is 1 and 2 in this research.

From the observation of the average surface roughness of tool one ($avgR_{a,T_1}$) and the average surface roughness of tool two ($avgR_{a,T_2}$), if the difference between these two average values was larger than 10 μin, which was larger than the tolerance of the industrial standard, the cutting tool could be considered as the factor that influenced the cutting surface roughness. Furthermore, the ANOVA table of each tool was applied to do the indirect analysis to analyze whether the cutting tool statistically influenced the surface roughness. If

either the observation or the statistical analysis could conclude that the tool would significantly affect the surface roughness when the tool was in good condition, under the circumstances, multiple tools will be used to develop the surface roughness prediction and control system.

To develop the NN-based surface roughness prediction or control system, it was important to select proper input factors for training. To discover the proper factors of cutting force, correlation analysis between surface roughness and different types of cutting force were applied. The Pearson product moment coefficient of correlation (r) is a measure of the strength of the linear relationship between two variables. The Pearson correlation in this research can be expressed as (McClave & Benson, 1994):

$$r_F = \frac{SS_{FRa}}{\sqrt{SS_{FF} \times SS_{RaRa}}}, \tag{3.11}$$

where SS represents the sum of the square, F indicates the cutting force, and Ra is the surface roughness.

To successfully develop the NN-IASRC system, the training data should be large enough to obtain an accurate prediction model. The sample size, which was 108 for statistical analysis, was probably not large enough to achieve the goal. Therefore, the experimental design should be expanded to obtain more data set for training. To decide which factor should be expanded, the matrix plot was applied to find the relationship between surface roughness and machining parameters, which were spindle speed, feed rate, and depth of cut. As the input factors of cutting force and expanded level of factor were decided, the NN-IASRC system was constructed.

PCN Training Procedure for BP

The PCN training procedure for backpropagation of neural networks was applied to build, train and test the NN-IASRC system. The PCN training procedure involved the following key steps:

Step 1: Determine the input and output variables to build the system.

Step 2: Collect the data for training the weight between each neuron and bias of each neuron.

Step 3: Preprocess the data to reduce the training error.

Step 4: Divide the data into training and testing data sets

Step 5: Train the data sets by using a learning process. According to the theorem discussed in Chapter 2, the learning process can be summarized as followed:

1. Given network parameters: Set all the necessary parameters such as the number of input neurons (i), the number of hidden layers and the number of neurons included in each hidden layer (h), the number of output neurons (j), etc.
2. Initialize the beginning weights and biases: Set all the initial weights and biases values by random.
3. Load the input vector X and the target output vector T of a training example.
4. Calculate and infer the actual output vector Y.
5. Calculate the error term e.
6. Calculate the revised weight ΔW of the weight matrix and the revised bias $\Delta\theta$ of the bias vector.
7. Adjust and renew the weight matrix W and the bias vector θ.
8. Repeat 3 through 7 until the energy function has converged or the specified learning cycles are completely executed.

Step 6: Recalling the training process: Set all the network parameters, such as hidden neurons, hidden layers, learning rate, learning cycle, and momentum factor, to read the weight and the bias.

Step 7: Use the trained weight and bias to build a system for prediction.

Adaptive Control System

The model-reference adaptive system (MRAS) was applied to construct the NN-IASRC system in this research. Figure 3.11 shows the diagram of an MRAS for adjustment. In figure 3.11, to adjust the δ value of this system, let the model have a transfer function *T(s)*, which was assumed to be known, to process the information. The δ^c was a known constant for the model. The error could be expressed as:

$$e = y - y_m = T(s)(\delta - \delta^c)Uc, \tag{3.12}$$

where Uc is the command signal, y_m is the model output, y is the process output, and δ is the adjustable parameter.

The sensitivity derivative of the error with respect to the adjustable parameter δ could be expressed as:

$$\frac{\partial e}{\partial \delta} = \frac{y_m}{\delta^c}. \tag{3.13}$$

Finally, the adaptive parameter δ within a period of time could be expressed as:

$$\frac{d\delta}{dt} = -\gamma \times e\frac{\partial e}{\partial \delta} = -\gamma \times ey_m, \tag{3.14}$$

where the γ indicates the adaptation rate.

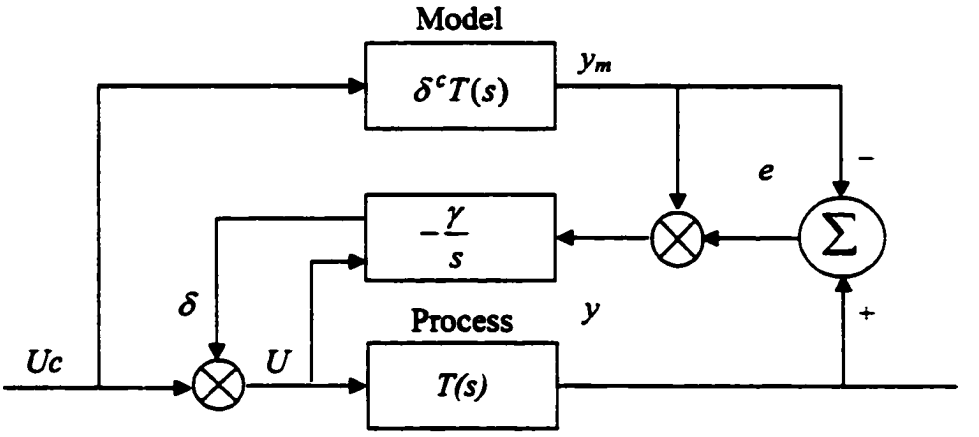

Figure 3.11. Block diagram of an MRAS for adjustment

According to the Figure 2.10 discussed in Chapter Two and Figure 3.11, in the NN-IASRC system, the machining parameters indicated command signal *Uc*. The *U* are the input factors consisting of both machining parameters and cutting force. The in-process NN-based surface roughness prediction (INN-SRP) system works as the plant to predict the surface roughness, and a neural networks algorithm plays as a transfer function in the plant to analyze the input factors and generate a predicted surface roughness. The output y of the plant is the predicted surface roughness. The model box has the desired surface roughness y_m required by the customers. The error indicated the difference between the predicted and desired surface roughness. Furthermore, the NN-based adaptive machining parameter control (NN-AMPC) system was applied to analyze the error and input factors to generate the adaptive degree of feed rate. The δ was the adaptive degree of feed rate, which fed back to the machine to adjust the machining parameter and generate a new surface roughness, which satisfied the desired surface roughness.

Summary of Methodologies

The methodologies of developing the NN-IASRC system have been proposed in this chapter. The experimental setup was designed to collect the data for analysis. The statistical approaches were used to discover the proper cutting force for the NN-IASRC system.

The discussion and analysis of the NN-IASRC system start after an understanding of the methodologies. The fourth chapter discusses the relationship between cutting force and surface roughness, and the INN-SRP system. Chapter five focuses on the development of the NN-AMPC subsystem and the NN-IASRC subsystem. Finally, Chapter six discusses the conclusions and further research of this study.

CHAPTER 4 - THE IN-PROCESS SURFACE ROUGHNESS PREDICTION SYSTEM

According to Figure 3.1,. architecture of the NN-IASRC system, the NN-IASRC system consists of two subsystems. One is the in-process NN-based surface roughness prediction (INN-SRP) subsystem and the other is the NN-based adaptive machining parameter control (NN-AMPC) subsystem. To successfully develop the NN-IASRC system, the INN-SRP subsystem must be developed first. The accuracy of the prediction system influences the accuracy of the NN-IASRC system. Developing an accurate ISRP system becomes a very important link for the NN-IASRC system.

In this chapter, the procedures of developing an in-process neural networks-based surface roughness prediction (INN-SRP) subsystem in an end milling operation are discussed. To successfully construct this subsystem, the statistics analysis of surface roughness and cutting force, and the INN-SRP subsystem are discussed.

Statistical Analysis for Cutting Force Selection

To develop the NN-IASRC system, the selection of input factors was the most important step for this system. The proper input factors decided the successful performance of the NN-IASRS system. In this section, the statistical approach was applied to discover the input factors for the NN-IASRC system.

In Chapter 3, there were two cutting tools selected in the experimental design to collect the data for analyzing. Intuitively, if the tool condition did not affect the surface roughness, randomly selecting one cutting tool to collect data could satisfy the needs of developing the NN-IASRC system. To understand whether the cutting tool influenced the surface roughness, the average surface roughness of each tool was calculated. The average surface roughness of each tool was expressed as:

$$avgR_{a,T_j} = \sum_{i=1}^{m} R_{a,i,T_j} / m, \qquad (4.1)$$

where m is the sample size of each tool, which is equal to 54 in this research, and j represents the numbered cutting tool, which is 1 and 2 in this research

The average surface roughness of tool one was 57.4 μin and 69.3 μin for tool two. From the observation, the difference of average surface roughness between tool one and two was 11.9 μin, which was larger than 10 μin. From the aspect of industry, this difference is larger than the tolerance of the industrial standard, and it could influence the quality performance of surface roughness. Therefore, from the observation, the cutting tool should be considered as an important factor that affected the cutting surface roughness.

Furthermore, the JMP software was applied to analyze the experimental design for each tool. The dependent variables were surface roughness. A significant level α was set as 0.01 to examine the factors of each tool. Table 4.1 and 4.2 show the ANOVA table for tool one and two, respectively. Comparing the same factor in each table, most of the factors significantly affect the surface roughness for both cutting tools. The only different was the factor, Feed x Depth, which significantly influenced the surface roughness in tool one, but didn't significantly influence the surface roughness in tool two. The result implied that the cutting tool would affect the surface roughness. Therefore, from the results of observation and ANOVA table analysis of each tool, multiple cutting tools would be applied to conduct the NN-IASRC system for the global industrial application. The results of both analyses also implied that the sensing technology must be properly applied to monitor the cutting tool conditions.

Table 4.1. ANOVA table for cutting tool one (T_1)

Source	DF	Sum of Squares	*F* Value	Pr>*F*
Block	1	0.074	0.0031	0.9564
Speed	2	1364.593	28.1169	0.0001*
Feed	2	14859.593	306.1765	0.0001*
Depth	2	296.037	6.0997	0.0067*
Speed*Feed	4	1687.519	17.3854	0.0001*
Speed*Depth	4	2320.407	23.9056	0.0001*
Feed*Depth	4	2382.074	24.5409	0.0001*
Speed*Feed*Depth	8	949.815	4.8926	0.0009*
Error	26	630.926	24.266	
Total	53	24491.037		

* represents that the factor significantly influences the dependent variable

Table 4.2. ANOVA table for cutting tool two (T_2)

Source	DF	Sum of Squares	*F* Value	Pr>*F*
Block	1	40.907	1.1308	0.2974
Speed	2	2096.704	28.9787	0.0001*
Feed	2	22616.148	312.5795	0.0001*
Depth	2	455.704	6.2983	0.0059*
Speed*Feed	4	932.296	6.4427	0.0010*
Speed*Depth	4	1422.407	9.8296	0.0001*
Feed*Depth	4	588.963	4.0701	0.0108
Speed*Feed*Depth	8	1285.926	4.4432	0.0017*
Error	26	940.593	36.18	
Total	53	30379.648		

* represents that the factor significantly influences the dependent variable

In the experimental design, the independent variables were spindle speed, feed rate, and depth of cut, and the dependent variables were surface roughness, average resultant peak force, average resultant force, and absolute average force. Tables 4.3 – 4.6 show the ANOVA table for surface roughness, average resultant peak force, average resultant force, and absolute average force, respectively. The significant level α was set at 0.01 for the *F*-

value to diagnose each factor. From these tables, the statistical analysis of the experimental design can be concluded as follows:

1. The cutting tools significantly influenced both surface roughness and cutting force. This information proved that the cutting tool was one of the important factors affecting surface roughness. Furthermore, since cutting force can respond to the difference in cutting tools, these results indicated that it a useful signal for monitoring tool conditions and predicting surface roughness.

Table 4.3. ANOVA table for surface roughness

Source	DF	Sum of Squares	*F* Value	Pr>*F*
Tool	1	3828.2314	73.8236	0.0001*
Speed	2	3374.3889	32.5358	0.0001*
Feed	2	37064.3889	357.3747	0.0001*
Depth	2	477.0556	4.5998	0.0129
Speed*Feed	4	2155.2222	10.3903	0.0001*
Speed*Depth	4	3443.5556	16.6014	0.0001*
Feed*Depth	4	2510.0556	12.1010	0.0001*
Speed*Feed*Depth	8	1697.5	4.0918	0.0004*
Error	80	4148.5185		
Total	107	58986.9167		

* represents that the factor significantly influences the dependent variable

Table 4.4. ANOVA table for average resultant peak force (F_{ap})

Source	DF	Sum of Squares	*F* Value	Pr>*F*
Tool	1	3019.8848	61.9109	0.0001*
Speed	2	825.7451	8.4643	0.0004*
Feed	2	8690.7741	89.0851	0.0001*
Depth	2	22750.6969	233.2068	0.0001*
Speed*Feed	4	113.7988	0.5832	0.6756
Speed*Depth	4	130.9312	0.6711	0.6139
Feed*Depth	4	261.8087	1.3418	0.2617
Speed*Feed*Depth	8	91.1738	0.2336	0.9835
Error	80	3902.2354		
Total	107			

* represents that the factor significantly influences the dependent variable

Table 4.5. ANOVA table for average resultant force (F_{avg})

Source	DF	Sum of Squares	*F* Value	Pr>*F*
Tool	1	916.3873	89.2537	0.0001*
Speed	2	504.9904	24.5924	0.0001*
Feed	2	5264.4042	256.3695	0.0001*
Depth	2	17326.2704	843.7662	0.0001*
Speed*Feed	4	71.8937	1.7506	0.1471
Speed*Depth	4	10.6656	0.2597	0.9029
Feed*Depth	4	134.1275	3.2659	0.0156
Speed*Feed*Depth	8	55.8473	0.6799	0.7078
Error	80	821.3777		
Total	107			

* represents that the factor significantly influences the dependent variable

Table 4.6. ANOVA table for absolute average force (F_{az})

Source	DF	Sum of Squares	*F* Value	Pr>*F*
Tool	1	6.5033	74.0180	0.0001*
Speed	2	2.0052	11.4114	0.0001*
Feed	2	146.1208	831.5447	0.0001*
Depth	2	463.4036	2637.1386	0.0001*
Speed*Feed	4	0.3252	0.9253	0.4535
Speed*Depth	4	0.8430	2.3986	0.0569
Feed*Depth	4	8.7230	24.8204	0.0001*
Speed*Feed*Depth	8	6.6243	9.4245	0.0001*
Error	80	7.0289		
Total	107			

* represents that the factor significantly influences the dependent variable

2. Depth of cut did not significantly affect the surface roughness. Statistically, if a surface roughness prediction model were constructed, depth of cut would not be an input factor.
3. The average resultant peak force, average resultant force, and absolute average force were significantly influenced by the machining parameters.

4. Both surface roughness and cutting force signals are significantly influenced by the machining parameters. It indicated that a certain correlation should exist between the surface roughness and these cutting force signals.
5. The cutting force signals were significantly influenced by the machining parameters. The cutting force signals are not independent to machining parameters. Therefore, if the regression model consisted of both machining parameters and cutting forces as explanation variables were built to predict the surface roughness, the cutting force signals should be filtered to represent the pure cutting conditions.

Since cutting force was a useful signal in monitoring the tool conditions in order to predict surface roughness, further analysis was used to discover the relative degree of association between surface roughness and cutting force. The Pearson correlation (r) was applied to determine the relative degree of association among machining parameters, surface roughness, and three different cutting forces, the average resultant peak force in the XY plane (F_{ap}), the average resultant force in the XY plane (F_{avg}), and the absolute average force in the Z direction (F_{az}). The Pearson correlation is a measure of the strength of the linear relationship between surface roughness and selected cutting force. For example, the Pearson correlation between the average resultant peak force (F_{ap}) and the surface roughness (R_a) could be defined as:

$$r_{Fap} = \frac{SS_{FapRa}}{\sqrt{SS_{FapFap} \times SS_{RaRa}}}, \tag{4.2}$$

where SS_{FapRa}, SS_{FapFap}, and SS_{RaRa} could be expressed as:

$$SS_{FapRa} = \sum_{i=1}^{2m} F_{ap,i} \times R_{a,i} - \left(\sum_{i=1}^{2m} F_{ap,i}\right)\left(\sum_{i=1}^{2m} R_{a,i}\right) / 2m, \tag{4.3}$$

$$SS_{RaRa} = \sum_{i=1}^{2m} R_{a,i}^2 - \left(\sum_{i=1}^{2m} R_{a,i}\right)^2 / 2m, \quad (4.4)$$

$$SS_{FapFap} = \sum_{i=1}^{2m} F_{ap,i}^2 - \left(\sum_{i=1}^{2m} F_{ap,i}\right)^2 / 2m, \quad (4.5)$$

where m is the sample size of each tool, which is equal to 54 in this research.

Table 4.7 shows the Pearson correlation values between each parameter. The scatter plot matrix (Figure 4.1) can also be used to understand the relationship among machining parameters, surface roughness, and cutting force. For example, the scatter plot of R_a and F_{ap} is shown in column five, row four of this figure. From Table 4.7 and Figure 4.1, the correlation of each parameter can be concluded as follows:

Table 4.7. Pearson correlation value

	Ra	F_{ap}	F_{avg}	F_{az}
Ra	1.0000	0.5718	0.4362	0.5190
Spindle Speed	-0.2296	-0.1407	-0.1408	-0.0558
Feed Rate	0.7919	0.4576	0.4522	0.4568
Depth of Cut	0.0783	0.7559	0.8307	0.8473

1. The correlative degrees to the surface roughness from the highest to the lowest were feed rate (0.79), F_{ap} (0.57), F_{az} (0.52), F_{avg} (0.44), spindle speed (-0.23), and depth of cut (0.08). Feed rate had the highest positive correlation to surface roughness: the higher the feed rate, the worse the surface roughness.
2. Spindle speed correlated negatively to surface roughness. Therefore, higher spindle speeds lead to better surface roughness.

3. Depth of cut had the highest correlation to the cutting forces, F_{ap}, F_{az} and F_{avg}, but the lowest correlation to surface roughness.
4. To build an in-process surface roughness prediction subsystem, the cutting forces, F_{ap}, F_{az}, and F_{avg}, can all be used as input factors. However, both F_{ap} and F_{avg} are collected from the same plane. To prevent the potential problem of covariance, the one with higher correlation to the surface roughness should be selected. Therefore, F_{ap} and F_{az} were selected as input factors for the surface roughness prediction system.

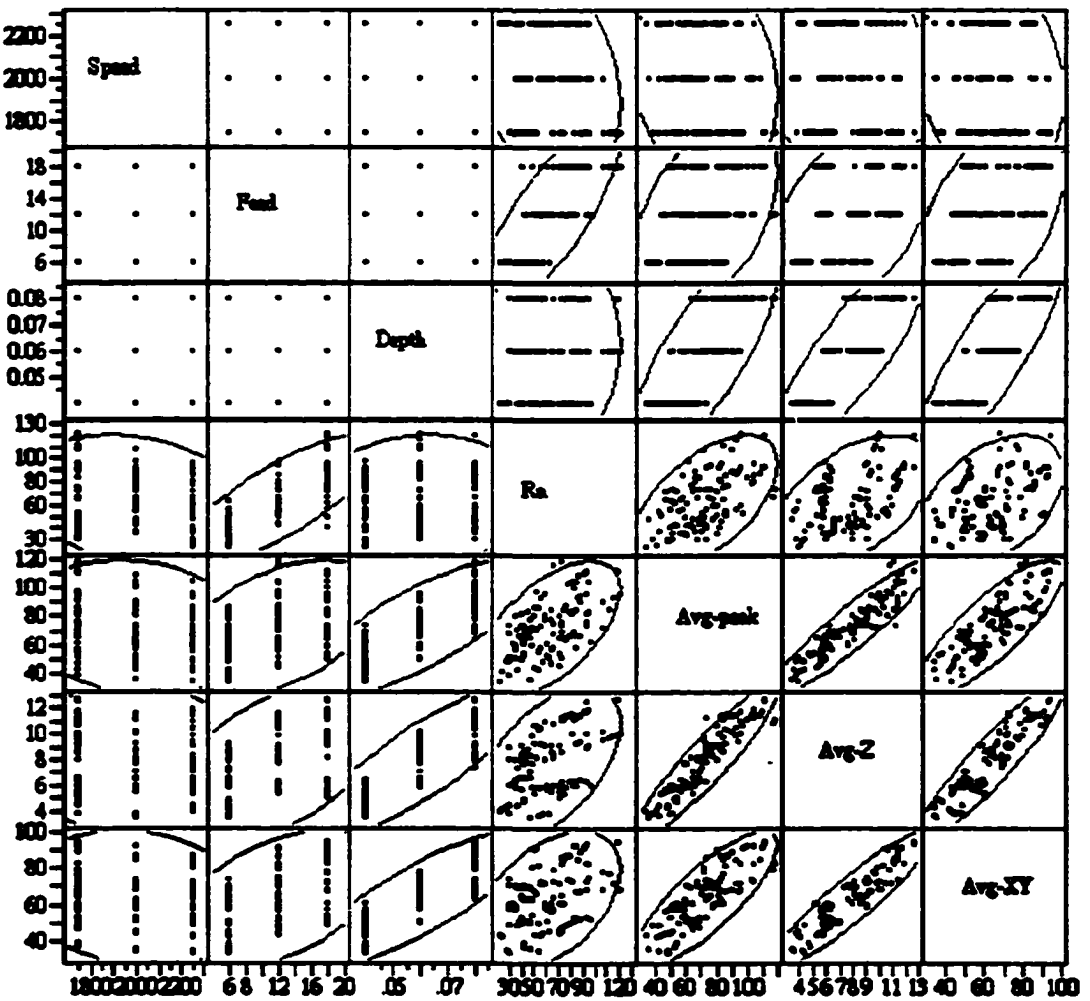

Figure 4.1. Scatter plot matrix

From the analysis of experimental design and Pearson correlation, the input factors for surface roughness prediction system could be decided. In the controllable factors, the spindle speed and feed rate were selected as input for this system. Since the depth of cut does not significantly influence the surface roughness, it was not used in this system. In the uncontrollable factors, the average resultant peak force in the XY plane and the absolute average force in the Z direction were used to monitor the tool conditions for a surface roughness prediction system. As the input factors were decided, the following stage was to use these factors to build the surface roughness prediction system.

In-process NN-based Surface Roughness Prediction (INN-SRP) Subsystem

The procedures of developing the INN-SRP subsystem are discussed in this section. Figure 4.2 shows the architecture of the INN-SRP subsystem. To develop this subsystem, the theorem of backproparation of neural networks was applied to build the decision-making algorithm, which can analyze the input data and then generate a predicted surface roughness.

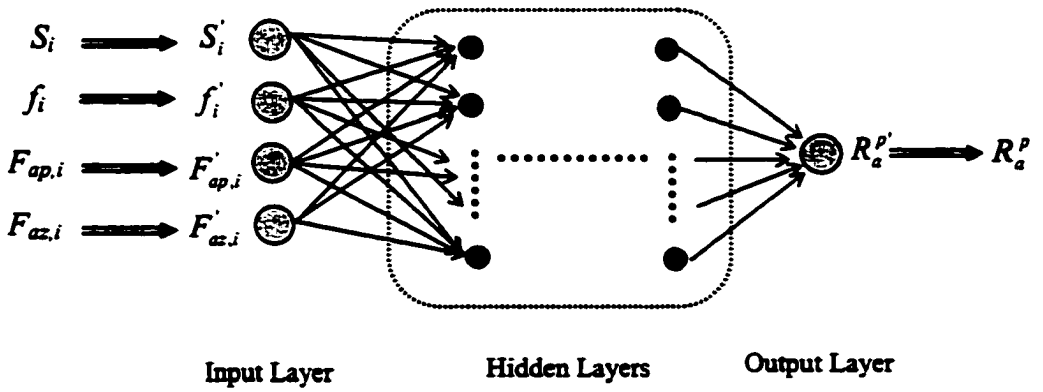

Figure 4.2. Architecture of the INN-SRP system

Relating to the PCN training procedures discussed in the Chapter 3, the following steps were used to construct the INN-SRP subsystem.

Step 1. Construct an experimental design to collect data for training

In order to achieve an accurate prediction system, it was necessary to provide sufficient data for the neural networks to train the INN-SRP subsystem. Basically, the data used for the statistical analysis was not enough to train the subsystem. Therefore, an experimental design was conducted again to collect more data for training. From the statistical analysis, feed rate had the most significant influence on surface roughness; spindle speed followed. The experimental design increased the levels of feed rate and spindle speed. Four levels of spindle speed (1750, 2000, 2250, and 2500 revolutions per minute (RPM)), eight levels of feed rate (6, 8, 10, 12, 14, 16, 18, and 20 in/min), and three levels of depth of cut (0.04, 0.06, and 0.08 inch), were selected. Two cutting tools (T_1 and T_2) with the same geometry were selected to cut the aluminum. Each tool executed two replications. Therefore, four replications were conducted, and there were a total of 384 data for training. Tables 4.8 through 4.11 show the experimental design and sequence for each replication. The numbers in the shaded area of each table represent the experimental sequence.

Table 4.8. Tool one (T_1) with first replication

Feed \ Speed / Depth / Seq.	1750			2000			2250			2500		
	4	6	8	4	6	8	4	6	8	4	6	8
6	13	3	9	7	20	16	6	21	5	72	28	60
8	31	62	44	96	56	71	89	77	36	53	66	54
10	82	33	57	61	42	76	52	95	68	43	59	39
12	17	15	27	14	25	2	26	18	22	47	90	83
14	75	88	50	93	32	49	87	91	81	78	34	48
16	51	63	67	58	84	69	74	37	64	38	86	79
18	8	24	1	19	10	23	11	4	12	55	73	35
20	45	85	41	70	80	30	94	46	92	29	40	65

Note: The unit of feed rate, depth of cut, and spindle speed is in/min, 0.01 in and RPM.

Table 4.9. Tool one (T_1) with second replication

Feed \ Speed / Depth / Seq.	1750			2000			2250			2500		
	4	6	8	4	6	8	4	6	8	4	6	8
6	10	25	3	11	26	5	1	22	14	71	77	32
8	85	37	56	65	39	46	58	45	52	96	31	60
10	66	50	78	81	59	62	40	93	68	44	89	88
12	27	9	24	16	2	23	20	15	12	82	74	51
14	76	36	92	35	47	79	49	28	87	33	53	54
16	84	61	75	55	29	69	73	83	41	64	95	30
18	8	18	17	4	19	13	6	7	21	94	43	72
20	38	70	91	48	86	34	57	63	90	42	80	67

Note: The unit of feed rate, depth of cut, and spindle speed is in/min, 0.01 in and RPM.

Table 4.10. Tool two (T_2) with first replication

Feed \ Speed / Depth / Seq.	1750			2000			2250			2500		
	4	6	8	4	6	8	4	6	8	4	6	8
6	12	3	7	23	15	10	25	16	21	66	48	76
8	73	56	85	43	53	64	33	87	34	29	95	37
10	96	41	62	84	31	61	83	60	77	70	47	58
12	27	19	11	2	5	18	4	26	9	38	94	82
14	92	42	72	89	40	52	68	49	51	80	57	28
16	67	88	32	63	44	78	30	93	59	46	91	65
18	1	24	6	14	20	13	22	17	8	86	36	81
20	90	55	79	54	71	74	45	69	35	39	75	50

Note: The unit of feed rate, depth of cut, and spindle speed is in/min, 0.01 in and RPM.

Table 4.11. Tool two (T_2) with second replication

Feed \ Speed / Depth / Seq.	1750			2000			2250			2500		
	4	6	8	4	6	8	4	6	8	4	6	8
6	*16*	*15*	*8*	*4*	*21*	*6*	*18*	*1*	*13*	*65*	*35*	*57*
8	*61*	*94*	*46*	*34*	*75*	*29*	*76*	*52*	*33*	*58*	*41*	*44*
10	*96*	*38*	*28*	*88*	*53*	*81*	*39*	*71*	*89*	*72*	*91*	*64*
12	*26*	*5*	*19*	*24*	*3*	*20*	*22*	*11*	*27*	*40*	*50*	*31*
14	*87*	*60*	*84*	*59*	*70*	*55*	*66*	*51*	*80*	*90*	*73*	*92*
16	*45*	*85*	*54*	*83*	*47*	*82*	*32*	*93*	*56*	*63*	*30*	*95*
18	*14*	*25*	*7*	*12*	*23*	*9*	*2*	*10*	*17*	*74*	*78*	*49*
20	*86*	*62*	*69*	*37*	*68*	*43*	*77*	*42*	*67*	*36*	*48*	*79*

Note: The unit of feed rate, depth of cut, and spindle speed is in/min, 0.01 in and RPM.

Step 2. Determine the input and output factors

After the experimental design was conducted, there were three hundred eighty four samples collected. All of the experimental samples, including the machining parameters, cutting force and measured surface roughness are shown in Appendix D in column two through column seven. After the data were collected, the input and output factors were then determined to construct the INN-SRP subsystem. As shown in Figure 4.2, there were four input factors in the INN-SRP subsystem, which were spindle speed (S), feed rate (f), average resultant peak force in the XY plane (F_{ap}), and absolute average force in the Z direction (F_{az}). The output factor was surface roughness measured by the stylus profiler. To create the INN-SRP subsystem, 384 pieces of data were applied. Each data set could be expressed as:

$$[S_i, f_i, F_{ap,i}, F_{az,i}; R_{a,i}], \qquad \text{for } i = 1 \text{ to } 384. \qquad (4.6)$$

These data are shown in Appendix D. For example, when i equals1, the data set can be expressed as [1750, 6, 39.060, 3.715; 30]

Step 3. Scale the data set

To avoid training error from bigger values of some data sets, some pre-processing was needed to obtain good training and prediction results. Data scaling was the method to make all input and output factors fall between 0 and 1. The principle of scaling depends on the distribution of each factor. Since the distributions of input and output factors were uniform, spindle speed and feed rate, or normal distribution without extreme values at each side, the average resultant peak force, the absolute average force and surface roughness. The simple linear mapping method was applied. This method can be expressed as:

$$V' = \frac{V - V_{min}}{V_{max} - V_{min}}, \tag{4.7}$$

where V' is the scaled value, V_{max} and V_{min} are the extremes of the factor, and V represents the original data.

For example, from the raw data set shown in Appendix D, the maximum value of spindle speed was 2500 RPM and the minimum value of spindle speed was 1750 RPM, the scaled value of the spindle speed can be expressed as:

$$S_i' = \frac{S_i - 1750}{750}. \tag{4.8}$$

After the pre-processing of scaling, the data set can be expressed as:

$$[S_i', f_i', F_{ap,i}', F_{az,i}^i; R_{a,i}'], \qquad \text{for } i = 1 \text{ to } 384 \tag{4.9}$$

All of the scaled data were shown in Appendix D from column seven to column eleven. For example, when i equals 1, the scaled data set can be expressed as [0.0, 0.0, 0.087, 0.028; 0.082].

Step 4. Training the data to obtain the weight between each neuron

The fifth step of the PCN training procedures discussed in the Chapter 3 was applied to execute the neural networks-BP training to obtain the weight between each neuron and the bias of each neuron. In the training process, it was difficult to decide the portion of training data and testing data, the layers and neurons of the hidden level, the learning rate and momentum factor. Therefore, the "learn-and-error" method was employed to adjust these training parameters until the smallest root mean square (*RMS*) error was achieved. The following procedures were applied to discover the optimal combination of these factors.

Procedure 1: Determine the ratio of training and testing data

The original data contained 384 samples and were randomized and separated into two data sets, the training data set and testing data set. Three different groups were applied to train the INN-SRP subsystem. The first group contained 250 training data and 134 testing data, the second group had 290 training data and 94 testing data, and the third one had 310 training data and 74 testing data. To compare the *RMS* error between each group, some parameters used in the training process should be fixed first. The initial number of hidden neurons was set at 4, and the hidden layer was set at 1. The learning rate and momentum factor were set at 1 and 0.7, respectively. The number of training cycles was 9000, and the testing period was 2. Table 4.12 shows the *RMS* error of each group. In this table, the *RMS* errors of both training and testing data in the group with 290 x 94 samples were 0.0838 and

0.1001, respectively, which were smaller than the *RMS* errors of both the training and testing data in the other two groups, which were 250 x 134 and 310 x 74. It indicated that the sample size 290 x 94 could provide higher accuracy in the prediction system. Consequently, the group contained 290 training data and 94 testing data and were employed for the neural networks training processes.

Table 4.12. Comparison of *RMS* error for different sample size

Training x Testing	Hidden Layer	Hidden Neuron	Learning Rate	Momentum Factor	*RMS* error of Training	*RMS* error of Testing
250 x 134	1	4	1	0.7	0.0942	0.1437
290 x 94	1	4	1	0.7	0.0838	0.1001
310 x 74	1	4	1	0.7	0.1132	0.1021

Procedure 2: Determine the hidden layer and hidden neuron

The initial number of hidden neurons and hidden layers was set at 4 and 1, respectively. Following that, different hidden neurons and layers were tested to determine which combination led to the smallest *RMS* error. Table 4.13 shows the results of the *RMS* error of training and testing with different layers and neurons. In the training processes, sometimes it was not easy to make one group have the *RMS* error of training and testing both smaller than other groups. Under the circumstances, the group with the smaller *RMS* error of training was selected because it provided sufficient information that allowed the system to predict. According to Table 4.13, the *RMS* error, 0.0821, of the training trail with 5 hidden neurons in hidden layer 1 and 5 hidden neurons in hidden layer 2 (shown in the shaded area of row eight) was less than it was in all other trails. Thus, the configuration contained the 2 layers with 5 hidden neurons in each layer was chosen because it led to the smallest *RMS*

error of training. Consequently, a 4-5-5-1 INN-SRP subsystem, which contained four input factors, 5 hidden neurons in hidden layer 1, 5 hidden neurons in hidden layer 2 and one output factor, was developed.

Table 4.13. Comparison of *RMS* error for different hidden neurons and layers

#	Neuron in Layer - 1	Neuron in Layer - 2	Learning Rate	Momentum Factor	*RMS* error of Training	*RMS* error of Testing
1	3	~	1	0.7	0.0841	0.0986
2	4	~	1	0.7	0.0838	0.1001
3	5	~	1	0.7	0.0841	0.0969
4	3	3	1	0.7	0.0837	0.0995
5	3	4	1	0.7	0.0834	0.0997
6	4	4	1	0.7	0.0837	0.0976
7	4	5	1	0.7	0.0847	0.0995
8	5	5	1	0.7	0.0821	0.0945
9	5	6	1	0.7	0.0831	0.0942
10	6	6	1	0.7	0.0825	0.0963

Procedure 3: Determine the learning rate (η)

It necessary to determine the optimal learning rate to minimize the *RMS* error of training and testing data. The initial learning rate was set as 1, which was able to simplify the adjustment of weight between each neuron and the bias of each neuron (shown in equations (2.18) and (2.19)). To obtain the optimal learning rate for the 4-5-5-1 INN-SRP subsystem, five additional learning rates, 0.5, 0.7, 0.9, 2 and 5, were used to compare with the initial one. Table 4.14 shows the training results with different learning rates for the 4-5-5-1 INN-SRP subsystem. From Table 4.14, the *RMS* error, 0.0764, of the learning rate of 0.7

had the smallest *RMS* error of both the training and testing data (shown in the shaded area of row five). To achieve the objective of finding the smallest *RMS* error, the learning rate of 0.7 was applied in the training processes to obtain the optimal weight between each neuron and the bias of each neuron.

Table 4.14 Comparison of *RMS* error of learning rate in the 4-5-5-1 INN-SRP subsystem

#	Learning Rate	*RMS* error of Training	*RMS* error of Testing
1	5	0.1022	0.1174
2	2	0.0964	0.1204
3	1	0.0821	0.0945
4	0.9	0.0806	0.0914
5	0.7	0.0764	0.0883
6	0.5	0.0794	0.0902

Procedure 4: Determine the momentum factor

The final procedure of the training process was changing the value of the momentum factor to obtain the configuration leading to the smallest *RMS* error for the prediction system using a neural networks approach. The initial value of the momentum factor was 0.7. Another four values, 0.8, 0.6,0.5, and 0.4 were selected to compare with the initial value. Table 4.15 shows the results of *RMS* error with different values for the momentum factor. From Table 4.15, the *RMS* errors, which were 0.0731 and 0.0826 for the training and tests data, respectively, of momentum factor, 0.5, had the smallest value (shown in the shaded area of row four). To achieve the high accuracy prediction system, the 0.5 momentum factor was used to train the INN-SRP subsystem.

Table 4.15. Comparison of *RMS* error of momentum factor in the 4-5-5-1 INN-SRP subsystem

#	Momentum Factor	*RMS* error of Training	*RMS* error of Testing
1	0.8	0.0802	0.0936
2	0.7	0.0764	0.0883
3	0.6	0.0752	0.0847
4	0.5	0.0731	0.0826
5	0.4	0.0737	0.0837

After the procedures of "learn and error" were used to adjust these training parameters in a neural networks, the smallest *RMS* error was discovered. A 4-5-5-1 INN-SRP subsystem, which set the learn rate as 0.7 and the momentum factor as 0.5, demonstrated the smallest *RMS* errors, which were 0.0731 and 0.0826 for both training and testing data, respectively. Figure 4.3 shows the architecture of the 4-5-5-1 INN-SRP subsystem.

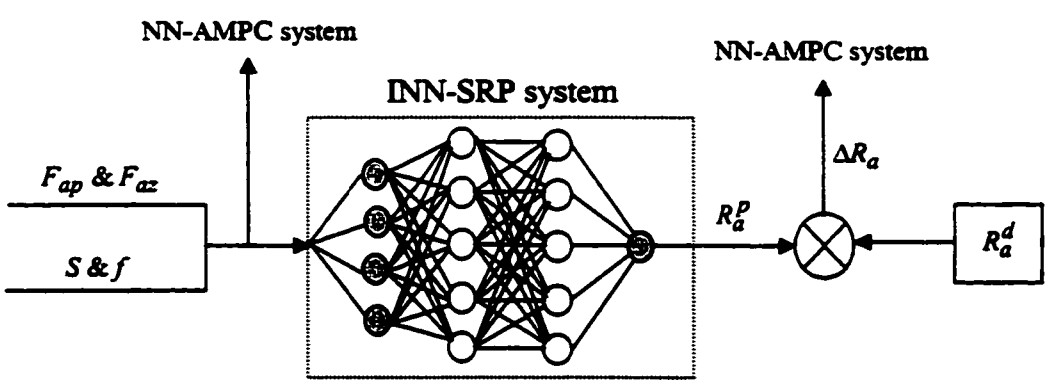

Figure 4.3. Architecture of the 4-5-5-1 INN-SRP system

Step 5. Build the INN-SRP subsystem

After completing the training procedures executed in step four, the weight between each neuron and the bias of each neuron shown in Table 4.16 were obtained. The decision-making algorithm used to predict surface roughness was expressed as:

$$R_{a,i}^{p} = \frac{1}{1+\exp-(\sum_{j=1}^{n} a_j^k \times W_j - \theta_{Ra})} \times (R_{a,\max} - R_{a,\min}) + R_{a,\min}, \qquad (4.10)$$

where n is the number of neurons in hidden layer k, θ_{Ra} is the bias of the output neuron, which was 0.021, $R_{a,\max}$ and $R_{a,\min}$ represent the maximum and minimum value of R_a from the data set, respectively.

Table 4.16. The weight between each neuron and bias of each neuron for the INN-SRP subsystem

		Inputs					
		S_i	f_i	$F_{ap,i}$	$F_{az,i}$	θ_j^1	
Hidden Layer 1	1	-0.4581	2.6490	-6.3270	-0.5697	1.7790	
	2	-2.3910	4.3420	1.2790	-2.3550	2.2470	
	3	-0.8417	8.5720	-1.3100	-0.2232	0.8322	
	4	-9.4440	6.3300	-0.3320	3.4010	6.7750	
	5	-0.6358	1.1140	-2.5020	-7.6860	-9.4270	
		Hidden Layer 1					
		1	2	3	4	5	θ_j^2
Hidden Layer 2	1	0.6004	-1.7240	3.8170	9.7690	-4.3710	2.0720
	2	-1.0030	0.3169	-0.8317	-2.9590	-0.7604	-0.0563
	3	1.3420	-0.5514	-1.6980	0.0233	0.5712	-0.0774
	4	-3.0630	1.7780	-3.2810	-3.5040	0.2006	-0.8216
	5	2.2380	-1.1190	-4.2040	3.1500	3.3270	0.2851
		Hidden Layer 2					
		1	2	3	4	5	θ_{Ra}
Output	1	4.1830	2.2100	-0.4757	4.2360	-5.0340	0.0021

In the INN-SRP subsystem, since there were 5 hidden neurons in hidden layer 2, and the $R_{a,\max}$ and $R_{a,\min}$ of the raw experimental data were 131 and 21 μin, respectively, the equation (4.10) can be further expressed as:

$$R_{a,i}^{p} = \frac{1}{1+\exp-(\sum_{j=1}^{5} a_j^2 \times W_j - 0.021)} \times 110 + 21 \qquad (4.11)$$

The training process was completed when the weight between each neuron and the bias of each neuron were obtained. The weight and bias can then be employed to build the INN-SRP subsystem. To perform the real time in-process prediction function, The INN-SRP subsystem was developed by the C++ programming language shown in Appendix E. In this program, the prediction algorithm of neural networks, which consisted of the weight and bias obtained from the training process, was built to perform the in-process prediction function. The program of the INN-SRP subsystem can collect and analyze the data in real-time and predict surface roughness value by the inference of neural networks prediction algorithm. The INN-SRP subsystem was completed when the program was finished. The next step is to apply the program of the INN-SRP subsystem to perform the real time in-process testing.

Step 6. Test the INN-SRP subsystem

To evaluate the accuracy of this subsystem, the average accuracy of the surface roughness and standard deviation of the average accuracy were applied. The equation of average accuracy of surface roughness (A_{Ra}) and standard deviation of the average surface roughness ($Std_{A_{Ra}}$) can be expressed as:

$$A_{Ra} = [1 - \sum_{i=1}^{n} \frac{|R_{a,i}^{p} - R_{a,i}|}{R_{a,i} \times n}] \times 100\% \ , \qquad (4.12)$$

$$Std_{A_{Ra}} = \sqrt{\frac{\sum_{i=1}^{n}(A_{Ra,i} - A_{Ra})^2}{n-1}}, \tag{4.13}$$

$$A_{Ra,i} = [1 - \frac{\left|R_{a,i}^{p} - R_{a,i}\right|}{R_{a,i}}] \times 100\%, \tag{4.14}$$

where the R_a^p is the predicted surface roughness, R_a represents the actual surface roughness measured off-line by the profilometer, and n is number of the samples.

As the method of evaluating the accuracy of the INN-SRP subsystem was determined, the testing process was conducted to discover the accuracy of this subsystem. The testing procedure included other machining parameters within the experimental range. The testing machining parameters, which were different from the original experimental ones, are shown in Table 4.17. Twenty-five samples were tested to find the flexibility of this system. Table 4.17 consists of the testing machining parameters, cutting force, predicted surface roughness obtained from the INN-SRP subsystem, actual surface roughness measured by the stylus profiler and the accuracy of each sample. For example, in sample one, the spindle speed (1750 PRM), feed rate (7 in/min), average resultant peak force (89.1083 N), and the absolute average force (9.0298 N), were employed as inputs in the INN-SRP subsystem to obtain the predicted surface roughness, 40 μ in. The actual surface roughness was 42 μ in. Finally, the accuracy of this sample was calculated at 95.2%.

Table 4.17. Results of testing data for the INN-SRP subsystem

#	Speed (RPM)	Feed (in/min)	Depth (in)	F_{ap} (N)	F_{ac} (N)	R_a^p	R_a	$A_{Ra,i}$
1	1750	7	0.065	89.1083	9.0298	40	42	0.952
2	1750	9	0.065	106.9291	9.2311	43	49	0.878
3	1750	11	0.065	102.9853	11.5246	57	57	1.000
4	1750	15	0.065	131.0221	13.4364	94	91	0.967
5	1800	7	0.05	62.6502	5.6725	39	32	0.781
6	1800	15	0.08	96.3554	11.1721	87	88	0.989
7	1850	7	0.04	46.9105	4.6894	35	30	0.833
8	2000	7	0.045	67.7542	5.0098	39	38	0.974
9	2000	11	0.045	60.5288	6.0721	55	54	0.981
10	2000	15	0.045	83.8719	11.0914	77	83	0.928
11	2000	17	0.045	91.4795	10.2466	82	86	0.953
12	2000	19	0.045	95.5351	11.1754	85	89	0.955
13	2050	8	0.06	58.4882	6.3472	36	43	0.837
14	2100	15	0.06	90.4283	8.4181	78	75	0.960
15	2250	7	0.05	62.0656	10.7142	39	39	1.000
16	2250	11	0.05	85.8351	7.1882	52	59	0.881
17	2250	15	0.05	99.7361	12.955	73	70	0.957
18	2250	17	0.05	88.6195	11.4961	82	81	0.988
19	2250	19	0.05	90.4723	12.2771	88	93	0.946
20	2300	19	0.05	73.2501	7.188	81	74	0.905
21	2350	17	0.048	73.6631	6.3407	76	68	0.882
22	2350	19	0.06	75.3982	8.8142	78	73	0.932
23	2450	18	0.05	64.1963	7.2495	70	61	0.852
24	2500	7	0.07	82.2235	7.6538	41	41	1.000
25	2500	11	0.07	96.3543	11.4371	54	51	0.941

Summary of the INN-SRP Subsystem

The average accuracy of surface roughness of the flexible testing samples tested in step six was 93% with a standard deviation of 5.6%. The high accuracy and low standard deviation of the flexible testing samples indicated that the INN-SRP subsystem had the ability to predict the surface roughness in any different machining parameter combination within the machining parameters of the experimental range. For an in-process surface roughness prediction system in end-milling operations with multiple cutting tools, high accuracy was achieved for the INN-SRP subsystem.

The surface roughness prediction system using neural networks algorithm was successfully developed. The development of the NN-based adaptive machining parameter control (NN-AMPC) system, which is the other subsystem of the NN-IASRC system, and testing of the NN-IASRC system is discussed in the following chapter.

CHAPTER 5 – NEURAL NETWORK BASED IN PROCESS ADAPTIVE SURFACE ROUGHNESS CONTROL SYSTEM

To successfully construct the NN-IASRC system, this system must provide the ability of adaptive control when the quality of surface roughness cannot achieve the need of the customers. In Chapter Four, the INN-SRP subsystem was developed. However, the INN-SRP subsystem can only predict the surface roughness. It cannot deal with the quality control situation when the predicted surface roughness cannot reach the need of the customers. Therefore, in this chapter, the other subsystem, the neural network based adaptive machining parameter control (NN-AMPC) subsystem was developed. The NN-AMPC subsystem and the INN-SRP subsystem was then integrated into the NN-IASRC system. Furthermore, the testing process was conducted to evaluate the performance of the NN-IASRC system.

Neural Network-based Adaptive Machining Parameter Control Subsystem

In the NN-IASRC system, the NN-AMPC subsystem works only when the predicted surface roughness is larger than the desired surface roughness. To develop the NN-AMPC subsystem (shown in Figure 5.1), the procedures are similar to the one used to develop the INN-SRP subsystem. The following steps are used to construct the NN-AMPC subsystem.

Step 1. Pre-process the experimental data

The purpose of this step is to obtain the training data for developing the NN-AMPC subsystem. The data used for the development of the INN-SRP subsystem were continuously applied. To build the NN-AMPC subsystem, one of the important input factors was to recognize the difference between the predicted surface roughness and the desired one.

Therefore, there was a need to know the difference between predicted surface roughness obtained from the INN-SRP subsystem and the desired surface roughness requested by the customers. Furthermore, the output of the NN-AMPC subsystem, which was the adaptive degree of feed rate, should also be known for training. However, the original data used in Chapter 4 for the INN-SPR subsystem didn't contain these two important factors. Therefore, the original data needed to be pre-processed to obtain these two important factors, which contained the adaptive degree of feed rate and the difference between the predicted surface roughness and the desired surface roughness.

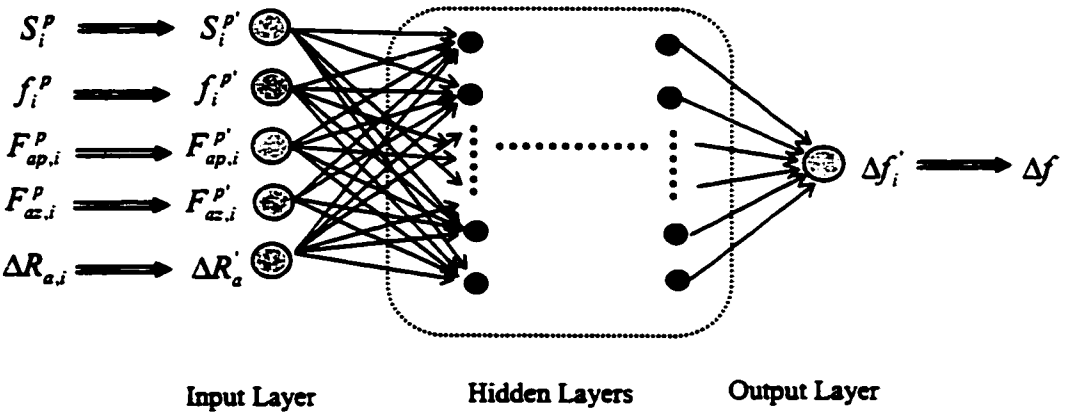

Figure 5.1. Architecture of the NN-AMPC system

To generate the difference between predicted and desired surface roughness and the adaptive degree of feed rate, basically, two samples with different R_a and feed rate needed to be selected to generate the difference of R_a (ΔR_a) and adaptive degree of feed rate (Δf). The following procedures were applied to generate the data set.

1. From the experimental samples for the INN-SRP subsystem, four replications were executed. Therefore, every combination of machining parameters had four samples. To reduce the sample size, every combination randomly selected one sample to put into the new data set. Therefore, 96 samples (384 samples divided by 4) were selected to form the new data set.
2. The target output factor of the NN-AMPC subsystem is the adaptive degree of feed rate. The spindle speed and depth of cut was not changed in this study. To generate the different feed rate without changing the spindle speed and depth of cut, these 96 samples were separated into twelve groups. Each group had a single spindle speed and depth of cut and eight different feed rates. For example, in Table 5.1, there are eight samples in group one, which contained only one spindle speed, 1750 RPM, and one depth of cut, 0.04 inches.

Table 5.1. Samples of group one for data pre-processing

Group One							
#	Speed (RPM)	Feed (in/min)	Depth (in)	F_{ap} (N)	F_{ac} (N)	R_a^p	R_a
1	1750	6	0.04	42.3023	4.4448	35	37
2	1750	8	0.04	61.2800	5.1687	41	39
3	1750	10	0.04	52.4374	5.2414	53	59
4	1750	12	0.04	56.7756	5.5821	68	64
5	1750	14	0.04	69.5485	6.6034	75	77
6	1750	16	0.04	71.8200	5.9493	78	79
7	1750	18	0.04	69.9409	6.2215	86	83
8	1750	20	0.04	63.7470	5.8242	100	102

3. In each group, two samples were chosen to create the ΔR_a and an adaptive degree of current feed rate (Δf). In these two samples, the sample with a larger surface roughness, the predicted surface roughness shown in column seven of Table 5.1, was assumed to be the predicted surface roughness obtained from the INN-SRP system. For the sample with the smaller surface roughness, the actual surface roughness shown in column eight of Table 5.1 was assumed to be the desired R_a (R_a^d). The new data set was expanded to 336 samples ($12 \times C_2^8$). The ΔR_a and Δf could be express as:

$$\Delta R_{a,i} = R_{a,i}^p - R_{a,j}^d, \qquad \text{for } i,j = 1 \text{ to } 96. \qquad (5.1)$$

$$\Delta f = (1 - \frac{f_{p,i} - f_{d,j}}{f_{p,i}}) \times 100\%, \qquad \text{for } i,j = 1 \text{ to } 96. \qquad (5.2)$$

where i represents the sample with the larger Ra (R_a^p), j is the sample with the smaller Ra (R_a^d), f_p is the feed rate of the INN-SRP subsystem and f_d is the desired feed rate to achieve the desired surface roughness.

For example, in Table 5.1, sample one and two were chosen to calculate the ΔR_a and Δf. The predicted surface roughness, 41 μ in, of sample two with a feed rate of 8 in/min, which contained the larger surface roughness, was assumed to be the predicted surface roughness. The actual surface roughness, 37 μ in, of sample one with a feed rate of 6 in/min was assumed to be the desired surface roughness. Therefore, the ΔR_a and Δf were calculated as 4 μ in and 75%, respectively. The machining parameters and cutting forces of sample two, which had a larger surface roughness than the one of sample one, were employed to form the new data set. Therefore, the new data set of these two samples

consisted of the machining parameters (1750 RPM, 8 in/min and 0.04 inches), cutting force of the prediction system (61.28 N and 5.1687 N), the difference between predicted surface roughness and desired surface roughness (4 μ in) and the adaptive degree of feed rate (75%).

Step 2. Determine the input and output factors

After the original data were pre-processed, a new data set with three hundred thirty six samples was obtained. The whole samples of the new data set contained the machining parameters (S^p, f^p), cutting force of the prediction system (F_{ap}^p, F_{az}^p), the difference between predicted surface roughness (ΔR_a) and desired surface roughness and the adaptive degree of feed rate (Δf) are shown in Appendix F in column two through column seven. After all data were pre-processed, the input and output factors were then determined for the NN-AMPC subsystem. The NN-AMPC subsystem consisted of five input factors, which were spindle speed from the prediction system (S^p), feed rate from the prediction system (f^p), average resultant peak force from the prediction system (F_{ap}^p), absolute average force in the Z direction from the prediction system (F_{az}^p), and the difference between predicted R_a and desired R_a (ΔR_a). Since the depth of cut was not used in the prediction system, it was not considered as an input factor in the NN-AMPC subsystem. The output factor was the adaptive degree of feed rate (Δf). Three hundred thirty six data were applied to develop the NN-AMPC subsystem. For each data set, it could be expressed as:

$$[S_i^p, f_i^p, F_{ap,i}^p, F_{az,i}^p, \Delta R_{a,i}; \Delta f_i], \qquad \text{for } i = 1 \text{ to } 336. \qquad (5.3)$$

For example, as shown in Appendix F, the data set of sample one can be expressed as [1750, 20, 63.747, 5.824, 17; 90].

Step 3. Scale the data set

To avoid training error from bigger values of some data sets, the data set was scaled to make the data of all input and output factors fall between 0 and 1. The equation (4.7) was applied again to scale the data set. For example, in the data set for developing the NN-AMPC subsystem, the maximum value of feed rate was 20 in/min, and 8 in/min was the minimum. The scaled feed rate can be expressed as:

$$f_i^{P'} = \frac{f_i^P - 8}{12}, \qquad \text{for } i = 1 \text{ to } 336 \qquad (5.4)$$

After all the input and output factors were scaled, the new data set for the training of neural networks could be expressed as:

$$[S_i^{P'}, f_i^{P'}, F_{ap,i}^{P'}, F_{az,i}^{P'}, \Delta R_{a,i}^{'}; \Delta f_i^{'}], \qquad \text{for } i = 1 \text{ to } 336 \qquad (5.5)$$

The whole scaled data were shown in Appendix F in column eight through column thirteen. For example, when i equals 1 the scaled data set can be expressed as [0.0, 1.0, 0.257, 0.137, 0.2; 0.857].

Step 4. Training the data to obtain the weight between each neuron

As the input-output factors were decided, the PCN training procedures were applied again to execute the neural network-BP training to obtain the weight between each neuron. The training procedures were the same as the ones applied in the INN-SRP subsystem. The "learn-and-error" method was used to adjust these training parameters until the smallest root mean square (*RMS*) error was achieved. The following procedures were applied to discover the optimal combination of these factors.

Procedure 1: Determine the ratio of training and testing data

Procedure 2: Determine the hidden layer and hidden neuron

Procedure 3: Determine the learning rate (η)

Procedure 4: Determine the momentum factor

The procedures of training for neural networks were used to adjust these training parameters until the smallest root mean square (*RMS*) error was discovered. A 5-8-7-1 NN-AMPC subsystem demonstrated the smallest *RMS* error for both training and testing data. Table 5.2 shows the optimal combination after the NN training procedures. There were 252 samples and 84 samples were employed in the training and testing data set, respectively.

Table 5.2. Optimal combination of the NN-AMPC subsystem

Item	Optimal value
Training data	252
Testing data	84
Hidden layer	2
Hidden neuron of layer 1	8
Hidden neuron of layer 2	7
Learn rate	0.7
Momentum factor	0.6
Training cycle	18000
RMS error of training	0.1031
RMS error of testing	0.1237

Step 5. Build the NN-AMPC subsystem

After completing the training procedures, the weight between each neuron and the bias of each neuron shown in Table 5.3 were obtained, the equations to adjust the degree of feed rate for the NN-AMPC subsystem were concluded. The final adaptive model could be expressed as:

$$\Delta f_i^p = \frac{1}{1+\exp-(\sum_{j=1}^{n} a_j^k \times W_j - \theta_{\Delta f})} \times (\Delta f_{\max} - \Delta f_{\min}) + \Delta f_{\min}, \quad (5.6)$$

where n is the number of neurons in hidden layer k, $\theta_{\Delta f}$ is the bias of output neuron $\Delta f_{\max}$ and $\Delta f_{\min}$ represents the maximum and minimum value of adaptive degree of feed rate from the new data set, and i represents the sample.

Table 5.3. The weight between each neuron and bias of each neuron for the NN-AMPC subsystem

		Inputs					
		S_i^p	f_i^p	$F_{ap,i}^p$	$F_{az,i}^p$	$\Delta R_{a,i}$	θ_j^1
Hidden Layer 1	1	0.956	-6.845	4.977	0.901	3.622	5.096
	2	13.940	-12.720	-3.587	-3.852	1.216	-0.965
	3	12.450	-16.270	-1.763	6.361	12.700	6.856
	4	-1.902	-14.630	-6.668	11.470	-13.450	-4.465
	5	1.991	-6.303	2.087	15.170	-23.800	-1.697
	6	7.351	-10.560	-1.440	3.087	-4.257	-2.729
	7	-4.407	-9.066	-0.302	1.678	-9.934	-6.046
	8	-4.232	3.032	-5.964	-15.140	10.620	-2.392

		Hidden Layer 1								
		1	2	3	4	5	6	7	8	θ_j^2
Hidden Layer 2	1	-7.441	-8.904	7.500	-2.540	-12.130	0.932	-3.764	-6.534	-1.260
	2	10.880	-1.626	-15.250	-0.868	-4.868	8.598	6.914	2.597	4.854
	3	3.890	-7.147	-4.278	7.134	1.296	0.142	-12.160	0.101	-2.337
	4	-3.914	-0.887	-4.484	-9.715	-5.116	6.762	13.100	-6.608	2.277
	5	3.643	-1.074	1.353	-4.294	-0.118	2.916	1.613	-4.493	5.393
	6	-8.477	-11.410	5.950	-3.269	-17.200	4.194	-0.923	-5.893	-0.681
	7	11.140	-3.871	-4.443	-5.152	2.843	-0.130	-15.280	-3.189	-3.060

		Hidden Layer 2							
		1	2	3	4	5	6	7	$\theta_{\Delta f}$
Output	1	7.701	18.880	-5.973	-15.900	-7.395	-10.470	6.053	0.008

For the NN-AMPC subsystem, this equation could be further expressed as:

$$\Delta f_i^P = \frac{1}{1+\exp-(\sum_{j=1}^{7} a_j^2 \times W_j - 0.008)} \times 70 + 30 . \qquad (5.7)$$

The training process was completed after the weight and bias was obtained. The adaptive machining parameter control system was developed using a neural networks algorithm. Figure 5.2 shows the architecture of the 5-8-7-1 NN-AMPC subsystem. All of the data from the NN-AMPC subsystem are shown in Appendix G. To evaluate the ability of the NN-AMPC subsystem, the testing process was conducted and discussed in the following section.

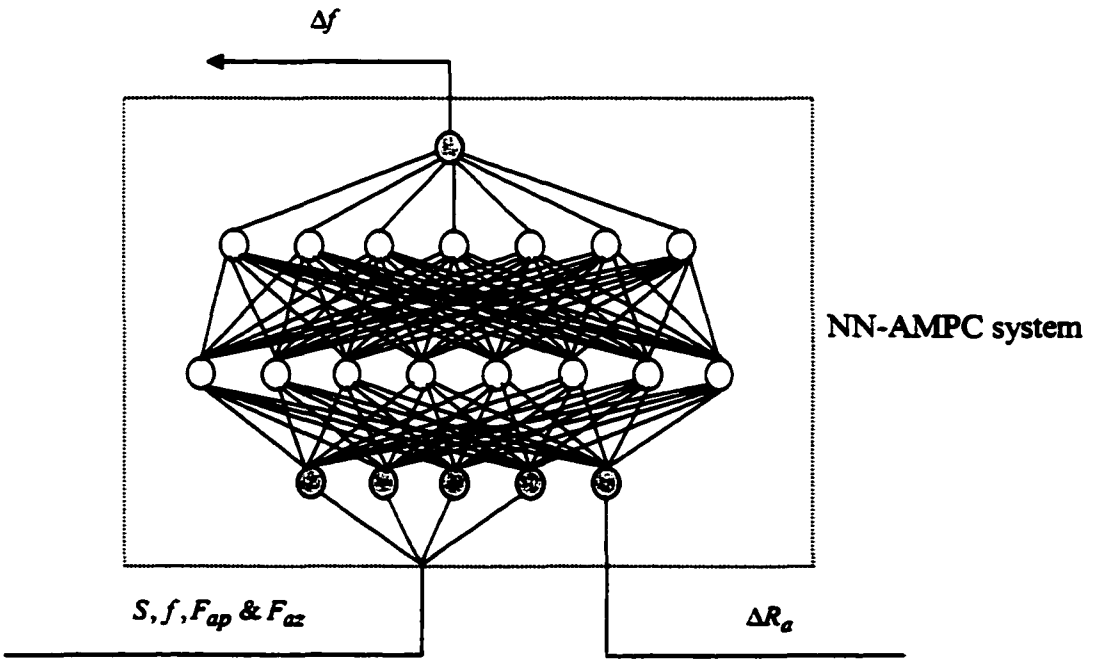

Figure 5.2. Architecture of the 5-8-7-1 NN-AMPC system

The Integration and Testing of the NN-IASRC System

The INN-SRP subsystem and the NN-AMPC subsystem were both developed to predict the surface roughness and adjust the feed rate if the predicted surface roughness could not satisfy the needs of customers. The final stage of the NN-IASRC system was to integrate these two subsystems together to perform the function of in-process surface roughness control. The INN-SRP and NN-AMPC subsystems were integrated into an NN-IASRC system by the C++ programming language (shown in Appendix H) to perform the predictive and adaptive function in an end milling operation. This program was able to collect the machining parameters and analyze the cutting force signals to predict the surface roughness and adjust the degree of feed rate to achieve the needs of the customers within the cutting process. Figure 5.3 shows the detailed architecture of the NN-IASRC system.

Finally, testing of the NN-IASRC system was executed. The experimental setup was set for the testing process. The experimental setup consisted of the hardware setup and software setup. In the hardware setup, another cutting tool (T_3), which was different from T_1 & T_2, utilized to collect the training data, was used to execute the testing process. The length of the workpiece was 2.5 inches (shown in Figure 5.4). The workpiece was separated into two sections. The first section was employed to produce the surface roughness of the original machining parameters of testing samples and the second section was used to produce a new surface roughness after the adjustment of the adaptive degree of feed rate obtained from the NN-IASRC system. Other equipment was the same as the experimental setup discussed in Chapter 3.

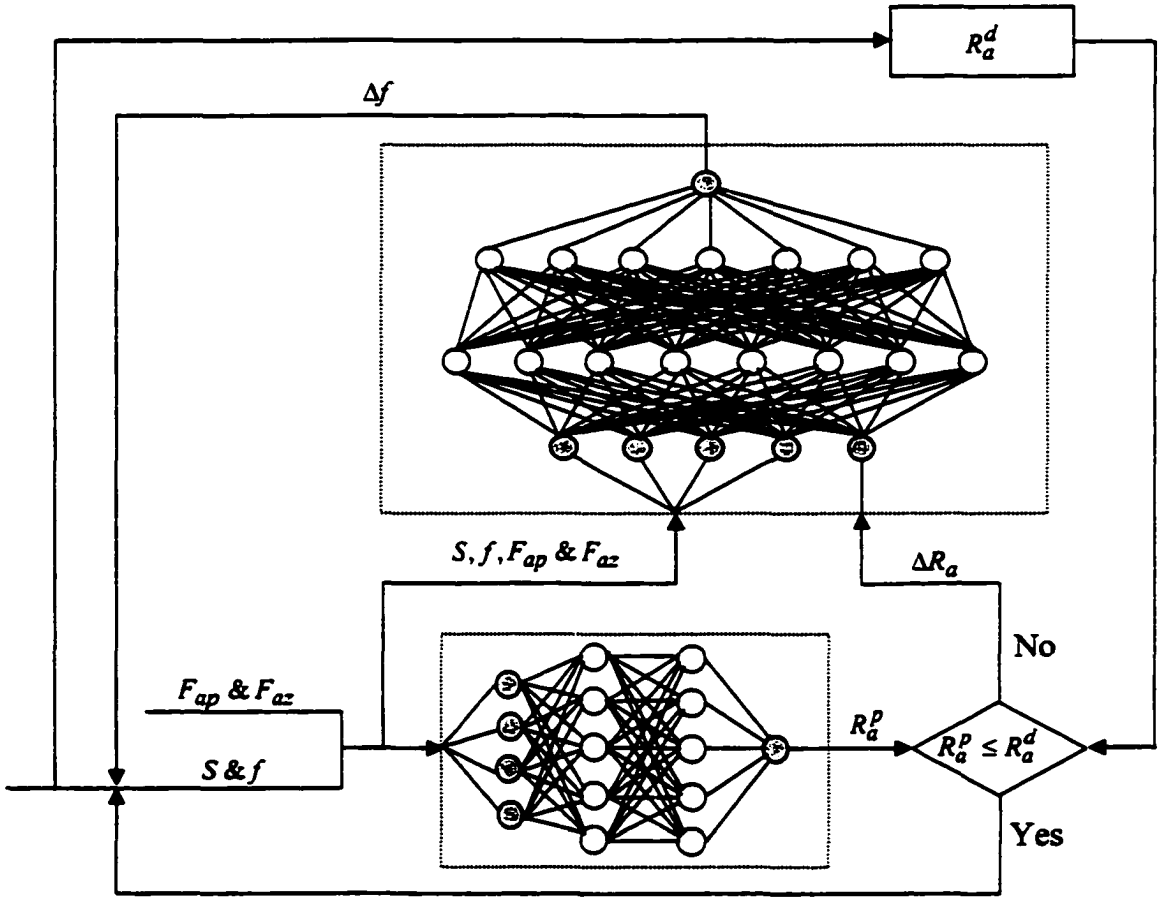

Figure 5.3. Detailed architecture of the NN-IASRC system

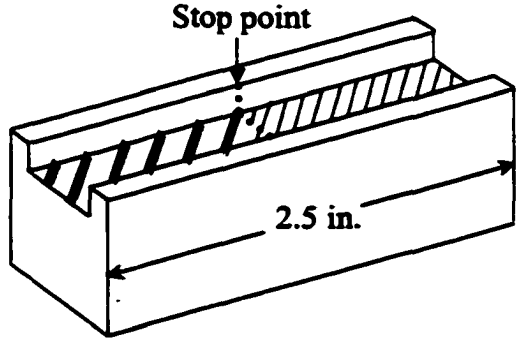

Figure 5.4. The material of testing for NN-IASRC system

The software setup consisted of a new NC program (shown in Appendix I) written to perform the cutting process for the testing of the NN-IASRC system, and the program for the NN-IASRC system, which was used to predict the surface roughness and the adaptive degree of feed rate when the predicted surface roughness was larger than the desired surface roughness.

In the new NC program, the cutting tool moved to cut the workpiece in the X-axis for 1.25 inches and then stopped. Within this length, the program of the NN-IASRC system was triggered to predict the surface roughness and provide the adaptive degree of feed rate when the predicted surface roughness was larger than the desired one. As the adaptive degree of feed rate was obtained, the knob for feed rate override, shown in Figure 5.5, was manually adjusted to change the current feed rate. For example, if the current feed rate was 20 in/min, and the adaptive degree of the current feed rate was 70% of the current feed rate obtained from the analysis of the NN-IASRC system, the knob for feed rate override was manually switched to the scale of 70 to reduce the feed rate to 14 in/min (20 x 70%). The cutting process was then restarted to the end of the workpiece to produce a product with desired surface roughness. Within this section, the actual surface roughness was measured off-line by the stylus profiler after the cutting process to check whether the actual surface roughness was smaller than the desired one.

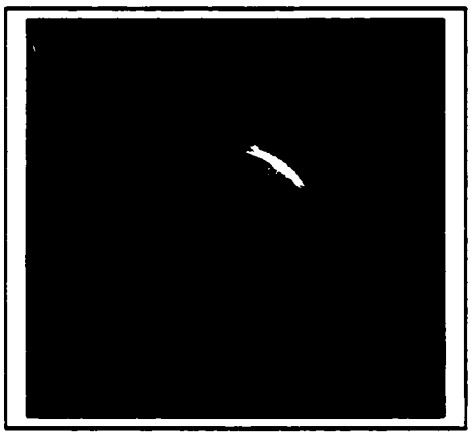

Figure 5.5. Feed rate override device

To execute the testing of the NN-IASRC system, the desired R_a (R_a^d) was first defined. The R_a^d was set at four different levels, which were 40, 50, 60 and 70 μin. The testing machining parameters and desired surface roughness of each testing sample were shown in Table 5.4. Forty samples were tested to evaluate the performance of the NN-IASRC system. Basically, to test the performance of the NN-IASRC system, most of the feed rates of testing samples were set higher than the average feed rate, which was 13 in/min. Each combination of machining parameters was cut twice to test the adaptive ability for different desired surface roughness.

The cutting process of a sample was separated into two sections. The first section of the cutting process generated the predicted R_a (R_a^{p1}) and the adaptive degree of feed rate when the predicted R_a (R_a^{p1}) was larger than R_a^d. The second section of cutting process was used to diagnose whether the new actual surface roughness (R_a^{new}) was smaller than the desired surface roughness. If the new surface roughness was smaller than the desired surface

roughness, it indicated that the NN-IASRC system was able to successfully adjust the feed rate to achieve the desired surface roughness.

Table 5.4. Testing machining parameters and R_a^d for the NN-IASRC system

	Speed	Depth	Feed	R_a^d		Speed	Depth	Feed	R_a^d
1A	2250	0.05	15	50	11A	2100	0.05	12	50
1B	2250	0.05	15	40	11B	2100	0.05	12	40
2A	1900	0.07	17	70	12A	2300	0.07	16	70
2B	1900	0.07	17	60	12B	2300	0.07	16	50
3A	2300	0.06	16	60	13A	2150	0.06	19	70
3B	2300	0.06	16	40	13B	2150	0.06	19	60
4A	1800	0.04	19	60	14A	1900	0.09	13	50
4B	1800	0.04	19	50	14B	1900	0.09	13	40
5A	2100	0.06	20	70	15A	2500	0.04	15	60
5B	2100	0.06	20	60	15B	2500	0.04	15	40
6A	2400	0.08	14	60	16A	1800	0.08	18	50
6B	2400	0.08	14	40	16B	1800	0.08	18	40
7A	2050	0.07	16	60	17A	2400	0.05	14	50
7B	2050	0.07	16	40	17B	2400	0.05	14	40
8A	1850	0.05	18	70	18A	1950	0.06	20	70
8B	1850	0.05	18	50	18B	1950	0.06	20	60
9A	2200	0.06	13	50	19A	2250	0.05	19	60
9B	2200	0.06	13	40	19B	2250	0.05	19	50
10A	2500	0.04	17	70	20A	1750	0.07	16	60
10B	2500	0.04	17	40	20B	1750	0.07	16	40

The result of the testing samples is shown in Table 5.5. For example, in sample 1A, the original spindle speed and feed rate of this testing sample were set as 2250 RPM and 15 in/min, respectively, the cutting force signals of this cutting process collected by the dynamometer sensor were 69.18 N and 9.974N. The machining parameters and cutting force signals were inputted into the NN-IASRC system to predict the surface roughness, 69 μ in, and the adaptive degree of feed rate, 80.7%. The knob for feed rate override was switched to

Table 5.5. Result of the testing for the NN-IASRC system

#	S	f	F_{ap}	F_{az}	R_a^{pl}	R_a^d	Δf	f^{new}	R_a^{new}	$R_a^{new} \le R_a^d$
1A	2250	15	69.180	9.974	69	50	80.7	12.1	41	Yes
1B	2250	15	64.224	7.512	68	40	35.9	5.4	29	Yes
2A	1900	17	128.782	12.791	122	70	72.5	12.3	65	Yes
2B	1900	17	132.753	12.251	115	60	68.1	11.6	53	Yes
3A	2300	16	103.382	9.317	78	60	60.9	9.7	42	Yes
3B	2300	16	100.798	8.103	79	40	58.8	9.4	38	Yes
4A	1800	19	91.793	8.685	107	60	60.9	11.6	57	Yes
4B	1800	19	83.944	8.707	106	50	58.8	11.2	39	Yes
5A	2100	20	98.046	13.746	111	70	68.1	13.6	70	Yes
5B	2100	20	91.783	11.544	87	60	68.1	13.6	54	Yes
6A	2400	14	73.232	11.238	69	60	56.7	7.9	33	Yes
6B	2400	14	81.601	9.739	67	40	64.7	9.1	30	Yes
7A	2050	16	111.524	11.935	92	60	67.1	10.7	53	Yes
7B	2050	16	102.449	9.380	84	40	42.7	6.8	33	Yes
8A	1850	18	98.666	10.317	97	70	68.4	12.3	60	Yes
8B	1850	18	92.265	8.930	84	50	54.6	9.8	42	Yes
9A	2200	13	79.186	6.508	67	50	61.9	8.0	44	Yes
9B	2200	13	71.365	7.088	65	40	30.1	3.9	33	Yes
10A	2500	17	79.897	5.566	76	70	60.3	10.3	44	Yes
10B	2500	17	92.937	5.796	78	40	65.2	11.1	36	Yes
11A	2100	12	62.142	6.501	60	50	95.2	11.4	46	Yes
11B	2100	12	56.924	6.120	58	40	90.1	10.8	33	Yes
12A	2300	16	72.779	10.584	72	70	77.6	12.4	59	Yes
12B	2300	16	82.507	10.231	75	50	70.3	11.2	45	Yes
13A	2150	19	81.172	7.323	89	70	70.1	13.3	59	Yes
13B	2150	19	75.398	8.168	84	60	64.8	12.3	53	Yes
14A	1900	13	102.359	9.943	73	50	65.9	8.6	45	Yes
14B	1900	13	93.646	8.681	74	40	60.1	7.8	39	Yes
15A	2500	15	76.914	7.487	68	60	96.3	14.4	58	Yes
15B	2500	15	83.581	6.818	69	40	30.7	4.6	32	Yes
16A	1800	18	109.779	9.588	105	50	58.7	10.6	44	Yes
16B	1800	18	94.954	8.438	93	40	59.5	10.7	39	Yes
17A	2400	14	91.335	7.054	67	50	77.8	10.9	47	Yes
17B	2400	14	79.683	8.099	66	40	47.9	6.7	32	Yes
18A	1950	20	113.073	10.851	97	70	76.0	15.2	64	Yes
18B	1950	20	108.350	9.265	88	60	68.3	13.7	57	Yes
19A	2250	19	105.654	8.469	91	60	48.0	9.1	51	Yes
19B	2250	19	92.949	9.168	86	50	41.3	7.8	38	Yes
20A	1750	16	67.255	6.867	74	60	59.8	9.6	53	Yes
20B	1750	16	69.693	6.864	76	40	52.0	8.3	40	Yes

the scale of 80.7 and then continued the cutting process to produce a product with a new surface roughness. The new surface roughness measured off-line was 41 μ in, which was smaller than the desired one. This sample was concluded as a successful sample for the testing of the NN-IASRC system.

In Table 5.5, all the new actual surface roughness (R_a^{new}) values were smaller than the desired surface roughness (R_a^d) in the test samples. This result indicated that the NN-IASRC system was successfully developed to adjust the feed rate to achieve the desired surface roughness requested from the customers.

Summary of the NN-IASRC System

The NN-AMPC subsystem was successfully developed to adjust the adaptive degree of feed rate when the predicted surface roughness was larger than the desired surface roughness. The INN-SRP and NN-AMPC subsystems have been successfully integrated into the NN-IASRC system. The NN-IASRC system provided not only the in-process surface roughness prediction ability but also machining parameter adaptive function. From the testing results of the NN-IASRC system, there was a 100% success rate. From the observation of the results shown in Table 5.5, the cutting force signals (F_{ap} and F_{ac}) play a very important role in determining the adaptive degree of feed rate. For example, in samples 1A and 8B, these two samples had the same desired surface roughness of 50 μ in. In sample 1A, the feed rate was reduced to 12.1 in/min (shown in column nine) to make the new surface roughness smaller than the desired one. However, sample 8B had to be reduced to 9.8 in/min for it to achieve the goal. It implied that the uncontrollable cutting tool conditions really influenced the result of surface roughness, and this uncontrollable factor must be

monitored to obtain the proper adaptive degree of feed rate for the NN-IASRC system. Therefore, the cutting force signals must be employed in the NN-IASRC system to monitor the cutting tool conditions to increase the accuracy of this system.

Furthermore, from the observation of Table 5.5, in sample 6A and 10A, relating to the desired surface roughness (shown in column seven), the new surface roughness (shown in column ten) was too small. Even though the new surface roughness achieved the goal of the NN-IASRC system. The low feed rate may influence the productivity. Discovering a new method for solving this problem could be considered for further research of the NN-IASRC system.

The NN-IASRC system allowed the CNC machine to perform the quality control of surface roughness by itself. From the testing results, all of the testing samples were successfully adapted to achieve the quality of the desired surface roughness. The NN-IASRC system can be concluded as a successful in-process surface roughness control system in end-milling operations.

CHAPTER 6 - CONCLUSIONS

Quality and productivity are both important in industry, and they always stand against each other; a successful performance of the in-process quality control system could solve the problem between quality and productivity. Since quality control is inspected by machines instead of human operators, the time and cost for off-line quality inspection no longer exist.

The major contribution of this research is that the in-process adaptive surface roughness control system in end-milling operations has been successfully developed by using neural networks. To control the quality of surface roughness, the NN-IASRC system not only provided the predictive function to accurately predict the surface roughness within the cutting process, but also possessed the adaptive function to adjust the machining parameter to generate the qualified surface roughness. The predictive function allowed the machines to measure the surface roughness, and the adaptive function assisted the machines and allowed them to adjust themselves when the quality of surface roughness was out of the control limit. In addition to the contributions of this system, the following conclusions were drawn based on the results of this research:

- A statistical approach was employed to analyze the relationship between the machining parameters and the surface roughness. From the statistical analysis, the feed rate provided the most significant positive effect on the surface roughness, and the spindle speed had a negative influence on the surface roughness. Therefore, the combination of high spindle speed and low feed rate were applied to obtain a fine surface roughness in end-milling operations.
- Statistically, the depth of cut did not significantly influence the surface roughness. This result allowed the NN-IASRC system to become more flexible to achieve the

need of the real industrial environment. In the real industrial environment, the depth of cut is not easy to control when the product has an uneven cutting surface, indicating that the depth of cut was not the same as was set in the CNC machine.

- An empirical approach was successfully applied to explore the correlation between the cutting force and the surface roughness. The average resultant peak force in the XY plane (F_{ap}) and the absolute average force in the Z direction (F_{az}) were examined as useful signals to represent the tool conditions related to the surface roughness in end-milling operations. These two cutting force signals were successfully utilized in the NN-IASRC system to represent the uncontrollable cutting tool conditions within the cutting process and to increase the accuracy of the surface roughness prediction and machining parameter adaptation.
- From the observation, the cutting tools influenced the surface roughness even though they were manufactured from the same company with the same geometry. This result indicated that the cutting tool conditions must be monitored by using sensing technology. Since cutting force signals are able to respond to the difference in cutting tools, they are useful signals for monitoring tool conditions and predicting surface roughness in end-milling operations.
- The spindle speed, feed rate, average resultant peak force in XY plane and absolute average force in the Z direction were successfully employed to develop the INN-SRP subsystem, which performed the in-process surface roughness prediction function with multiple cutting tools in end-milling operations. The neural networks algorithm was successfully employed to work as an in-process decision-making technique in the INN-SRP subsystem to prediction the surface roughness. From the result of testing

samples, the INN-SRP subsystem enabled the prediction accuracy of the surface roughness in 93%. Therefore, this system, which accurately predicted the surface roughness within a wide range of machining parameters, has practical application in industry.

- The spindle speed, feed rate, average resultant peak force and absolute average force in the prediction system, and the difference between predicted surface roughness and desired surface roughness was successfully employed to develop the NN-AMPC subsystem, which adjusted the degree of the original feed rate, and then generated a new surface roughness satisfying the desired one. The neural networks algorithm was successfully applied to work as an in-process decision-making technique in the NN-AMPC subsystem to adjust the feed rate.
- The INN-SRP subsystem and the NN-AMPC subsystem were successfully integrated to become the NN-IASRC system. The NN-IASRC system provided the CNC machines to automatically execute the quality control of surface roughness without human operators in end-milling operations. Based on the testing result, the NN-IASRC system was considered a successful system since after the adaptive control function was executed; all of the new surface roughness values were smaller than the desired ones.

A successful development of the NN-IASRC system, which performed the real time in-process surface roughness control in end-milling operations with multiple cutting tools, was concluded. This system, which can accurately predict the surface roughness and properly adjust the feed rate within a wide range of machining parameters, can be practical application in industry.

Recommendations for Further Research

In this research, the NN-IASRC system was successfully developed and applied in end-milling operations with multiple cutting tools. Basing on the analysis of the results of the research experiment, the following recommendations are made for the further research.

- The NN-IASRC system can adjust the adaptive degree of original feed rate only when the predicted surface roughness is larger than the desired surface roughness. This is a unidirectional adaptive control function. From Table 5.5 results from the testing for the NN-IASRC system, all of the samples were successfully adapted to make the new surface roughness become smaller than the desired one. However, some of them were too small. Since the surface roughness had a high positive correlation to the feed rate, the smaller the surface roughness is, the lower speed of the feed rate. Under the circumstances, the lower speed of feed rate reduced the productivity. Therefore, a bi-directional adaptive control function should be developed. Eventually, the goal of the NN-IASRC system is to make the $\Delta R_a = 0$ instead of $\Delta R_a \leq 0$.
- The NN-IASRC system adjusted the adaptive degree of the original feed rate to achieve the desired surface roughness. Nevertheless, from the statistical analysis, the spindle speed was also a significant factor in influencing the surface roughness. In the further research, the output of the adaptive machining parameter control system may consider two output factors, the feed rate and spindle speed, to adjust at the same time. The increased rate of the spindle feed could reduce the decrease rate of the feed rate, which could increase the productivity of the system.

- In this research, only one type of workpiece, 6061 aluminum, and one type of cutting tool, high-speed steel milling cutting tool with 0.5" diameter, were used to execute the experiment. The hardness of the material can be considered as an input factor for two or more different types of workpieces. Different types of cutting tools, such as a carbide cutting tool, could be selected to perform the experiment in further research to confirm the efficiency of the NN-IASRC system.
- The software of the NN-IASRC system has been successfully developed in this research. However, the software still has difficulty connecting to the CNC machine to perform the real feed rate adaptive function. The goal of this research is to develop a hardware chip to install in the CNC machine to control the servo drive amplifier for driving the axis control motors. Furthermore, when the chip has been developed and installed in the CNC machine, the responding time of both predicted surface roughness and adaptive degree of feed rate should be faster than the current situation, 1.02 sec, to achieve the objective of a real-time surface roughness control system.
- The dynamometer and proximity sensors, which were used to monitor the cutting force signals and spindle revolutions within the cutting process in this research, were inconvenient for industrial installation because of the wire connection. To search for sensors with a wireless function would be another direction to study to fully develop the NN-IASRC system. Furthermore, multiple sensors could be employed together to monitor different types of signals. The signals could compensate each other to fully monitor the uncontrollable cutting tool condition and increase the accuracy of the NN-IASRC system.

- A neural networks algorithm has been successfully applied as a decision-making technique to develop the NN-IASRC system. To increase the accuracy of the NN-IASRC system, different decision-making techniques, such as fuzzy neural modeling and a generic algorithm, could also be tried to construct the IASRC system, which could be compared with the present system to determine which system is the best.

These recommendations will be continuously studied in the future to make the in-process adaptive surface roughness control system more robust for eventual implementation. Hopefully, the smart CNC control system, which can integrate the surface roughness control, tool breakage monitoring, and tool wear detection, can be well developed and employed in the real industry.

APPENDIX A - NC PROGRAM FOR DATA COLLECTION

```
%
N5 O9993                                /* Program number */
N10 G90 G80 G40 G17                     /* Safety feature */
N20 T16 M6                              /* Change tool to tool #16 */
N30 E7 G0 X-.3 Y.35 Z0.3                /* Set program zero & move to (-.3,.35,.3) */
N40 S2000 M3                            /* Control the spindle speed */
N50 G1 Z-0.005 F15. M49                 /* Control the feed rate and depth of cut */
N60 G1 X1.5
N70 G0 Z0.2
N80 G0 X-.3
N90 G1 Z-0.045                          /* Control the depth of cut */
N100 G1 X1.7
N110 G0 Z0.2
N120 G91 G28 X0.0 Y0.0 Z1.0 M5
N130 M30                                /* End of program */
%
```

APPENDIX B - A/D CONVERTING PROGRAM

```
#include "stdio.h"
#include "conio.h"
#include "dos.h"
#include "cb.h"
#include "time.h"
#define number 2300
typedef unsigned int WORD;                          / * 16-bit unsigned int */
clock_t begin,end;

void ClearScreen (void);                            /* Prototypes */
void GetTextCursor (int *x, int *y);
void MoveCursor (int x, int y);

void main ()
  {
  FILE *fptr;
  char *filename;

  int Row,Col,Row2,Col2;

  int BoardNum = 0;
  int UDStat = 0;

  int Chan0=0,Chan1=1,Chan2=2,Chan3=3,int I=0;

  int Gain0 = BIP10VOLTS;                           /*Proximity data channel*/
  int Gain1 = BIP10VOLTS;                           /*X channel*/
  int Gain2 = BIP10VOLTS;                           /*Y channel*/
  int Gain3 = BIP10VOLTS;                           /*Z channel*/

  float data[2300][4], EngUnits,RevLevel = (float)CURRENTREVNUM;
  WORD DataValue0 = 0;
  WORD DataValue1 = 0;
  WORD DataValue2 = 0;
  WORD DataValue3 = 0;

  UDStat = cbDeclareRevision(&RevLevel);            /* Declare UL Revision Level */

  /* Initiate error handling
    Parameters:
        PRINTALL :all warnings and errors encountered will be printed
        STOPALL  :if any error is encountered, the program will stop */

  cbErrHandling (PRINTALL, STOPALL);

  /* set up the screen */
  ClearScreen();
  printf ("Demonstration of cbAIn()\n");
  printf("Press any key to start A/D converting.\n");
  getchar();
  begin=clock();                    /* clock starts      */
```

```
/* collect the sample from the channel until a key is pressed */
for (I=0;I<number;I++)
        {
        UDStat =cbAIn (BoardNum, Chan0, Gain0, &DataValue0);
        UDStat =cbToEngUnits (BoardNum, Gain0, DataValue0, &EngUnits);
        data[I][0]=EngUnits;

        UDStat =cbAIn (BoardNum, Chan1, Gain1, &DataValue1);
         UDStat =cbToEngUnits (BoardNum, Gain1, DataValue1, &EngUnits);
        data[I][1]=EngUnits;

         UDStat =cbAIn (BoardNum, Chan2, Gain2, &DataValue2);
        UDStat =cbToEngUnits (BoardNum, Gain2, DataValue2, &EngUnits);
        data[I][2]=EngUnits;

        UDStat =cbAIn (BoardNum, Chan3, Gain3, &DataValue3);
        UDStat =cbToEngUnits (BoardNum, Gain3, DataValue3, &EngUnits);
        data[I][3]=EngUnits;
        }

end=clock();
printf(" A/D Convert is finished and the converted time is %7.4f\n seconds",(end-begin)/CLK_TCK);

 for (I=0; I<number; I++)
 {
  data[I][1]=(data[I][1]+data[I+1][1])/2;
  data[I][2]=(data[I][2]+data[I+1][2])/2;
  data[I][3]=(data[I][3]+data[I+1][3])/2;
 }

 printf(" \n Please keyin filename:");
        scanf("%s",filename);

        if((fptr=fopen(filename,"w"))==NULL)
        {
                printf(" Can't open file.\n");
                exit(1);
        }

 for(I=0; I<number;I++)
 {
        fprintf(fptr,"%d %7.4f %7.4f %7.4f %7.4f\n",I,data[I][0],data[I][1],
        data[I][2],data[I][3]);
 }
 fclose(fptr);

 exit(0);
 return;
}
```

```
/*****************************************************************************
* Name:     ClearScreen
* Arguments: ---
* Returns:  ---
* Clears the screen.
*****************************************************************************/
#define BIOS_VIDEO  0x10
void
ClearScreen (void)
{
   union REGS InRegs,OutRegs;
   InRegs.h.ah = 0;
   InRegs.h.al = 2;
   int86 (BIOS_VIDEO, &InRegs, &OutRegs);

   return;
}

/*****************************************************************************
* Name:     MoveCursor
* Arguments: x,y - screen coordinates of new cursor position
* Returns:  ---
* Positions the cursor on screen.
*****************************************************************************/
void
MoveCursor (int x, int y)
{
   union REGS InRegs,OutRegs;
   InRegs.h.ah = 2;
   InRegs.h.dl = (char) x;
   InRegs.h.dh = (char) y;
   InRegs.h.bh = 0;
   int86 (BIOS_VIDEO, &InRegs, &OutRegs);

   return;
}

/*****************************************************************************
* Name:     GetTextCursor
* Arguments: x,y - screen coordinates of new cursor position
* Returns:  *x and *y
* Returns the current (text) cursor position.
*****************************************************************************/
void
GetTextCursor (int *x, int *y)
{
   union REGS InRegs,OutRegs;
   InRegs.h.ah = 3;
   InRegs.h.bh = 0;
   int86 (BIOS_VIDEO, &InRegs, &OutRegs);
   *x = OutRegs.h.dl;
   *y = OutRegs.h.dh;
   return;
}
```

APPENDIX C - CUTTING FORCE ANALYTICAL PROGRAM

```
/* ----------------------------*/
/* Data Analysis Program */
/* ---------------------------- */

#include "stdio.h"
#include "stdlib.h"
#include "dos.h"
#include "time.h"
#include "math.h"
# define MAX(i,j) (i>j)?i:j
#define ABS(i)(i<0)?-i:i
#define number 2000   /* transform 2000 data for A/D conv. */

int main(void)
 {
 FILE *fptr;
 char *filename;
 float data[number][4],combxy[number],Max[80];
 int point[4];
 int i,j,k,pmax,per_tooth,range,length,peak1;
 float h_peak,avg1,avg_xy,avg_z,sumf_xy,sumf_z,g,t;

 /* input the file name */
 printf(" \nPlease key in the filename: ");
 scanf("%s",filename);


 if ((fptr=fopen(filename,"r"))==NULL)
  {
  printf("\n Can't open the file.\n");
  exit(1);
  }

 for(i=0; i<number; ++i)
   fscanf(fptr, "%d %f %f %f %f\n", &i, &data[i][0], &data[i][1],
                    &data[i][2], &data[i][3]);
   fclose(fptr);

 for(i=0; i<number; i++)
 {
  combxy[i]=sqrt( pow(data[i][1],2) + pow(data[i][2],2));
  data[i][3]=ABS(data[i][3]);
 }

 for(h_peak=combxy[50], i=50; i<number; ++i)       /* find the max. value of voltage */
    if (h_peak<combxy[i])
    {
          h_peak=combxy[i];
          pmax=i;
    }
```

```
j=0;
for(i=50; i<number; i++)                    /* find the value of range and per tooth */
  if (data[i-1][0]<1 && data[i][0]>1)
  {
   point[j] = i;
   j++;
  }

range=point[2]-point[0];
per_tooth=(point[2]-point[0])/4;

printf("Range = %d from point %d to point %d\n",range,point[0],point[2]);
printf("The total points per tooth are %d\n",per_tooth);
printf("The max voltage is %7.4f\n",combxy[pmax]);
printf("The point of max. voltage is %d\n",pmax);

length=pmax-per_tooth;                      /* find the first peak value */
while (length>50)
{
  pmax=pmax-per_tooth;
  length=pmax-per_tooth;
}
peak1=pmax;

/* find all peak of the data */
i=peak1;
k=0;

while (k<81)
{
 g=0;
   for (i=peak1; i<peak1+5; i++)
   g=MAX(combxy[i-2],g);
 Max[k]=g;
 peak1=peak1+per_tooth;
 k=k+1;
}

t=0;                                        /* find the max. peak force for 17 rev. */
for (i=0; i<67; i++)
   t=MAX(Max[i],t);
printf("The Max. peak force of 17 rev.= %7.4f\n",t*50);

avg1=0;                                     /* Calculate the average peak force for 17 rev. */
for (i=0; i<67; i++)
   avg1=Max[i]+avg1;
avg1=avg1/68;

printf("Average peak force for 17 rev. = %7.4f\n", avg1*50);

sumf_xy=0;                                  /* Calculate the average force for 17 rev. */
sumf_z=0;
```

```
 for (i=point[0]; i<point[0]+range*17; i++)
 {
  sumf_xy=combxy[i]+sumf_xy;
  sumf_z=data[i][3]+sumf_z;
 }
 avg_xy=sumf_xy/(range*17);
 avg_z=sumf_z/(range*17);
 printf("average force in XY for 17 Rev.= %7.4f\n", avg_xy*50);
 printf("average force in Z for 17 Rev.= %7.4f\n", avg_z*50);


 exit(0);
 return 0;
}
```

APPENDIX D - EXPERIMENTAL DATA FOR INN-SRP SYSTEM

	Raw Data Set						Scaled Data Set				
#	Speed	Feed	Depth	F_{ap}	F_{az}	R_a	S'	f'	F'_{ap}	F'_{az}	R'_a
1	1750	6	0.04	39.060	3.715	30	0.000	0.000	0.087	0.028	0.082
2	1750	6	0.04	52.050	4.842	42	0.000	0.000	0.222	0.135	0.191
3	1750	6	0.04	42.302	4.445	37	0.000	0.000	0.121	0.097	0.145
4	1750	6	0.04	54.297	4.759	43	0.000	0.000	0.246	0.127	0.200
5	1750	6	0.06	50.947	5.986	31	0.000	0.000	0.211	0.243	0.091
6	1750	6	0.06	61.463	6.064	33	0.000	0.000	0.320	0.251	0.109
7	1750	6	0.06	68.710	6.531	44	0.000	0.000	0.396	0.295	0.209
8	1750	6	0.06	68.962	6.629	47	0.000	0.000	0.398	0.304	0.236
9	1750	6	0.08	73.190	9.013	30	0.000	0.000	0.443	0.530	0.082
10	1750	6	0.08	82.250	9.094	40	0.000	0.000	0.537	0.538	0.173
11	1750	6	0.08	86.238	9.180	51	0.000	0.000	0.578	0.546	0.273
12	1750	6	0.08	67.547	8.062	30	0.000	0.000	0.384	0.440	0.082
13	1750	8	0.04	44.849	4.000	31	0.000	0.143	0.147	0.055	0.091
14	1750	8	0.04	52.965	4.170	33	0.000	0.143	0.232	0.071	0.109
15	1750	8	0.04	61.280	5.169	39	0.000	0.143	0.318	0.166	0.164
16	1750	8	0.04	62.421	7.694	57	0.000	0.143	0.330	0.405	0.327
17	1750	8	0.06	55.167	7.143	51	0.000	0.143	0.255	0.353	0.273
18	1750	8	0.06	62.793	5.385	39	0.000	0.143	0.334	0.186	0.164
19	1750	8	0.06	78.875	7.769	61	0.000	0.143	0.502	0.412	0.364
20	1750	8	0.06	73.218	9.422	33	0.000	0.143	0.443	0.569	0.109
21	1750	8	0.08	83.801	9.453	35	0.000	0.143	0.553	0.572	0.127
22	1750	8	0.08	100.96	9.486	37	0.000	0.143	0.732	0.575	0.145
23	1750	8	0.08	79.120	8.499	64	0.000	0.143	0.504	0.481	0.391
24	1750	8	0.08	102.31	9.795	38	0.000	0.143	0.746	0.604	0.155
25	1750	10	0.04	44.491	5.042	58	0.000	0.286	0.144	0.154	0.336
26	1750	10	0.04	58.419	5.418	63	0.000	0.286	0.289	0.190	0.382
27	1750	10	0.04	52.437	5.241	59	0.000	0.286	0.226	0.173	0.345
28	1750	10	0.04	58.020	5.266	61	0.000	0.286	0.285	0.175	0.364
29	1750	10	0.06	59.117	7.015	37	0.000	0.286	0.296	0.341	0.145
30	1750	10	0.06	67.395	7.043	42	0.000	0.286	0.382	0.343	0.191
31	1750	10	0.06	90.708	7.943	56	0.000	0.286	0.625	0.429	0.318
32	1750	10	0.06	91.350	8.257	67	0.000	0.286	0.632	0.458	0.418
33	1750	10	0.08	76.743	9.639	39	0.000	0.286	0.480	0.589	0.164
34	1750	10	0.08	88.551	9.692	41	0.000	0.286	0.602	0.594	0.182
35	1750	10	0.08	111.83	9.944	46	0.000	0.286	0.845	0.618	0.227
36	1750	10	0.08	113.40	10.512	57	0.000	0.286	0.861	0.672	0.327
37	1750	12	0.04	47.218	5.609	64	0.000	0.429	0.172	0.208	0.391
38	1750	12	0.04	56.776	5.582	64	0.000	0.429	0.272	0.205	0.391
39	1750	12	0.04	65.390	5.972	72	0.000	0.429	0.361	0.242	0.464
40	1750	12	0.04	69.685	6.307	73	0.000	0.429	0.406	0.274	0.473
41	1750	12	0.06	75.247	8.505	66	0.000	0.429	0.464	0.482	0.409
42	1750	12	0.06	75.772	8.596	74	0.000	0.429	0.469	0.491	0.482
43	1750	12	0.06	83.101	9.072	60	0.000	0.429	0.546	0.536	0.355
44	1750	12	0.06	75.940	8.966	64	0.000	0.429	0.471	0.526	0.391
45	1750	12	0.08	80.418	10.589	51	0.000	0.429	0.518	0.679	0.273
46	1750	12	0.08	97.224	10.685	52	0.000	0.429	0.693	0.688	0.282
47	1750	12	0.08	116.52	10.788	66	0.000	0.429	0.894	0.698	0.409

48	1750	12	0.08	119.01	11.091	74	0.000	0.429	0.920	0.727	0.482
49	1750	14	0.04	49.132	5.499	64	0.000	0.571	0.192	0.197	0.391
50	1750	14	0.04	69.549	6.603	77	0.000	0.571	0.405	0.302	0.509
51	1750	14	0.04	70.310	7.001	84	0.000	0.571	0.413	0.340	0.573
52	1750	14	0.04	58.165	5.750	74	0.000	0.571	0.286	0.221	0.482
53	1750	14	0.06	66.779	8.927	80	0.000	0.571	0.376	0.522	0.536
54	1750	14	0.06	78.885	9.164	86	0.000	0.571	0.502	0.544	0.591
55	1750	14	0.06	96.280	9.943	90	0.000	0.571	0.683	0.618	0.627
56	1750	14	0.06	95.094	9.006	99	0.000	0.571	0.671	0.529	0.709
57	1750	14	0.08	98.592	11.246	82	0.000	0.571	0.707	0.741	0.555
58	1750	14	0.08	104.29	11.552	99	0.000	0.571	0.766	0.770	0.709
59	1750	14	0.08	82.638	10.961	70	0.000	0.571	0.541	0.715	0.445
60	1750	14	0.08	102.42	11.525	88	0.000	0.571	0.747	0.768	0.609
61	1750	16	0.04	50.015	5.270	61	0.000	0.714	0.201	0.176	0.364
62	1750	16	0.04	60.089	5.739	68	0.000	0.714	0.306	0.220	0.427
63	1750	16	0.04	70.391	5.892	69	0.000	0.714	0.413	0.234	0.436
64	1750	16	0.04	71.820	5.949	79	0.000	0.714	0.428	0.240	0.527
65	1750	16	0.06	81.745	8.738	80	0.000	0.714	0.532	0.504	0.536
66	1750	16	0.06	96.510	8.819	85	0.000	0.714	0.685	0.512	0.582
67	1750	16	0.06	96.554	9.007	89	0.000	0.714	0.686	0.529	0.618
68	1750	16	0.06	68.916	8.331	72	0.000	0.714	0.398	0.465	0.464
69	1750	16	0.08	93.983	11.815	104	0.000	0.714	0.659	0.795	0.755
70	1750	16	0.08	96.750	11.891	110	0.000	0.714	0.688	0.803	0.809
71	1750	16	0.08	100.54	12.253	114	0.000	0.714	0.727	0.837	0.845
72	1750	16	0.08	118.60	12.469	122	0.000	0.714	0.915	0.857	0.918
73	1750	18	0.04	65.363	5.402	75	0.000	0.857	0.361	0.188	0.491
74	1750	18	0.04	69.941	6.222	83	0.000	0.857	0.409	0.266	0.564
75	1750	18	0.04	73.090	6.264	93	0.000	0.857	0.441	0.270	0.655
76	1750	18	0.04	53.280	5.108	72	0.000	0.857	0.235	0.160	0.464
77	1750	18	0.06	85.370	9.657	112	0.000	0.857	0.569	0.591	0.827
78	1750	18	0.06	93.810	9.803	116	0.000	0.857	0.657	0.605	0.864
79	1750	18	0.06	95.613	10.067	122	0.000	0.857	0.676	0.630	0.918
80	1750	18	0.06	72.527	9.556	107	0.000	0.857	0.436	0.581	0.782
81	1750	18	0.08	110.50	11.729	92	0.000	0.857	0.831	0.787	0.645
82	1750	18	0.08	112.15	12.757	119	0.000	0.857	0.848	0.884	0.891
83	1750	18	0.08	90.180	11.371	88	0.000	0.857	0.619	0.753	0.609
84	1750	18	0.08	111.06	12.611	93	0.000	0.857	0.837	0.871	0.655
85	1750	20	0.04	52.592	5.351	91	0.000	1.000	0.228	0.183	0.636
86	1750	20	0.04	76.368	5.883	100	0.000	1.000	0.476	0.234	0.718
87	1750	20	0.04	79.060	6.395	118	0.000	1.000	0.504	0.282	0.882
88	1750	20	0.04	63.747	5.824	102	0.000	1.000	0.344	0.228	0.736
89	1750	20	0.06	72.850	9.311	98	0.000	1.000	0.439	0.558	0.700
90	1750	20	0.06	94.337	9.329	101	0.000	1.000	0.663	0.560	0.727
91	1750	20	0.06	104.14	9.407	103	0.000	1.000	0.765	0.567	0.745
92	1750	20	0.06	106.82	10.000	117	0.000	1.000	0.793	0.623	0.873
93	1750	20	0.08	90.229	12.638	93	0.000	1.000	0.620	0.873	0.655
94	1750	20	0.08	111.27	12.703	110	0.000	1.000	0.839	0.879	0.809
95	1750	20	0.08	123.54	13.463	111	0.000	1.000	0.967	0.951	0.818
96	1750	20	0.08	126.72	13.976	131	0.000	1.000	1.000	1.000	1.000
97	2000	6	0.04	35.239	3.416	47	0.333	0.000	0.047	0.000	0.236
98	2000	6	0.04	39.669	4.808	31	0.333	0.000	0.093	0.132	0.091
99	2000	6	0.04	48.990	3.730	44	0.333	0.000	0.190	0.030	0.209
100	2000	6	0.04	42.190	3.689	41	0.333	0.000	0.120	0.026	0.182
101	2000	6	0.06	51.712	5.844	35	0.333	0.000	0.219	0.230	0.127

102	2000	6	0.06	56.178	6.375	35	0.333	0.000	0.265	0.280	0.127
103	2000	6	0.06	66.479	6.666	38	0.333	0.000	0.373	0.308	0.155
104	2000	6	0.06	69.120	7.087	48	0.333	0.000	0.400	0.348	0.245
105	2000	6	0.08	63.144	8.110	42	0.333	0.000	0.338	0.445	0.191
106	2000	6	0.08	73.106	8.701	43	0.333	0.000	0.442	0.500	0.200
107	2000	6	0.08	80.570	7.986	36	0.333	0.000	0.519	0.433	0.136
108	2000	6	0.08	83.030	8.804	46	0.333	0.000	0.545	0.510	0.227
109	2000	8	0.04	41.384	4.545	32	0.333	0.143	0.111	0.107	0.100
110	2000	8	0.04	51.489	5.181	35	0.333	0.143	0.216	0.167	0.127
111	2000	8	0.04	46.262	4.835	34	0.333	0.143	0.162	0.134	0.118
112	2000	8	0.04	52.860	5.784	38	0.333	0.143	0.231	0.224	0.155
113	2000	8	0.06	55.149	6.931	35	0.333	0.143	0.255	0.333	0.127
114	2000	8	0.06	59.705	7.390	35	0.333	0.143	0.302	0.376	0.127
115	2000	8	0.06	73.897	7.506	37	0.333	0.143	0.450	0.387	0.145
116	2000	8	0.06	86.880	7.912	38	0.333	0.143	0.585	0.426	0.155
117	2000	8	0.08	69.640	8.581	29	0.333	0.143	0.406	0.489	0.073
118	2000	8	0.08	87.019	9.049	36	0.333	0.143	0.587	0.533	0.136
119	2000	8	0.08	92.596	8.958	36	0.333	0.143	0.645	0.525	0.136
120	2000	8	0.08	90.630	8.867	36	0.333	0.143	0.624	0.516	0.136
121	2000	10	0.04	42.815	4.554	49	0.333	0.286	0.126	0.108	0.255
122	2000	10	0.04	49.153	5.103	51	0.333	0.286	0.192	0.160	0.273
123	2000	10	0.04	53.303	5.579	54	0.333	0.286	0.235	0.205	0.300
124	2000	10	0.04	57.330	6.655	59	0.333	0.286	0.277	0.307	0.345
125	2000	10	0.06	67.658	7.855	38	0.333	0.286	0.385	0.420	0.155
126	2000	10	0.06	80.030	8.300	50	0.333	0.286	0.514	0.462	0.264
127	2000	10	0.06	81.362	8.251	50	0.333	0.286	0.528	0.458	0.264
128	2000	10	0.06	59.017	7.286	38	0.333	0.286	0.295	0.366	0.155
129	2000	10	0.08	71.119	9.455	36	0.333	0.286	0.421	0.572	0.136
130	2000	10	0.08	82.335	9.640	38	0.333	0.286	0.538	0.589	0.155
131	2000	10	0.08	94.517	10.461	45	0.333	0.286	0.665	0.667	0.218
132	2000	10	0.08	97.930	10.673	54	0.333	0.286	0.700	0.687	0.300
133	2000	12	0.04	50.724	5.766	73	0.333	0.429	0.209	0.223	0.473
134	2000	12	0.04	64.599	6.792	54	0.333	0.429	0.353	0.320	0.300
135	2000	12	0.04	46.145	5.508	72	0.333	0.429	0.161	0.198	0.464
136	2000	12	0.04	64.513	6.581	58	0.333	0.429	0.352	0.300	0.336
137	2000	12	0.06	61.011	7.667	54	0.333	0.429	0.316	0.403	0.300
138	2000	12	0.06	70.990	7.832	56	0.333	0.429	0.420	0.418	0.318
139	2000	12	0.06	80.550	7.947	59	0.333	0.429	0.519	0.429	0.345
140	2000	12	0.06	85.494	8.663	64	0.333	0.429	0.571	0.497	0.391
141	2000	12	0.08	74.099	11.294	74	0.333	0.429	0.452	0.746	0.482
142	2000	12	0.08	87.826	11.383	77	0.333	0.429	0.595	0.754	0.509
143	2000	12	0.08	105.09	11.583	81	0.333	0.429	0.775	0.773	0.545
144	2000	12	0.08	103.40	11.488	78	0.333	0.429	0.757	0.764	0.518
145	2000	14	0.04	53.569	5.844	54	0.333	0.571	0.238	0.230	0.300
146	2000	14	0.04	62.680	5.259	58	0.333	0.571	0.332	0.175	0.336
147	2000	14	0.04	63.576	6.457	65	0.333	0.571	0.342	0.288	0.400
148	2000	14	0.04	66.758	7.785	54	0.333	0.571	0.376	0.414	0.300
149	2000	14	0.06	74.068	8.422	71	0.333	0.571	0.452	0.474	0.455
150	2000	14	0.06	74.812	8.627	76	0.333	0.571	0.459	0.493	0.500
151	2000	14	0.06	77.480	9.878	77	0.333	0.571	0.487	0.612	0.509
152	2000	14	0.06	85.886	9.927	90	0.333	0.571	0.575	0.617	0.627
153	2000	14	0.08	91.994	11.238	68	0.333	0.571	0.638	0.741	0.427
154	2000	14	0.08	106.07	11.655	86	0.333	0.571	0.785	0.780	0.591
155	2000	14	0.08	106.89	12.150	93	0.333	0.571	0.793	0.827	0.655

156	2000	14	0.08	79.861	10.693	78	0.333	0.571	0.512	0.689	0.518
157	2000	16	0.04	51.018	5.725	76	0.333	0.714	0.212	0.219	0.500
158	2000	16	0.04	54.772	5.836	87	0.333	0.714	0.251	0.229	0.600
159	2000	16	0.04	65.462	6.109	90	0.333	0.714	0.362	0.255	0.627
160	2000	16	0.04	68.500	6.177	97	0.333	0.714	0.394	0.261	0.691
161	2000	16	0.06	66.895	7.804	67	0.333	0.714	0.377	0.415	0.418
162	2000	16	0.06	96.970	8.679	73	0.333	0.714	0.690	0.498	0.473
163	2000	16	0.06	97.458	9.306	91	0.333	0.714	0.695	0.558	0.636
164	2000	16	0.06	76.181	8.245	71	0.333	0.714	0.474	0.457	0.455
165	2000	16	0.08	82.548	10.269	76	0.333	0.714	0.540	0.649	0.500
166	2000	16	0.08	110.79	11.511	81	0.333	0.714	0.834	0.767	0.545
167	2000	16	0.08	110.91	11.729	88	0.333	0.714	0.835	0.787	0.609
168	2000	16	0.08	96.607	11.305	77	0.333	0.714	0.686	0.747	0.509
169	2000	18	0.04	52.218	5.598	62	0.333	0.857	0.224	0.207	0.373
170	2000	18	0.04	58.617	5.951	66	0.333	0.857	0.291	0.240	0.409
171	2000	18	0.04	66.020	6.039	84	0.333	0.857	0.368	0.248	0.573
172	2000	18	0.04	66.500	6.482	89	0.333	0.857	0.373	0.290	0.618
173	2000	18	0.06	73.731	9.201	77	0.333	0.857	0.448	0.548	0.509
174	2000	18	0.06	81.744	10.010	82	0.333	0.857	0.532	0.624	0.555
175	2000	18	0.06	82.120	10.033	93	0.333	0.857	0.536	0.627	0.655
176	2000	18	0.06	90.528	10.223	91	0.333	0.857	0.623	0.645	0.636
177	2000	18	0.08	85.343	11.118	75	0.333	0.857	0.569	0.729	0.491
178	2000	18	0.08	100.92	11.182	84	0.333	0.857	0.731	0.735	0.573
179	2000	18	0.08	104.15	11.337	86	0.333	0.857	0.765	0.750	0.591
180	2000	18	0.08	108.39	11.398	87	0.333	0.857	0.809	0.756	0.600
181	2000	20	0.04	51.605	5.877	62	0.333	1.000	0.218	0.233	0.373
182	2000	20	0.04	62.319	6.126	71	0.333	1.000	0.329	0.257	0.455
183	2000	20	0.04	70.057	6.148	86	0.333	1.000	0.410	0.259	0.591
184	2000	20	0.04	70.890	6.597	89	0.333	1.000	0.419	0.301	0.618
185	2000	20	0.06	68.735	8.572	71	0.333	1.000	0.396	0.488	0.455
186	2000	20	0.06	78.524	9.179	71	0.333	1.000	0.498	0.546	0.455
187	2000	20	0.06	91.110	9.917	90	0.333	1.000	0.629	0.616	0.627
188	2000	20	0.06	91.234	10.068	90	0.333	1.000	0.630	0.630	0.627
189	2000	20	0.08	86.967	11.850	84	0.333	1.000	0.586	0.799	0.573
190	2000	20	0.08	112.89	12.374	113	0.333	1.000	0.856	0.848	0.836
191	2000	20	0.08	99.498	12.011	93	0.333	1.000	0.716	0.814	0.655
192	2000	20	0.08	107.75	12.279	93	0.333	1.000	0.802	0.839	0.655
193	2250	6	0.04	34.382	3.945	23	0.667	0.000	0.038	0.050	0.018
194	2250	6	0.04	47.640	4.286	28	0.667	0.000	0.176	0.082	0.064
195	2250	6	0.04	48.244	4.350	30	0.667	0.000	0.183	0.088	0.082
196	2250	6	0.04	41.449	4.063	25	0.667	0.000	0.112	0.061	0.036
197	2250	6	0.06	59.891	6.242	35	0.667	0.000	0.304	0.268	0.127
198	2250	6	0.06	64.750	6.571	41	0.667	0.000	0.355	0.299	0.182
199	2250	6	0.06	49.955	5.897	30	0.667	0.000	0.201	0.235	0.082
200	2250	6	0.06	64.846	7.103	48	0.667	0.000	0.356	0.349	0.245
201	2250	6	0.08	72.959	8.256	40	0.667	0.000	0.440	0.458	0.173
202	2250	6	0.08	78.415	8.268	48	0.667	0.000	0.497	0.459	0.245
203	2250	6	0.08	70.339	7.398	37	0.667	0.000	0.413	0.377	0.145
204	2250	6	0.08	73.930	7.795	40	0.667	0.000	0.450	0.415	0.173
205	2250	8	0.04	43.048	4.811	35	0.667	0.143	0.129	0.132	0.127
206	2250	8	0.04	51.440	5.252	42	0.667	0.143	0.216	0.174	0.191
207	2250	8	0.04	52.279	5.278	47	0.667	0.143	0.225	0.176	0.236
208	2250	8	0.04	39.431	4.633	34	0.667	0.143	0.091	0.115	0.118
209	2250	8	0.06	58.950	6.791	35	0.667	0.143	0.294	0.320	0.127

210	2250	8	0.06	61.982	6.907	52	0.667	0.143	0.326	0.331	0.282
211	2250	8	0.06	56.462	6.613	30	0.667	0.143	0.268	0.303	0.082
212	2250	8	0.06	61.982	6.801	52	0.667	0.143	0.326	0.321	0.282
213	2250	8	0.08	66.773	9.339	45	0.667	0.143	0.376	0.561	0.218
214	2250	8	0.08	74.837	9.418	48	0.667	0.143	0.460	0.568	0.245
215	2250	8	0.08	82.779	8.912	33	0.667	0.143	0.542	0.520	0.109
216	2250	8	0.08	87.400	9.025	41	0.667	0.143	0.590	0.531	0.182
217	2250	10	0.04	41.061	4.936	31	0.667	0.286	0.108	0.144	0.091
218	2250	10	0.04	49.197	5.081	32	0.667	0.286	0.193	0.158	0.100
219	2250	10	0.04	50.395	5.150	35	0.667	0.286	0.205	0.164	0.127
220	2250	10	0.04	54.710	5.425	45	0.667	0.286	0.250	0.190	0.218
221	2250	10	0.06	66.539	7.650	51	0.667	0.286	0.373	0.401	0.273
222	2250	10	0.06	68.381	8.102	59	0.667	0.286	0.392	0.444	0.345
223	2250	10	0.06	74.250	8.148	62	0.667	0.286	0.454	0.448	0.373
224	2250	10	0.06	57.331	7.638	47	0.667	0.286	0.277	0.400	0.236
225	2250	10	0.08	69.434	9.379	42	0.667	0.286	0.403	0.565	0.191
226	2250	10	0.08	81.610	9.644	34	0.667	0.286	0.530	0.590	0.118
227	2250	10	0.08	86.830	9.868	37	0.667	0.286	0.585	0.611	0.145
228	2250	10	0.08	87.318	9.772	35	0.667	0.286	0.590	0.602	0.127
229	2250	12	0.04	58.233	5.805	56	0.667	0.429	0.287	0.226	0.318
230	2250	12	0.04	60.870	5.961	62	0.667	0.429	0.314	0.241	0.373
231	2250	12	0.04	43.957	5.290	51	0.667	0.429	0.138	0.177	0.273
232	2250	12	0.04	55.128	5.763	54	0.667	0.429	0.254	0.222	0.300
233	2250	12	0.06	59.259	7.708	49	0.667	0.429	0.297	0.406	0.255
234	2250	12	0.06	77.168	9.070	59	0.667	0.429	0.484	0.535	0.345
235	2250	12	0.06	71.057	8.103	52	0.667	0.429	0.420	0.444	0.282
236	2250	12	0.06	77.170	9.092	64	0.667	0.429	0.484	0.537	0.391
237	2250	12	0.08	93.880	10.497	56	0.667	0.429	0.658	0.671	0.318
238	2250	12	0.08	96.108	11.041	59	0.667	0.429	0.681	0.722	0.345
239	2250	12	0.08	72.385	9.948	50	0.667	0.429	0.434	0.619	0.264
240	2250	12	0.08	86.370	10.362	54	0.667	0.429	0.580	0.658	0.300
241	2250	14	0.04	52.872	5.848	51	0.667	0.571	0.231	0.230	0.273
242	2250	14	0.04	55.447	6.016	59	0.667	0.571	0.258	0.246	0.345
243	2250	14	0.04	60.400	6.726	64	0.667	0.571	0.309	0.313	0.391
244	2250	14	0.04	44.164	5.759	47	0.667	0.571	0.140	0.222	0.236
245	2250	14	0.06	64.645	8.820	76	0.667	0.571	0.354	0.512	0.500
246	2250	14	0.06	77.687	9.441	82	0.667	0.571	0.489	0.571	0.555
247	2250	14	0.06	80.720	9.523	77	0.667	0.571	0.521	0.578	0.509
248	2250	14	0.06	83.020	9.737	81	0.667	0.571	0.545	0.599	0.545
249	2250	14	0.08	77.530	10.105	61	0.667	0.571	0.488	0.633	0.364
250	2250	14	0.08	93.029	10.248	61	0.667	0.571	0.649	0.647	0.364
251	2250	14	0.08	95.504	11.598	74	0.667	0.571	0.675	0.775	0.482
252	2250	14	0.08	103.38	12.824	89	0.667	0.571	0.757	0.891	0.618
253	2250	16	0.04	53.255	6.125	74	0.667	0.714	0.235	0.257	0.482
254	2250	16	0.04	58.140	6.201	78	0.667	0.714	0.286	0.264	0.518
255	2250	16	0.04	63.895	6.786	82	0.667	0.714	0.346	0.319	0.555
256	2250	16	0.04	53.054	6.114	60	0.667	0.714	0.233	0.255	0.355
257	2250	16	0.06	64.725	8.197	63	0.667	0.714	0.354	0.453	0.382
258	2250	16	0.06	76.164	8.351	65	0.667	0.714	0.473	0.467	0.400
259	2250	16	0.06	87.920	8.863	82	0.667	0.714	0.596	0.516	0.555
260	2250	16	0.06	83.527	8.426	80	0.667	0.714	0.550	0.474	0.536
261	2250	16	0.08	92.429	11.108	75	0.667	0.714	0.643	0.728	0.491
262	2250	16	0.08	93.437	12.051	97	0.667	0.714	0.653	0.818	0.691
263	2250	16	0.08	107.17	12.064	99	0.667	0.714	0.796	0.819	0.709

264	2250	16	0.08	79.292	10.601	70	0.667	0.714	0.506	0.680	0.445
265	2250	18	0.04	59.588	5.754	50	0.667	0.857	0.301	0.221	0.264
266	2250	18	0.04	63.963	5.786	76	0.667	0.857	0.346	0.224	0.500
267	2250	18	0.04	67.110	6.286	80	0.667	0.857	0.379	0.272	0.536
268	2250	18	0.04	49.773	5.710	48	0.667	0.857	0.199	0.217	0.245
269	2250	18	0.06	67.927	8.170	66	0.667	0.857	0.388	0.450	0.409
270	2250	18	0.06	80.373	9.024	72	0.667	0.857	0.517	0.531	0.464
271	2250	18	0.06	85.584	9.211	85	0.667	0.857	0.572	0.549	0.582
272	2250	18	0.06	94.080	9.390	88	0.667	0.857	0.660	0.566	0.609
273	2250	18	0.08	83.630	11.371	80	0.667	0.857	0.551	0.753	0.536
274	2250	18	0.08	93.199	11.400	87	0.667	0.857	0.651	0.756	0.600
275	2250	18	0.08	96.452	11.825	93	0.667	0.857	0.685	0.796	0.655
276	2250	18	0.08	104.04	11.893	96	0.667	0.857	0.764	0.803	0.682
277	2250	20	0.04	48.980	5.752	72	0.667	1.000	0.190	0.221	0.464
278	2250	20	0.04	59.335	5.822	86	0.667	1.000	0.298	0.228	0.591
279	2250	20	0.04	65.413	7.135	92	0.667	1.000	0.362	0.352	0.645
280	2250	20	0.04	70.120	7.520	94	0.667	1.000	0.411	0.389	0.664
281	2250	20	0.06	68.784	8.780	77	0.667	1.000	0.397	0.508	0.509
282	2250	20	0.06	82.886	9.586	84	0.667	1.000	0.543	0.584	0.573
283	2250	20	0.06	89.610	10.682	86	0.667	1.000	0.614	0.688	0.591
284	2250	20	0.06	86.084	9.788	86	0.667	1.000	0.577	0.603	0.591
285	2250	20	0.08	86.787	11.460	86	0.667	1.000	0.584	0.762	0.591
286	2250	20	0.08	99.785	11.860	90	0.667	1.000	0.719	0.800	0.627
287	2250	20	0.08	100.11	12.058	93	0.667	1.000	0.723	0.818	0.655
288	2250	20	0.08	111.33	12.141	99	0.667	1.000	0.840	0.826	0.709
289	2500	6	0.04	36.423	3.903	46	1.000	0.000	0.060	0.046	0.227
290	2500	6	0.04	39.254	4.110	39	1.000	0.000	0.089	0.066	0.164
291	2500	6	0.04	39.285	3.963	41	1.000	0.000	0.089	0.052	0.182
292	2500	6	0.04	30.702	3.596	54	1.000	0.000	0.000	0.017	0.300
293	2500	6	0.06	46.163	5.449	50	1.000	0.000	0.161	0.193	0.264
294	2500	6	0.06	54.825	5.763	55	1.000	0.000	0.251	0.222	0.309
295	2500	6	0.06	61.909	5.806	61	1.000	0.000	0.325	0.226	0.364
296	2500	6	0.06	62.660	6.176	62	1.000	0.000	0.333	0.261	0.373
297	2500	6	0.08	58.827	7.259	26	1.000	0.000	0.293	0.364	0.045
298	2500	6	0.08	69.825	7.528	27	1.000	0.000	0.407	0.389	0.055
299	2500	6	0.08	78.350	8.781	44	1.000	0.000	0.496	0.508	0.209
300	2500	6	0.08	70.983	8.515	42	1.000	0.000	0.420	0.483	0.191
301	2500	8	0.04	39.066	4.121	26	1.000	0.143	0.087	0.067	0.045
302	2500	8	0.04	40.340	4.331	28	1.000	0.143	0.100	0.087	0.064
303	2500	8	0.04	51.514	4.607	35	1.000	0.143	0.217	0.113	0.127
304	2500	8	0.04	51.100	4.415	32	1.000	0.143	0.212	0.095	0.100
305	2500	8	0.06	51.896	6.183	21	1.000	0.143	0.221	0.262	0.000
306	2500	8	0.06	74.923	6.753	39	1.000	0.143	0.461	0.316	0.164
307	2500	8	0.06	62.292	6.621	27	1.000	0.143	0.329	0.303	0.055
308	2500	8	0.06	67.340	6.751	28	1.000	0.143	0.382	0.316	0.064
309	2500	8	0.08	62.583	8.067	25	1.000	0.143	0.332	0.440	0.036
310	2500	8	0.08	80.097	9.534	34	1.000	0.143	0.514	0.579	0.118
311	2500	8	0.08	76.025	8.187	26	1.000	0.143	0.472	0.452	0.045
312	2500	8	0.08	81.870	9.569	40	1.000	0.143	0.533	0.583	0.173
313	2500	10	0.04	40.144	4.941	32	1.000	0.286	0.098	0.144	0.100
314	2500	10	0.04	47.929	5.034	34	1.000	0.286	0.179	0.153	0.118
315	2500	10	0.04	56.760	5.304	36	1.000	0.286	0.271	0.179	0.136
316	2500	10	0.04	55.536	5.066	35	1.000	0.286	0.259	0.156	0.127
317	2500	10	0.06	54.145	7.060	31	1.000	0.286	0.244	0.345	0.091

318	2500	10	0.06	66.890	7.267	34	1.000	0.286	0.377	0.365	0.118
319	2500	10	0.06	67.708	7.956	39	1.000	0.286	0.385	0.430	0.164
320	2500	10	0.06	67.813	7.841	38	1.000	0.286	0.387	0.419	0.155
321	2500	10	0.08	65.044	8.413	35	1.000	0.286	0.358	0.473	0.127
322	2500	10	0.08	79.518	8.866	36	1.000	0.286	0.508	0.516	0.136
323	2500	10	0.08	87.474	9.721	41	1.000	0.286	0.591	0.597	0.182
324	2500	10	0.08	88.550	10.054	46	1.000	0.286	0.602	0.629	0.227
325	2500	12	0.04	47.730	5.590	41	1.000	0.429	0.177	0.206	0.182
326	2500	12	0.04	56.570	5.724	45	1.000	0.429	0.269	0.219	0.218
327	2500	12	0.04	57.830	5.626	51	1.000	0.429	0.283	0.209	0.273
328	2500	12	0.04	42.036	5.260	39	1.000	0.429	0.118	0.175	0.164
329	2500	12	0.06	67.805	7.555	38	1.000	0.429	0.386	0.392	0.155
330	2500	12	0.06	79.370	7.806	45	1.000	0.429	0.507	0.416	0.218
331	2500	12	0.06	57.629	7.489	38	1.000	0.429	0.280	0.386	0.155
332	2500	12	0.06	71.498	7.746	42	1.000	0.429	0.425	0.410	0.191
333	2500	12	0.08	70.876	9.885	57	1.000	0.429	0.418	0.613	0.327
334	2500	12	0.08	79.475	10.558	59	1.000	0.429	0.508	0.676	0.345
335	2500	12	0.08	90.710	10.559	65	1.000	0.429	0.625	0.676	0.400
336	2500	12	0.08	91.859	10.940	71	1.000	0.429	0.637	0.712	0.455
337	2500	14	0.04	43.057	5.835	63	1.000	0.571	0.129	0.229	0.382
338	2500	14	0.04	52.956	5.941	67	1.000	0.571	0.232	0.239	0.418
339	2500	14	0.04	59.082	5.943	73	1.000	0.571	0.296	0.239	0.473
340	2500	14	0.04	60.420	5.994	75	1.000	0.571	0.310	0.244	0.491
341	2500	14	0.06	68.068	8.505	73	1.000	0.571	0.389	0.482	0.473
342	2500	14	0.06	80.995	9.002	75	1.000	0.571	0.524	0.529	0.491
343	2500	14	0.06	82.700	9.321	79	1.000	0.571	0.542	0.559	0.527
344	2500	14	0.06	60.571	8.121	67	1.000	0.571	0.311	0.445	0.418
345	2500	14	0.08	74.639	10.406	53	1.000	0.571	0.458	0.662	0.291
346	2500	14	0.08	93.800	10.795	54	1.000	0.571	0.657	0.699	0.300
347	2500	14	0.08	94.457	11.285	68	1.000	0.571	0.664	0.745	0.427
348	2500	14	0.08	96.645	11.509	79	1.000	0.571	0.687	0.766	0.527
349	2500	16	0.04	45.160	6.031	55	1.000	0.714	0.151	0.248	0.309
350	2500	16	0.04	55.103	6.184	65	1.000	0.714	0.254	0.262	0.400
351	2500	16	0.04	58.107	6.210	74	1.000	0.714	0.285	0.265	0.482
352	2500	16	0.04	62.110	6.278	75	1.000	0.714	0.327	0.271	0.491
353	2500	16	0.06	69.410	5.597	63	1.000	0.714	0.403	0.206	0.382
354	2500	16	0.06	72.408	8.609	68	1.000	0.714	0.434	0.492	0.427
355	2500	16	0.06	74.180	9.463	71	1.000	0.714	0.453	0.573	0.455
356	2500	16	0.06	81.052	9.503	77	1.000	0.714	0.524	0.576	0.509
357	2500	16	0.08	91.537	11.756	84	1.000	0.714	0.634	0.790	0.573
358	2500	16	0.08	75.726	11.749	81	1.000	0.714	0.469	0.789	0.545
359	2500	16	0.08	99.341	13.048	114	1.000	0.714	0.715	0.912	0.845
360	2500	16	0.08	105.130	13.476	122	1.000	0.714	0.775	0.953	0.918
361	2500	18	0.04	46.438	5.517	48	1.000	0.857	0.164	0.199	0.245
362	2500	18	0.04	54.963	5.626	57	1.000	0.857	0.253	0.209	0.327
363	2500	18	0.04	58.236	6.209	62	1.000	0.857	0.287	0.264	0.373
364	2500	18	0.04	64.310	6.514	77	1.000	0.857	0.350	0.293	0.509
365	2500	18	0.06	78.738	9.005	70	1.000	0.857	0.500	0.529	0.445
366	2500	18	0.06	80.035	9.009	74	1.000	0.857	0.514	0.530	0.482
367	2500	18	0.06	85.040	9.032	75	1.000	0.857	0.566	0.532	0.491
368	2500	18	0.06	64.121	8.929	61	1.000	0.857	0.348	0.522	0.364
369	2500	18	0.08	79.804	10.062	56	1.000	0.857	0.511	0.629	0.318
370	2500	18	0.08	97.086	10.541	65	1.000	0.857	0.691	0.675	0.400
371	2500	18	0.08	106.220	11.357	84	1.000	0.857	0.787	0.752	0.573

372	2500	18	0.08	97.857	11.563	92	1.000	0.857	0.699	0.771	0.645
373	2500	20	0.04	48.236	5.930	50	1.000	1.000	0.183	0.238	0.264
374	2500	20	0.04	55.443	6.179	53	1.000	1.000	0.258	0.262	0.291
375	2500	20	0.04	61.790	6.673	73	1.000	1.000	0.324	0.308	0.473
376	2500	20	0.04	64.110	6.675	80	1.000	1.000	0.348	0.309	0.536
377	2500	20	0.06	77.190	8.966	77	1.000	1.000	0.484	0.526	0.509
378	2500	20	0.06	84.950	9.716	79	1.000	1.000	0.565	0.597	0.527
379	2500	20	0.06	85.243	9.908	79	1.000	1.000	0.568	0.615	0.527
380	2500	20	0.06	65.742	8.376	73	1.000	1.000	0.365	0.470	0.473
381	2500	20	0.08	83.796	11.551	93	1.000	1.000	0.553	0.770	0.655
382	2500	20	0.08	92.411	12.237	93	1.000	1.000	0.643	0.835	0.655
383	2500	20	0.08	105.32	12.311	96	1.000	1.000	0.777	0.842	0.682
384	2500	20	0.08	111.25	12.493	99	1.000	1.000	0.839	0.860	0.709

APPENDIX E - THE PROGRAM OF THE INN-SRP SYSTEM

```
/* ------------------------------------*/
/* The INN-SRP System Program */
/* ------------------------------------ */

#include "stdio.h"
#include "conio.h"
#include "dos.h"
#include "cb.h"
#include "time.h"
# define MAX(i,j) (i>j)?i:j
#define ABS(i)(i<0)?-i:i
#define number 2000
#define e 2.718282
typedef unsigned int WORD;                    /* 16-bit unsigned int */
clock_t begin,end;

void ClearScreen (void);                      /* Prototypes */
void GetTextCursor (int *x, int *y);
void MoveCursor (int x, int y);

void main ()
   {
   float data[number][4],combxy[number],Max[80];
   int point[4];
   int i,j,k,pmax,per_tooth,range,length,peak1;
   float h_peak,avg1,avg_z,sumf_z,g,t;
   float S,f;
   float h11,h12,h13,h14,h15,h21,h22,h23,h24,h25,pra;

   int Row,Col,Row2,Col2;
   int BoardNum = 0;
   int UDStat = 0;
   int Chan0=0,Chan1=1,Chan2=2,Chan3=3,int I=0;
   int Gain0 = BIP10VOLTS;                    /*Proximity data channel*/
   int Gain1 = BIP10VOLTS;                    /*X channel*/
   int Gain2 = BIP10VOLTS;                     /*Y channel*/
   int Gain3 = BIP10VOLTS;                     /*Z channel*/
   float data[2000][4], EngUnits,RevLevel = (float)CURRENTREVNUM;
   WORD DataValue0 = 0;
   WORD DataValue1 = 0;
   WORD DataValue2 = 0;
   WORD DataValue3 = 0;

    UDStat = cbDeclareRevision(&RevLevel);        /* Declare UL Revision Level */

   cbErrHandling (PRINTALL, STOPALL);

/*************************************************/
/* set up the screen  & input the machining parameters */
/*************************************************/
```

```
ClearScreen();
   printf("input the spindle speed : ");
   scanf("%f", &S);
   printf("input the feed rate : ");
   scanf("%f", &f);
   getchar();

  printf ("Demonstration of cbAIn()\n");
  printf("Press any key to start A/D converting.\n");
  getchar();
  begin=clock();                    /* clock starts        */

 /* collect the sample from the channel until a key is pressed */
  for (I=0;I<number;I++)
        {
        UDStat =cbAIn (BoardNum, Chan0, Gain0, &DataValue0);
        UDStat =cbToEngUnits (BoardNum, Gain0, DataValue0, &EngUnits);
        data[I][0]=EngUnits;

        UDStat =cbAIn (BoardNum, Chan1, Gain1, &DataValue1);
         UDStat =cbToEngUnits (BoardNum, Gain1, DataValue1, &EngUnits);
        data[I][1]=EngUnits;

         UDStat =cbAIn (BoardNum, Chan2, Gain2, &DataValue2);
        UDStat =cbToEngUnits (BoardNum, Gain2, DataValue2, &EngUnits);
        data[I][2]=EngUnits;

        UDStat =cbAIn (BoardNum, Chan3, Gain3, &DataValue3);
        UDStat =cbToEngUnits (BoardNum, Gain3, DataValue3, &EngUnits);
        data[I][3]=EngUnits;
        }

 end=clock();
 printf(" A/D Convert is finished and the converted time is %7.4f\n seconds",(end-begin)/CLK_TCK);

  for (I=0; I<number; I++)
  {
   data[I][1]=(data[I][1]+data[I+1][1])/2;
   data[I][2]=(data[I][2]+data[I+1][2])/2;
   data[I][3]=(data[I][3]+data[I+1][3])/2;
  }

/* obtain the resultant force in XY plant and absolute force in Z direction */
 for(i=0; i<number; i++)
 {
  combxy[i]=sqrt( pow(data[i][1],2) + pow(data[i][2],2));
  data[i][3]=ABS(data[i][3]);
 }

 for(h_peak=combxy[50], i=50; i<number; ++i)       /* find the max. value of voltage */
   if (h_peak<combxy[i])
   {
        h_peak=combxy[i];
```

```
        pmax=i;
    }

 j=0;
 for(i=50; i<number; i++)                    /* find the value of range and per tooth */
   if (data[i-1][0]<1 && data[i][0]>1)
   {
    point[j] = i;
    j++;
   }

 range=point[2]-point[0];
 per_tooth=(point[2]-point[0])/4;

 length=pmax-per_tooth;                      /* find the first peak value */
 while (length>50)
 {
   pmax=pmax-per_tooth;
   length=pmax-per_tooth;
 }
 peak1=pmax;

 /* find all peak of the data */
 i=peak1;
 k=0;

 while (k<68)
 {
  g=0;
    for (i=peak1; i<peak1+5; i++)
    g=MAX(combxy[i-2],g);
  Max[k]=g;
  peak1=peak1+per_tooth;
  k=k+1;
 }


/*****************************************/
/* Calculate the average peak force for 17 rev. */
/*****************************************/
   avg1=0;
   for (i=0; i<67; i++)
      avg1=Max[i]+avg1;
   avg1=50*avg1/68;

   printf("Average peak force for 17 rev. = %7.4f\n", avg1);


/*********************************/
/* Calculate the average force for 17 rev. */
/*********************************/
   sumf_z=0;
   for (i=point[0]; i<point[0]+range*17; i++)
      sumf_z=data[i][3]+sumf_z;
```

```
   avg_z=50*sumf_z/(range*17);
   printf("average force in Z for 17 Rev.= %7.4f\n", avg_z);


/*************************************/
/* Calculate the predicted surface roughness */
/*************************************/

  /* neurons in hidden layer 1 */
   h11=1/(1+pow(e,-((S*(-0.4581)+f*2.649+avg1*(-6.3270)+avg_z*(-0.5697))-1.7790)));
   h12=1/(1+pow(e,-((S*(-2.391)+f*4.342+avg1*1.279+avg_z*(-2.355))-2.247)));
   h13=1/(1+pow(e,-((S*(-0.8417)+f*8.572+avg1*(-1.31)+avg_z*(-0.2232))-0.8322)));
   h14=1/(1+pow(e,-((S*(-9.444)+f*6.33+avg1*(-0.332)+avg_z*3.401)-6.775)));
   h15=1/(1+pow(e,-((S*(-0.6358)+f*1.114+avg1*(-2.5)+avg_z*(-7.686))+9.427)));

  /* neurons in hidden layer 2 */
   h21=1/(1+pow(e,-((h11*0.6004+h12*(-1.724)+h13*3.817+h14*9.769+h15*(-4.371))-2.072)));
   h22=1/(1+pow(e,-((h11*(-1.003)+h12*0.3169+h13*(-0.8317)+h14*(-2.959)+h15*(-0.7604))+0.0563)));
   h23=1/(1+pow(e,-((h11*1.342+h12*(-0.5514)+h13*(-1.698)+h14*0.0233+h15*0.5712)+0.0774)));
   h24=1/(1+pow(e,-((h11*(-3.063)+h12*1.778+h13*(-3.281)+h14*(-3.504)+h15*0.2006)+0.8216)));
   h25=1/(1+pow(e,-((h11*2.238+h12*(-1.119)+h13*(-4.204)+h14*3.15+h15*3.327)-0.2851)));

  /* output layer */
   pra=1/(1+pow(e,-((h21*4.183+h22*2.21+h23*(-0.4757)+h24*4.236+h25*(-5.034))-0.0021)));

   pra=pra*110+21;

   printf("The predicted surface roughness =  %4.0f\n", pra);

   exit(0);
   return;
 }


/*****************************************************************************
* Name:    ClearScreen
*****************************************************************************/
#define BIOS_VIDEO   0x10

void
ClearScreen (void)
{
   union REGS InRegs,OutRegs;
   InRegs.h.ah = 0;
   InRegs.h.al = 2;
   int86 (BIOS_VIDEO, &InRegs, &OutRegs);

   return;
}


/*****************************************************************************
* Name:    MoveCursor
*****************************************************************************/
```

```
void
MoveCursor (int x, int y)
{
   union REGS InRegs,OutRegs;
   InRegs.h.ah = 2;
   InRegs.h.dl = (char) x;
   InRegs.h.dh = (char) y;
   InRegs.h.bh = 0;
   int86 (BIOS_VIDEO, &InRegs, &OutRegs);

   return;
}


/*****************************************************************************
* Name:     GetTextCursor
*****************************************************************************/
void
GetTextCursor (int *x, int *y)
{
   union REGS InRegs,OutRegs;
   InRegs.h.ah = 3;
   InRegs.h.bh = 0;
   int86 (BIOS_VIDEO, &InRegs, &OutRegs);
   *x = OutRegs.h.dl;
   *y = OutRegs.h.dh;

   return;
}
```

APPENDIX F - SAMPLES FOR THE DEVELOPMENT OF NN-AMPC SYSTEM

(336 samples)

	Raw Data Set						Scaled Data Set					
#	S^p	f^p	F_{ap}^p	F_{ax}^p	ΔR_a	Δf	$S^{p'}$	$f^{p'}$	$F_{ap}^{p'}$	$F_{ax}^{p'}$	$\Delta R_a'$	$\Delta f'$
1	1750	20	63.747	5.824	17	90.0	0.000	1.000	0.257	0.137	0.200	0.857
2	1750	20	63.747	5.824	21	80.0	0.000	1.000	0.257	0.137	0.247	0.714
3	1750	20	63.747	5.824	23	70.0	0.000	1.000	0.257	0.137	0.271	0.571
4	1750	20	63.747	5.824	36	60.0	0.000	1.000	0.257	0.137	0.424	0.429
5	1750	20	63.747	5.824	41	50.0	0.000	1.000	0.257	0.137	0.482	0.286
6	1750	20	63.747	5.824	61	40.0	0.000	1.000	0.257	0.137	0.718	0.143
7	1750	20	63.747	5.824	63	30.0	0.000	1.000	0.257	0.137	0.741	0.000
8	1750	18	69.941	6.222	7	88.9	0.000	0.833	0.334	0.182	0.082	0.841
9	1750	18	69.941	6.222	9	77.8	0.000	0.833	0.334	0.182	0.106	0.683
10	1750	18	69.941	6.222	22	66.7	0.000	0.833	0.334	0.182	0.259	0.524
11	1750	18	69.941	6.222	27	55.6	0.000	0.833	0.334	0.182	0.318	0.365
12	1750	18	69.941	6.222	47	44.4	0.000	0.833	0.334	0.182	0.553	0.206
13	1750	18	69.941	6.222	49	33.3	0.000	0.833	0.334	0.182	0.576	0.048
14	1750	16	71.820	5.949	1	87.5	0.000	0.667	0.357	0.152	0.012	0.821
15	1750	16	71.820	5.949	14	75.0	0.000	0.667	0.357	0.152	0.165	0.643
16	1750	16	71.820	5.949	19	62.5	0.000	0.667	0.357	0.152	0.224	0.464
17	1750	16	71.820	5.949	39	50.0	0.000	0.667	0.357	0.152	0.459	0.286
18	1750	16	71.820	5.949	41	37.5	0.000	0.667	0.357	0.152	0.482	0.107
19	1750	14	69.549	6.603	11	85.7	0.000	0.500	0.329	0.225	0.129	0.796
20	1750	14	69.549	6.603	16	71.4	0.000	0.500	0.329	0.225	0.188	0.592
21	1750	14	69.549	6.603	36	57.1	0.000	0.500	0.329	0.225	0.424	0.388
22	1750	14	69.549	6.603	38	42.9	0.000	0.500	0.329	0.225	0.447	0.184
23	1750	12	56.776	5.582	9	83.3	0.000	0.333	0.171	0.110	0.106	0.762
24	1750	12	56.776	5.582	29	66.7	0.000	0.333	0.171	0.110	0.341	0.524
25	1750	12	56.776	5.582	31	50.0	0.000	0.333	0.171	0.110	0.365	0.286
26	1750	10	52.437	5.241	14	80.0	0.000	0.167	0.117	0.072	0.165	0.714
27	1750	10	52.437	5.241	16	60.0	0.000	0.167	0.117	0.072	0.188	0.429
28	1750	8	61.280	5.169	4	75.0	0.000	0.000	0.227	0.063	0.047	0.643
29	1750	20	104.140	9.407	0	100	0.000	1.000	0.759	0.542	0.000	1.000
30	1750	20	104.140	9.407	21	80.0	0.000	1.000	0.759	0.542	0.247	0.714
31	1750	20	104.140	9.407	26	70.0	0.000	1.000	0.759	0.542	0.306	0.571
32	1750	20	104.140	9.407	42	60.0	0.000	1.000	0.759	0.542	0.494	0.429
33	1750	20	104.140	9.407	50	50.0	0.000	1.000	0.759	0.542	0.588	0.286
34	1750	20	104.140	9.407	67	40.0	0.000	1.000	0.759	0.542	0.788	0.143
35	1750	20	104.140	9.407	75	30.0	0.000	1.000	0.759	0.542	0.882	0.000
36	1750	18	72.527	9.556	20	88.9	0.000	0.833	0.366	0.559	0.235	0.841
37	1750	18	72.527	9.556	25	77.8	0.000	0.833	0.366	0.559	0.294	0.683
38	1750	18	72.527	9.556	41	66.7	0.000	0.833	0.366	0.559	0.482	0.524
39	1750	18	72.527	9.556	49	55.6	0.000	0.833	0.366	0.559	0.576	0.365
40	1750	18	72.527	9.556	66	44.4	0.000	0.833	0.366	0.559	0.776	0.206
41	1750	18	72.527	9.556	74	33.3	0.000	0.833	0.366	0.559	0.871	0.048
42	1750	16	96.510	8.819	8	87.5	0.000	0.667	0.664	0.476	0.094	0.821
43	1750	16	96.510	8.819	24	75.0	0.000	0.667	0.664	0.476	0.282	0.643
44	1750	16	96.510	8.819	32	62.5	0.000	0.667	0.664	0.476	0.376	0.464
45	1750	16	96.510	8.819	49	50.0	0.000	0.667	0.664	0.476	0.576	0.286

46	1750	16	96.510	8.819	57	37.5	0.000	0.667	0.664	0.476	0.671	0.107
47	1750	14	66.779	8.927	4	85.7	0.000	0.500	0.295	0.488	0.047	0.796
48	1750	14	66.779	8.927	12	71.4	0.000	0.500	0.295	0.488	0.141	0.592
49	1750	14	66.779	8.927	29	57.1	0.000	0.500	0.295	0.488	0.341	0.388
50	1750	14	66.779	8.927	37	42.9	0.000	0.500	0.295	0.488	0.435	0.184
51	1750	12	75.940	8.966	6	83.3	0.000	0.333	0.409	0.492	0.071	0.762
52	1750	12	75.940	8.966	23	66.7	0.000	0.333	0.409	0.492	0.271	0.524
53	1750	12	75.940	8.966	31	50.0	0.000	0.333	0.409	0.492	0.365	0.286
54	1750	10	90.708	7.943	13	80.0	0.000	0.167	0.592	0.377	0.153	0.714
55	1750	10	90.708	7.943	21	60.0	0.000	0.167	0.592	0.377	0.247	0.429
56	1750	8	62.793	5.385	10	75.0	0.000	0.000	0.245	0.088	0.118	0.643
57	1750	20	123.540	13.463	22	90.0	0.000	1.000	1.000	1.000	0.259	0.857
58	1750	20	123.540	13.463	11	80.0	0.000	1.000	1.000	1.000	0.129	0.714
59	1750	20	123.540	13.463	16	70.0	0.000	1.000	1.000	1.000	0.188	0.571
60	1750	20	123.540	13.463	41	60.0	0.000	1.000	1.000	1.000	0.482	0.429
61	1750	20	123.540	13.463	58	50.0	0.000	1.000	1.000	1.000	0.682	0.286
62	1750	20	123.540	13.463	77	40.0	0.000	1.000	1.000	1.000	0.906	0.143
63	1750	20	123.540	13.463	85	30.0	0.000	1.000	1.000	1.000	1.000	0.000
64	1750	18	111.061	12.611	4	88.9	0.000	0.833	0.845	0.904	0.047	0.841
65	1750	18	111.061	12.611	9	77.8	0.000	0.833	0.845	0.904	0.106	0.683
66	1750	18	111.061	12.611	34	66.7	0.000	0.833	0.845	0.904	0.400	0.524
67	1750	18	111.061	12.611	51	55.6	0.000	0.833	0.845	0.904	0.600	0.365
68	1750	18	111.061	12.611	70	44.4	0.000	0.833	0.845	0.904	0.824	0.206
69	1750	18	111.061	12.611	78	33.3	0.000	0.833	0.845	0.904	0.918	0.048
70	1750	16	93.983	11.815	12	87.5	0.000	0.667	0.633	0.814	0.141	0.821
71	1750	16	93.983	11.815	37	75.0	0.000	0.667	0.633	0.814	0.435	0.643
72	1750	16	93.983	11.815	54	62.5	0.000	0.667	0.633	0.814	0.635	0.464
73	1750	16	93.983	11.815	73	50.0	0.000	0.667	0.633	0.814	0.859	0.286
74	1750	16	93.983	11.815	81	37.5	0.000	0.667	0.633	0.814	0.953	0.107
75	1750	14	104.290	11.552	23	85.7	0.000	0.500	0.761	0.784	0.271	0.796
76	1750	14	104.290	11.552	40	71.4	0.000	0.500	0.761	0.784	0.471	0.592
77	1750	14	104.290	11.552	59	57.1	0.000	0.500	0.761	0.784	0.694	0.388
78	1750	14	104.290	11.552	67	42.9	0.000	0.500	0.761	0.784	0.788	0.184
79	1750	12	119.010	11.091	11	83.3	0.000	0.333	0.944	0.732	0.129	0.762
80	1750	12	119.010	11.091	30	66.7	0.000	0.333	0.944	0.732	0.353	0.524
81	1750	12	119.010	11.091	38	50.0	0.000	0.333	0.944	0.732	0.447	0.286
82	1750	10	113.400	10.512	10	80.0	0.000	0.167	0.874	0.667	0.118	0.714
83	1750	10	113.400	10.512	18	60.0	0.000	0.167	0.874	0.667	0.212	0.429
84	1750	8	102.310	9.795	11	75.0	0.000	0.000	0.736	0.586	0.129	0.643
85	2000	20	70.057	6.148	2	90.0	0.333	1.000	0.336	0.174	0.024	0.857
86	2000	20	70.057	6.148	10	80.0	0.333	1.000	0.336	0.174	0.118	0.714
87	2000	20	70.057	6.148	21	70.0	0.333	1.000	0.336	0.174	0.247	0.571
88	2000	20	70.057	6.148	28	60.0	0.333	1.000	0.336	0.174	0.329	0.429
89	2000	20	70.057	6.148	35	50.0	0.333	1.000	0.336	0.174	0.412	0.286
90	2000	20	70.057	6.148	51	40.0	0.333	1.000	0.336	0.174	0.600	0.143
91	2000	20	70.057	6.148	55	30.0	0.333	1.000	0.336	0.174	0.647	0.000
92	2000	18	66.020	6.039	8	88.9	0.333	0.833	0.285	0.162	0.094	0.841
93	2000	18	66.020	6.039	19	77.8	0.333	0.833	0.285	0.162	0.224	0.683
94	2000	18	66.020	6.039	26	66.7	0.333	0.833	0.285	0.162	0.306	0.524
95	2000	18	66.020	6.039	33	55.6	0.333	0.833	0.285	0.162	0.388	0.365
96	2000	18	66.020	6.039	49	44.4	0.333	0.833	0.285	0.162	0.576	0.206
97	2000	18	66.020	6.039	53	33.3	0.333	0.833	0.285	0.162	0.624	0.048
98	2000	16	51.018	5.725	3	87.5	0.333	0.667	0.099	0.126	0.035	0.821
99	2000	16	51.018	5.725	10	75.0	0.333	0.667	0.099	0.126	0.118	0.643

100	2000	16	51.018	5.725	17	62.5	0.333	0.667	0.099	0.126	0.200	0.464
101	2000	16	51.018	5.725	33	50.0	0.333	0.667	0.099	0.126	0.388	0.286
102	2000	16	51.018	5.725	37	37.5	0.333	0.667	0.099	0.126	0.435	0.107
103	2000	14	63.576	6.457	15	85.7	0.333	0.500	0.255	0.209	0.176	0.796
104	2000	14	63.576	6.457	22	71.4	0.333	0.500	0.255	0.209	0.259	0.592
105	2000	14	63.576	6.457	38	57.1	0.333	0.500	0.255	0.209	0.447	0.388
106	2000	14	63.576	6.457	42	42.9	0.333	0.500	0.255	0.209	0.494	0.184
107	2000	12	64.513	6.581	12	83.3	0.333	0.333	0.267	0.223	0.141	0.762
108	2000	12	64.513	6.581	28	66.7	0.333	0.333	0.267	0.223	0.329	0.524
109	2000	12	64.513	6.581	32	50.0	0.333	0.333	0.267	0.223	0.376	0.286
110	2000	10	49.153	5.103	10	80.0	0.333	0.167	0.076	0.056	0.118	0.714
111	2000	10	49.153	5.103	14	60.0	0.333	0.167	0.076	0.056	0.165	0.429
112	2000	8	51.489	5.181	4	75.0	0.333	0.000	0.105	0.065	0.047	0.643
113	2000	20	91.110	9.917	7	90.0	0.333	1.000	0.597	0.600	0.082	0.857
114	2000	20	91.110	9.917	17	80.0	0.333	1.000	0.597	0.600	0.200	0.714
115	2000	20	91.110	9.917	13	70.0	0.333	1.000	0.597	0.600	0.153	0.571
116	2000	20	91.110	9.917	20	60.0	0.333	1.000	0.597	0.600	0.235	0.429
117	2000	20	91.110	9.917	34	50.0	0.333	1.000	0.597	0.600	0.400	0.286
118	2000	20	91.110	9.917	46	40.0	0.333	1.000	0.597	0.600	0.541	0.143
119	2000	20	91.110	9.917	49	30.0	0.333	1.000	0.597	0.600	0.576	0.000
120	2000	18	73.731	9.201	12	88.9	0.333	0.833	0.381	0.519	0.141	0.841
121	2000	18	73.731	9.201	8	77.8	0.333	0.833	0.381	0.519	0.094	0.683
122	2000	18	73.731	9.201	15	66.7	0.333	0.833	0.381	0.519	0.176	0.524
123	2000	18	73.731	9.201	29	55.6	0.333	0.833	0.381	0.519	0.341	0.365
124	2000	18	73.731	9.201	41	44.4	0.333	0.833	0.381	0.519	0.482	0.206
125	2000	18	73.731	9.201	44	33.3	0.333	0.833	0.381	0.519	0.518	0.048
126	2000	16	66.895	7.804	5	87.5	0.333	0.667	0.296	0.361	0.059	0.821
127	2000	16	66.895	7.804	12	75.0	0.333	0.667	0.296	0.361	0.141	0.643
128	2000	16	66.895	7.804	26	62.5	0.333	0.667	0.296	0.361	0.306	0.464
129	2000	16	66.895	7.804	38	50.0	0.333	0.667	0.296	0.361	0.447	0.286
130	2000	16	66.895	7.804	41	37.5	0.333	0.667	0.296	0.361	0.482	0.107
131	2000	14	74.068	8.422	9	85.7	0.333	0.500	0.385	0.431	0.106	0.796
132	2000	14	74.068	8.422	23	71.4	0.333	0.500	0.385	0.431	0.271	0.592
133	2000	14	74.068	8.422	35	57.1	0.333	0.500	0.385	0.431	0.412	0.388
134	2000	14	74.068	8.422	38	42.9	0.333	0.500	0.385	0.431	0.447	0.184
135	2000	12	85.494	8.663	13	83.3	0.333	0.333	0.527	0.458	0.153	0.762
136	2000	12	85.494	8.663	25	66.7	0.333	0.333	0.527	0.458	0.294	0.524
137	2000	12	85.494	8.663	28	50.0	0.333	0.333	0.527	0.458	0.329	0.286
138	2000	10	81.362	8.251	7	80.0	0.333	0.167	0.476	0.411	0.082	0.714
139	2000	10	81.362	8.251	10	60.0	0.333	0.167	0.476	0.411	0.118	0.429
140	2000	8	86.880	7.912	4	75.0	0.333	0.000	0.545	0.373	0.047	0.643
141	2000	20	112.892	12.374	22	90.0	0.333	1.000	0.868	0.877	0.259	0.857
142	2000	20	112.892	12.374	33	80.0	0.333	1.000	0.868	0.877	0.388	0.714
143	2000	20	112.892	12.374	41	70.0	0.333	1.000	0.868	0.877	0.482	0.571
144	2000	20	112.892	12.374	35	60.0	0.333	1.000	0.868	0.877	0.412	0.429
145	2000	20	112.892	12.374	55	50.0	0.333	1.000	0.868	0.877	0.647	0.286
146	2000	20	112.892	12.374	73	40.0	0.333	1.000	0.868	0.877	0.859	0.143
147	2000	20	112.892	12.374	73	30.0	0.333	1.000	0.868	0.877	0.859	0.000
148	2000	18	108.386	11.398	13	88.9	0.333	0.833	0.812	0.767	0.153	0.841
149	2000	18	108.386	11.398	21	77.8	0.333	0.833	0.812	0.767	0.247	0.683
150	2000	18	108.386	11.398	15	66.7	0.333	0.833	0.812	0.767	0.176	0.524
151	2000	18	108.386	11.398	35	55.6	0.333	0.833	0.812	0.767	0.412	0.365
152	2000	18	108.386	11.398	53	44.4	0.333	0.833	0.812	0.767	0.624	0.206
153	2000	18	108.386	11.398	53	33.3	0.333	0.833	0.812	0.767	0.624	0.048

154	2000	16	82.548	10.269	10	87.5	0.333	0.667	0.491	0.639	0.118	0.821
155	2000	16	82.548	10.269	4	75.0	0.333	0.667	0.491	0.639	0.047	0.643
156	2000	16	82.548	10.269	24	62.5	0.333	0.667	0.491	0.639	0.282	0.464
157	2000	16	82.548	10.269	42	50.0	0.333	0.667	0.491	0.639	0.494	0.286
158	2000	16	82.548	10.269	42	37.5	0.333	0.667	0.491	0.639	0.494	0.107
159	2000	14	91.994	11.238	3	85.7	0.333	0.500	0.608	0.749	0.035	0.796
160	2000	14	91.994	11.238	23	71.4	0.333	0.500	0.608	0.749	0.271	0.592
161	2000	14	91.994	11.238	41	57.1	0.333	0.500	0.608	0.749	0.482	0.388
162	2000	14	91.994	11.238	41	42.9	0.333	0.500	0.608	0.749	0.482	0.184
163	2000	12	74.099	11.294	10	83.3	0.333	0.333	0.386	0.755	0.118	0.762
164	2000	12	74.099	11.294	28	66.7	0.333	0.333	0.386	0.755	0.329	0.524
165	2000	12	74.099	11.294	28	50.0	0.333	0.333	0.386	0.755	0.329	0.286
166	2000	10	97.930	10.673	11	80.0	0.333	0.167	0.682	0.685	0.129	0.714
167	2000	10	97.930	10.673	11	60.0	0.333	0.167	0.682	0.685	0.129	0.429
168	2000	8	87.019	9.049	3	75.0	0.333	0.000	0.546	0.502	0.035	0.643
169	2250	20	70.120	7.520	6	90.0	0.667	1.000	0.336	0.329	0.071	0.857
170	2250	20	70.120	7.520	22	80.0	0.667	1.000	0.336	0.329	0.259	0.714
171	2250	20	70.120	7.520	23	70.0	0.667	1.000	0.336	0.329	0.271	0.571
172	2250	20	70.120	7.520	26	60.0	0.667	1.000	0.336	0.329	0.306	0.429
173	2250	20	70.120	7.520	37	50.0	0.667	1.000	0.336	0.329	0.435	0.286
174	2250	20	70.120	7.520	47	40.0	0.667	1.000	0.336	0.329	0.553	0.143
175	2250	20	70.120	7.520	52	30.0	0.667	1.000	0.336	0.329	0.612	0.000
176	2250	18	63.963	5.786	17	88.9	0.667	0.833	0.260	0.133	0.200	0.841
177	2250	18	63.963	5.786	18	77.8	0.667	0.833	0.260	0.133	0.212	0.683
178	2250	18	63.963	5.786	21	66.7	0.667	0.833	0.260	0.133	0.247	0.524
179	2250	18	63.963	5.786	32	55.6	0.667	0.833	0.260	0.133	0.376	0.365
180	2250	18	63.963	5.786	42	44.4	0.667	0.833	0.260	0.133	0.494	0.206
181	2250	18	63.963	5.786	47	33.3	0.667	0.833	0.260	0.133	0.553	0.048
182	2250	16	53.054	6.114	6	87.5	0.667	0.667	0.124	0.170	0.071	0.821
183	2250	16	53.054	6.114	9	75.0	0.667	0.667	0.124	0.170	0.106	0.643
184	2250	16	53.054	6.114	20	62.5	0.667	0.667	0.124	0.170	0.235	0.464
185	2250	16	53.054	6.114	30	50.0	0.667	0.667	0.124	0.170	0.353	0.286
186	2250	16	53.054	6.114	35	37.5	0.667	0.667	0.124	0.170	0.412	0.107
187	2250	14	55.447	6.016	7	85.7	0.667	0.500	0.154	0.159	0.082	0.796
188	2250	14	55.447	6.016	18	71.4	0.667	0.500	0.154	0.159	0.212	0.592
189	2250	14	55.447	6.016	28	57.1	0.667	0.500	0.154	0.159	0.329	0.388
190	2250	14	55.447	6.016	33	42.9	0.667	0.500	0.154	0.159	0.388	0.184
191	2250	12	58.233	5.805	11	83.3	0.667	0.333	0.189	0.135	0.129	0.762
192	2250	12	58.233	5.805	21	66.7	0.667	0.333	0.189	0.135	0.247	0.524
193	2250	12	58.233	5.805	26	50.0	0.667	0.333	0.189	0.135	0.306	0.286
194	2250	10	54.710	5.425	5	80.0	0.667	0.167	0.145	0.092	0.059	0.714
195	2250	10	54.710	5.425	10	60.0	0.667	0.167	0.145	0.092	0.118	0.429
196	2250	8	43.048	4.811	2	75.0	0.667	0.000	0.000	0.023	0.024	0.643
197	2250	20	89.610	10.682	1	90.0	0.667	1.000	0.578	0.686	0.012	0.857
198	2250	20	89.610	10.682	23	80.0	0.667	1.000	0.578	0.686	0.271	0.714
199	2250	20	89.610	10.682	9	70.0	0.667	1.000	0.578	0.686	0.106	0.571
200	2250	20	89.610	10.682	34	60.0	0.667	1.000	0.578	0.686	0.400	0.429
201	2250	20	89.610	10.682	39	50.0	0.667	1.000	0.578	0.686	0.459	0.286
202	2250	20	89.610	10.682	51	40.0	0.667	1.000	0.578	0.686	0.600	0.143
203	2250	20	89.610	10.682	56	30.0	0.667	1.000	0.578	0.686	0.659	0.000
204	2250	18	85.584	9.211	18	88.9	0.667	0.833	0.528	0.520	0.212	0.841
205	2250	18	85.584	9.211	4	77.8	0.667	0.833	0.528	0.520	0.047	0.683
206	2250	18	85.584	9.211	29	66.7	0.667	0.833	0.528	0.520	0.341	0.524
207	2250	18	85.584	9.211	34	55.6	0.667	0.833	0.528	0.520	0.400	0.365

208	2250	18	85.584	9.211	46	44.4	0.667	0.833	0.528	0.520	0.541	0.206
209	2250	18	85.584	9.211	51	33.3	0.667	0.833	0.528	0.520	0.600	0.048
210	2250	16	64.725	8.197	0	100.	0.667	0.667	0.269	0.405	0.000	1.000
211	2250	16	64.725	8.197	18	75.0	0.667	0.667	0.269	0.405	0.212	0.643
212	2250	16	64.725	8.197	23	62.5	0.667	0.667	0.269	0.405	0.271	0.464
213	2250	16	64.725	8.197	35	50.0	0.667	0.667	0.269	0.405	0.412	0.286
214	2250	16	64.725	8.197	40	37.5	0.667	0.667	0.269	0.405	0.471	0.107
215	2250	14	80.720	9.523	17	85.7	0.667	0.500	0.468	0.555	0.200	0.796
216	2250	14	80.720	9.523	22	71.4	0.667	0.500	0.468	0.555	0.259	0.592
217	2250	14	80.720	9.523	34	57.1	0.667	0.500	0.468	0.555	0.400	0.388
218	2250	14	80.720	9.523	39	42.9	0.667	0.500	0.468	0.555	0.459	0.184
219	2250	12	71.057	8.103	9	83.3	0.667	0.333	0.348	0.395	0.106	0.762
220	2250	12	71.057	8.103	21	66.7	0.667	0.333	0.348	0.395	0.247	0.524
221	2250	12	71.057	8.103	26	50.0	0.667	0.333	0.348	0.395	0.306	0.286
222	2250	10	57.331	7.638	5	80.0	0.667	0.167	0.177	0.342	0.059	0.714
223	2250	10	57.331	7.638	10	60.0	0.667	0.167	0.177	0.342	0.118	0.429
224	2250	8	58.950	6.791	5	75.0	0.667	0.000	0.198	0.247	0.059	0.643
225	2250	20	100.105	12.058	12	90.0	0.667	1.000	0.709	0.841	0.141	0.857
226	2250	20	100.105	12.058	17	80.0	0.667	1.000	0.709	0.841	0.200	0.714
227	2250	20	100.105	12.058	18	70.0	0.667	1.000	0.709	0.841	0.212	0.571
228	2250	20	100.105	12.058	33	60.0	0.667	1.000	0.709	0.841	0.388	0.429
229	2250	20	100.105	12.058	50	50.0	0.667	1.000	0.709	0.841	0.588	0.286
230	2250	20	100.105	12.058	59	40.0	0.667	1.000	0.709	0.841	0.694	0.143
231	2250	20	100.105	12.058	55	30.0	0.667	1.000	0.709	0.841	0.647	0.000
232	2250	18	83.630	11.371	6	88.9	0.667	0.833	0.504	0.764	0.071	0.841
233	2250	18	83.630	11.371	7	77.8	0.667	0.833	0.504	0.764	0.082	0.683
234	2250	18	83.630	11.371	22	66.7	0.667	0.833	0.504	0.764	0.259	0.524
235	2250	18	83.630	11.371	39	55.6	0.667	0.833	0.504	0.764	0.459	0.365
236	2250	18	83.630	11.371	48	44.4	0.667	0.833	0.504	0.764	0.565	0.206
237	2250	18	83.630	11.371	44	33.3	0.667	0.833	0.504	0.764	0.518	0.048
238	2250	16	92.429	11.108	6	87.5	0.667	0.667	0.613	0.734	0.071	0.821
239	2250	16	92.429	11.108	21	75.0	0.667	0.667	0.613	0.734	0.247	0.643
240	2250	16	92.429	11.108	38	62.5	0.667	0.667	0.613	0.734	0.447	0.464
241	2250	16	92.429	11.108	47	50.0	0.667	0.667	0.613	0.734	0.553	0.286
242	2250	16	92.429	11.108	43	37.5	0.667	0.667	0.613	0.734	0.506	0.107
243	2250	14	95.504	11.598	20	85.7	0.667	0.500	0.652	0.789	0.235	0.796
244	2250	14	95.504	11.598	37	71.4	0.667	0.500	0.652	0.789	0.435	0.592
245	2250	14	95.504	11.598	46	57.1	0.667	0.500	0.652	0.789	0.541	0.388
246	2250	14	95.504	11.598	42	42.9	0.667	0.500	0.652	0.789	0.494	0.184
247	2250	12	96.108	11.041	20	83.3	0.667	0.333	0.659	0.727	0.235	0.762
248	2250	12	96.108	11.041	29	66.7	0.667	0.333	0.659	0.727	0.341	0.524
249	2250	12	96.108	11.041	25	50.0	0.667	0.333	0.659	0.727	0.294	0.286
250	2250	10	69.434	9.379	7	80.0	0.667	0.167	0.328	0.539	0.082	0.714
251	2250	10	69.434	9.379	3	60.0	0.667	0.167	0.328	0.539	0.035	0.429
252	2250	8	82.779	8.912	1	75.0	0.667	0.000	0.494	0.486	0.012	0.643
253	2500	20	64.110	6.675	9	90.0	1.000	1.000	0.262	0.234	0.106	0.857
254	2500	20	64.110	6.675	6	80.0	1.000	1.000	0.262	0.234	0.071	0.714
255	2500	20	64.110	6.675	18	70.0	1.000	1.000	0.262	0.234	0.212	0.571
256	2500	20	64.110	6.675	20	60.0	1.000	1.000	0.262	0.234	0.235	0.429
257	2500	20	64.110	6.675	35	50.0	1.000	1.000	0.262	0.234	0.412	0.286
258	2500	20	64.110	6.675	36	40.0	1.000	1.000	0.262	0.234	0.424	0.143
259	2500	20	64.110	6.675	40	30.0	1.000	1.000	0.262	0.234	0.471	0.000
260	2500	18	58.236	6.209	1	88.9	1.000	0.833	0.189	0.181	0.012	0.841
261	2500	18	58.236	6.209	13	77.8	1.000	0.833	0.189	0.181	0.153	0.683

262	2500	18	58.236	6.209	15	66.7	1.000	0.833	0.189	0.181	0.176	0.524
263	2500	18	58.236	6.209	30	55.6	1.000	0.833	0.189	0.181	0.353	0.365
264	2500	18	58.236	6.209	31	44.4	1.000	0.833	0.189	0.181	0.365	0.206
265	2500	18	58.236	6.209	35	33.3	1.000	0.833	0.189	0.181	0.412	0.048
266	2500	16	55.103	6.184	9	87.5	1.000	0.667	0.150	0.178	0.106	0.821
267	2500	16	55.103	6.184	11	75.0	1.000	0.667	0.150	0.178	0.129	0.643
268	2500	16	55.103	6.184	26	62.5	1.000	0.667	0.150	0.178	0.306	0.464
269	2500	16	55.103	6.184	27	50.0	1.000	0.667	0.150	0.178	0.318	0.286
270	2500	16	55.103	6.184	31	37.5	1.000	0.667	0.150	0.178	0.365	0.107
271	2500	14	43.057	5.835	1	85.7	1.000	0.500	0.000	0.139	0.012	0.796
272	2500	14	43.057	5.835	16	71.4	1.000	0.500	0.000	0.139	0.188	0.592
273	2500	14	43.057	5.835	17	57.1	1.000	0.500	0.000	0.139	0.200	0.388
274	2500	14	43.057	5.835	21	42.9	1.000	0.500	0.000	0.139	0.247	0.184
275	2500	12	57.830	5.626	15	83.3	1.000	0.333	0.184	0.115	0.176	0.762
276	2500	12	57.830	5.626	16	66.7	1.000	0.333	0.184	0.115	0.188	0.524
277	2500	12	57.830	5.626	20	50.0	1.000	0.333	0.184	0.115	0.235	0.286
278	2500	10	56.760	5.304	2	80.0	1.000	0.167	0.170	0.079	0.024	0.714
279	2500	10	56.760	5.304	6	60.0	1.000	0.167	0.170	0.079	0.071	0.429
280	2500	8	51.514	4.607	4	75.0	1.000	0.000	0.105	0.000	0.047	0.643
281	2500	20	85.243	9.908	5	90.0	1.000	1.000	0.524	0.599	0.059	0.857
282	2500	20	85.243	9.908	11	80.0	1.000	1.000	0.524	0.599	0.129	0.714
283	2500	20	85.243	9.908	12	70.0	1.000	1.000	0.524	0.599	0.141	0.571
284	2500	20	85.243	9.908	34	60.0	1.000	1.000	0.524	0.599	0.400	0.429
285	2500	20	85.243	9.908	41	50.0	1.000	1.000	0.524	0.599	0.482	0.286
286	2500	20	85.243	9.908	51	40.0	1.000	1.000	0.524	0.599	0.600	0.143
287	2500	20	85.243	9.908	53	30.0	1.000	1.000	0.524	0.599	0.624	0.000
288	2500	18	80.035	9.009	6	88.9	1.000	0.833	0.460	0.497	0.071	0.841
289	2500	18	80.035	9.009	7	77.8	1.000	0.833	0.460	0.497	0.082	0.683
290	2500	18	80.035	9.009	29	66.7	1.000	0.833	0.460	0.497	0.341	0.524
291	2500	18	80.035	9.009	36	55.6	1.000	0.833	0.460	0.497	0.424	0.365
292	2500	18	80.035	9.009	46	44.4	1.000	0.833	0.460	0.497	0.541	0.206
293	2500	18	80.035	9.009	48	33.3	1.000	0.833	0.460	0.497	0.565	0.048
294	2500	16	72.408	8.609	2	87.5	1.000	0.667	0.365	0.452	0.024	0.821
295	2500	16	72.408	8.609	24	75.0	1.000	0.667	0.365	0.452	0.282	0.643
296	2500	16	72.408	8.609	31	62.5	1.000	0.667	0.365	0.452	0.365	0.464
297	2500	16	72.408	8.609	41	50.0	1.000	0.667	0.365	0.452	0.482	0.286
298	2500	16	72.408	8.609	43	37.5	1.000	0.667	0.365	0.452	0.506	0.107
299	2500	14	60.571	8.121	16	85.7	1.000	0.500	0.218	0.397	0.188	0.796
300	2500	14	60.571	8.121	23	71.4	1.000	0.500	0.218	0.397	0.271	0.592
301	2500	14	60.571	8.121	33	57.1	1.000	0.500	0.218	0.397	0.388	0.388
302	2500	14	60.571	8.121	35	42.9	1.000	0.500	0.218	0.397	0.412	0.184
303	2500	12	79.370	7.806	12	83.3	1.000	0.333	0.451	0.361	0.141	0.762
304	2500	12	79.370	7.806	22	66.7	1.000	0.333	0.451	0.361	0.259	0.524
305	2500	12	79.370	7.806	24	50.0	1.000	0.333	0.451	0.361	0.282	0.286
306	2500	10	67.813	7.841	9	80.0	1.000	0.167	0.308	0.365	0.106	0.714
307	2500	10	67.813	7.841	11	60.0	1.000	0.167	0.308	0.365	0.129	0.429
308	2500	8	67.340	6.751	9	75.0	1.000	0.000	0.302	0.242	0.106	0.643
309	2500	20	111.250	12.493	14	90.0	1.000	1.000	0.847	0.890	0.165	0.857
310	2500	20	111.250	12.493	14	80.0	1.000	1.000	0.847	0.890	0.165	0.714
311	2500	20	111.250	12.493	19	70.0	1.000	1.000	0.847	0.890	0.224	0.571
312	2500	20	111.250	12.493	39	60.0	1.000	1.000	0.847	0.890	0.459	0.429
313	2500	20	111.250	12.493	52	50.0	1.000	1.000	0.847	0.890	0.612	0.286
314	2500	20	111.250	12.493	58	40.0	1.000	1.000	0.847	0.890	0.682	0.143
315	2500	20	111.250	12.493	71	30.0	1.000	1.000	0.847	0.890	0.835	0.000

316	2500	18	106.220	11.357	2	88.9	1.000	0.833	0.785	0.762	0.024	0.841
317	2500	18	106.220	11.357	7	77.8	1.000	0.833	0.785	0.762	0.082	0.683
318	2500	18	106.220	11.357	27	66.7	1.000	0.833	0.785	0.762	0.318	0.524
319	2500	18	106.220	11.357	40	55.6	1.000	0.833	0.785	0.762	0.471	0.365
320	2500	18	106.220	11.357	46	44.4	1.000	0.833	0.785	0.762	0.541	0.206
321	2500	18	106.220	11.357	59	33.3	1.000	0.833	0.785	0.762	0.694	0.048
322	2500	16	91.537	11.756	3	87.5	1.000	0.667	0.602	0.807	0.035	0.821
323	2500	16	91.537	11.756	23	75.0	1.000	0.667	0.602	0.807	0.271	0.643
324	2500	16	91.537	11.756	36	62.5	1.000	0.667	0.602	0.807	0.424	0.464
325	2500	16	91.537	11.756	42	50.0	1.000	0.667	0.602	0.807	0.494	0.286
326	2500	16	91.537	11.756	55	37.5	1.000	0.667	0.602	0.807	0.647	0.107
327	2500	14	96.645	11.509	18	85.7	1.000	0.500	0.666	0.779	0.212	0.796
328	2500	14	96.645	11.509	31	71.4	1.000	0.500	0.666	0.779	0.365	0.592
329	2500	14	96.645	11.509	37	57.1	1.000	0.500	0.666	0.779	0.435	0.388
330	2500	14	96.645	11.509	50	42.9	1.000	0.500	0.666	0.779	0.588	0.184
331	2500	12	79.475	10.558	8	83.3	1.000	0.333	0.453	0.672	0.094	0.762
332	2500	12	79.475	10.558	14	66.7	1.000	0.333	0.453	0.672	0.165	0.524
333	2500	12	79.475	10.558	27	50.0	1.000	0.333	0.453	0.672	0.318	0.286
334	2500	10	88.550	10.054	0	100.	1.000	0.167	0.565	0.615	0.000	1.000
335	2500	10	88.550	10.054	13	60.0	1.000	0.167	0.565	0.615	0.153	0.429
336	2500	8	81.870	9.569	12	75.0	1.000	0.000	0.482	0.560	0.141	0.643

APPENDIX G - PCN TRAINING AND TESTING DATA FOR THE NN-AMPC SYSTEM

Training Data (252 samples)

#	S^p (RPM)	f^p (in/min)	Depth (in)	F_{ap}^p (N)	F_{az}^p (N)	ΔR_a	Δf^p	Δf
1	1750	8	0.06	62.7933	5.3854	10	82.00	75.00
2	1750	8	0.08	102.3100	9.7952	11	80.00	75.00
3	1750	10	0.04	52.4374	5.2414	16	72.60	60.00
4	1750	10	0.04	52.4374	5.2414	14	100.00	80.00
5	1750	10	0.06	90.7082	7.9431	13	96.02	80.00
6	1750	10	0.06	90.7082	7.9431	21	72.30	60.00
7	1750	10	0.08	113.4000	10.5116	18	70.00	60.00
8	1750	10	0.08	113.4000	10.5116	10	95.00	80.00
9	1750	12	0.04	56.7756	5.5821	29	84.11	66.67
10	1750	12	0.04	56.7756	5.5821	31	61.00	50.00
11	1750	12	0.06	75.9400	8.9656	23	61.66	66.67
12	1750	12	0.06	75.9400	8.9656	31	65.35	50.00
13	1750	12	0.06	75.9400	8.9656	6	65.40	83.33
14	1750	12	0.08	119.0100	11.0908	11	63.10	83.33
15	1750	12	0.08	119.0100	11.0908	30	69.16	66.67
16	1750	14	0.04	69.5485	6.6034	38	56.36	42.86
17	1750	14	0.04	69.5485	6.6034	11	62.33	85.71
18	1750	14	0.06	66.7785	8.9267	29	73.23	57.14
19	1750	14	0.06	66.7785	8.9267	12	63.39	71.43
20	1750	14	0.06	66.7785	8.9267	4	66.30	85.71
21	1750	14	0.06	66.7785	8.9267	37	56.30	42.86
22	1750	14	0.08	104.2900	11.5517	59	68.10	57.14
23	1750	14	0.08	104.2900	11.5517	23	67.12	85.71
24	1750	14	0.08	104.2900	11.5517	40	67.69	71.43
25	1750	16	0.04	71.8200	5.9493	41	51.75	37.50
26	1750	16	0.04	71.8200	5.9493	1	72.00	87.50
27	1750	16	0.04	71.8200	5.9493	14	62.10	75.00
28	1750	16	0.06	96.5100	8.8189	49	62.60	50.00
29	1750	16	0.06	96.5100	8.8189	8	68.57	87.50
30	1750	16	0.06	96.5100	8.8189	24	70.77	75.00
31	1750	16	0.06	96.5100	8.8189	32	68.37	62.50
32	1750	16	0.08	93.9825	11.8150	81	52.90	37.50
33	1750	16	0.08	93.9825	11.8150	12	66.75	87.50
34	1750	16	0.08	93.9825	11.8150	54	50.45	62.50
35	1750	16	0.08	93.9825	11.8150	73	60.28	50.00
36	1750	18	0.04	69.9409	6.2215	49	50.76	33.33
37	1750	18	0.04	69.9409	6.2215	22	50.93	66.67
38	1750	18	0.04	69.9409	6.2215	9	53.84	77.78
39	1750	18	0.04	69.9409	6.2215	7	75.50	88.89
40	1750	18	0.04	69.9409	6.2215	47	50.73	44.44
41	1750	18	0.06	72.5272	9.5555	25	77.65	77.78
42	1750	18	0.06	72.5272	9.5555	66	52.62	44.44
43	1750	18	0.06	72.5272	9.5555	20	68.70	88.89
44	1750	18	0.06	72.5272	9.5555	74	52.20	33.33
45	1750	18	0.08	111.0609	12.6109	4	67.92	88.89
46	1750	18	0.08	111.0609	12.6109	70	50.04	44.44

47	1750	18	0.08	111.0609	12.6109	78	48.00	33.33
48	1750	18	0.08	111.0609	12.6109	51	76.06	55.56
49	1750	18	0.08	111.0609	12.6109	34	68.03	66.67
50	1750	20	0.04	63.7470	5.8242	63	40.40	30.00
51	1750	20	0.04	63.7470	5.8242	23	50.34	70.00
52	1750	20	0.04	63.7470	5.8242	21	62.30	80.00
53	1750	20	0.04	63.7470	5.8242	17	68.40	90.00
54	1750	20	0.04	63.7470	5.8242	41	50.31	50.00
55	1750	20	0.04	63.7470	5.8242	36	50.31	60.00
56	1750	20	0.04	63.7470	5.8242	61	50.40	40.00
57	1750	20	0.06	104.1400	9.4066	50	63.60	50.00
58	1750	20	0.06	104.1400	9.4066	75	42.10	30.00
59	1750	20	0.06	104.1400	9.4066	67	58.69	40.00
60	1750	20	0.06	104.1400	9.4066	0	76.10	100.00
61	1750	20	0.06	104.1400	9.4066	42	53.03	60.00
62	1750	20	0.06	104.1400	9.4066	26	79.42	70.00
63	1750	20	0.06	104.1400	9.4066	21	71.72	80.00
64	1750	20	0.08	123.5400	13.4634	41	68.22	60.00
65	1750	20	0.08	123.5400	13.4634	16	67.97	70.00
66	1750	20	0.08	123.5400	13.4634	11	67.99	80.00
67	1750	20	0.08	123.5400	13.4634	77	49.54	40.00
68	1750	20	0.08	123.5400	13.4634	22	67.96	90.00
69	2000	8	0.04	51.4891	5.1813	4	85.00	75.00
70	2000	8	0.06	86.8800	7.9123	4	82.30	75.00
71	2000	8	0.08	87.0187	9.0494	3	65.99	75.00
72	2000	10	0.04	49.1525	5.1028	14	72.00	60.00
73	2000	10	0.04	49.1525	5.1028	10	88.00	80.00
74	2000	10	0.06	81.3621	8.2507	7	76.50	80.00
75	2000	10	0.06	81.3621	8.2507	10	42.70	60.00
76	2000	10	0.08	97.9300	10.6725	11	59.40	80.00
77	2000	10	0.08	97.9300	10.6725	11	45.40	60.00
78	2000	12	0.04	64.5132	6.5808	12	98.54	83.33
79	2000	12	0.04	64.5132	6.5808	28	84.00	66.67
80	2000	12	0.06	85.4937	8.6628	13	81.19	83.33
81	2000	12	0.06	85.4937	8.6628	28	43.80	50.00
82	2000	12	0.06	85.4937	8.6628	25	53.88	66.67
83	2000	12	0.08	74.0992	11.2944	28	49.60	66.67
84	2000	12	0.08	74.0992	11.2944	28	32.59	50.00
85	2000	12	0.08	74.0992	11.2944	10	66.80	83.33
86	2000	14	0.04	63.5755	6.4570	15	93.37	85.71
87	2000	14	0.04	63.5755	6.4570	22	87.90	71.43
88	2000	14	0.04	63.5755	6.4570	42	56.30	42.86
89	2000	14	0.04	63.5755	6.4570	38	70.60	57.14
90	2000	14	0.06	74.0680	8.4221	35	35.69	57.14
91	2000	14	0.06	74.0680	8.4221	38	38.74	42.86
92	2000	14	0.06	74.0680	8.4221	23	57.44	71.43
93	2000	14	0.06	74.0680	8.4221	9	63.96	85.71
94	2000	14	0.08	91.9936	11.2381	23	64.36	71.43
95	2000	14	0.08	91.9936	11.2381	3	72.40	85.71
96	2000	14	0.08	91.9936	11.2381	41	71.37	57.14
97	2000	16	0.04	51.0175	5.7246	37	54.07	37.50
98	2000	16	0.04	51.0175	5.7246	17	67.05	62.50
99	2000	16	0.04	51.0175	5.7246	33	55.94	50.00
100	2000	16	0.06	66.8951	7.8037	38	62.94	50.00

101	2000	16	0.06	66.8951	7.8037	26	67.30	62.50
102	2000	16	0.06	66.8951	7.8037	5	67.43	87.50
103	2000	16	0.06	66.8951	7.8037	12	67.80	75.00
104	2000	16	0.08	82.5480	10.2688	24	67.44	62.50
105	2000	16	0.08	82.5480	10.2688	42	48.46	50.00
106	2000	18	0.04	66.0202	6.0393	8	69.80	88.89
107	2000	18	0.04	66.0202	6.0393	26	52.47	66.67
108	2000	18	0.04	66.0202	6.0393	33	51.66	55.56
109	2000	18	0.06	73.7309	9.2007	29	73.56	55.56
110	2000	18	0.06	73.7309	9.2007	12	70.00	88.89
111	2000	18	0.06	73.7309	9.2007	15	68.13	66.67
112	2000	18	0.06	73.7309	9.2007	44	45.10	33.33
113	2000	18	0.08	108.3861	11.3984	13	72.80	88.89
114	2000	18	0.08	108.3861	11.3984	53	46.39	33.33
115	2000	18	0.08	108.3861	11.3984	15	67.83	66.67
116	2000	18	0.08	108.3861	11.3984	35	68.19	55.56
117	2000	18	0.08	108.3861	11.3984	21	67.86	77.78
118	2000	18	0.08	108.3861	11.3984	53	46.39	44.44
119	2000	20	0.04	70.0569	6.1482	55	44.50	30.00
120	2000	20	0.04	70.0569	6.1482	2	72.40	90.00
121	2000	20	0.04	70.0569	6.1482	51	50.53	40.00
122	2000	20	0.04	70.0569	6.1482	35	50.70	50.00
123	2000	20	0.06	91.1100	9.9167	49	47.87	30.00
124	2000	20	0.06	91.1100	9.9167	17	68.22	80.00
125	2000	20	0.06	91.1100	9.9167	20	68.33	60.00
126	2000	20	0.06	91.1100	9.9167	7	67.99	90.00
127	2000	20	0.06	91.1100	9.9167	34	55.38	50.00
128	2000	20	0.08	112.8915	12.3742	73	44.09	30.00
129	2000	20	0.08	112.8915	12.3742	73	44.09	40.00
130	2000	20	0.08	112.8915	12.3742	33	68.13	80.00
131	2000	20	0.08	112.8915	12.3742	22	67.96	90.00
132	2000	20	0.08	112.8915	12.3742	55	45.04	50.00
133	2250	8	0.04	43.0480	4.8108	2	64.17	75.00
134	2250	8	0.06	58.9500	6.7910	5	63.84	75.00
135	2250	8	0.08	82.7786	8.9116	1	63.86	75.00
136	2250	10	0.04	54.7100	5.4249	5	59.84	80.00
137	2250	10	0.04	54.7100	5.4249	10	63.82	60.00
138	2250	10	0.08	69.4344	9.3792	7	53.02	80.00
139	2250	12	0.04	58.2334	5.8052	26	60.60	50.00
140	2250	12	0.04	58.2334	5.8052	11	82.52	83.33
141	2250	12	0.04	58.2334	5.8052	21	51.36	66.67
142	2250	12	0.06	71.0565	8.1031	26	55.78	50.00
143	2250	12	0.06	71.0565	8.1031	9	80.51	83.33
144	2250	12	0.08	96.1082	11.0414	20	73.22	83.33
145	2250	12	0.08	96.1082	11.0414	25	63.90	50.00
146	2250	14	0.04	55.4474	6.0157	28	75.10	57.14
147	2250	14	0.04	55.4474	6.0157	18	90.00	71.43
148	2250	14	0.04	55.4474	6.0157	33	61.70	42.86
149	2250	14	0.06	80.7202	9.5229	39	58.40	42.86
150	2250	14	0.06	80.7202	9.5229	17	96.19	85.71
151	2250	14	0.08	95.5042	11.5980	20	83.83	85.71
152	2250	14	0.08	95.5042	11.5980	46	75.90	57.14
153	2250	14	0.08	95.5042	11.5980	37	86.20	71.43
154	2250	16	0.04	53.0544	6.1137	20	81.50	62.50

155	2250	16	0.04	53.0544	6.1137	9	89.80	75.00
156	2250	16	0.04	53.0544	6.1137	30	69.70	50.00
157	2250	16	0.04	53.0544	6.1137	6	99.30	87.50
158	2250	16	0.06	64.7254	8.1973	40	59.10	37.50
159	2250	16	0.06	64.7254	8.1973	0	79.20	100.00
160	2250	16	0.06	64.7254	8.1973	18	70.16	75.00
161	2250	16	0.06	64.7254	8.1973	35	58.09	50.00
162	2250	16	0.06	64.7254	8.1973	23	44.40	62.50
163	2250	16	0.08	92.4288	11.1076	38	74.10	62.50
164	2250	16	0.08	92.4288	11.1076	43	55.40	37.50
165	2250	16	0.08	92.4288	11.1076	6	72.10	87.50
166	2250	16	0.08	92.4288	11.1076	21	55.72	75.00
167	2250	18	0.04	63.9631	5.7857	32	55.58	55.56
168	2250	18	0.04	63.9631	5.7857	42	50.49	44.44
169	2250	18	0.04	63.9631	5.7857	21	66.03	66.67
170	2250	18	0.04	63.9631	5.7857	18	69.95	77.78
171	2250	18	0.04	63.9631	5.7857	17	71.25	88.89
172	2250	18	0.06	85.5838	9.2114	4	65.68	77.78
173	2250	18	0.06	85.5838	9.2114	46	39.47	44.44
174	2250	18	0.06	85.5838	9.2114	29	66.24	66.67
175	2250	18	0.06	85.5838	9.2114	34	41.75	55.56
176	2250	18	0.08	83.6297	11.3713	39	70.40	55.56
177	2250	18	0.08	83.6297	11.3713	44	49.10	33.33
178	2250	18	0.08	83.6297	11.3713	7	62.51	77.78
179	2250	18	0.08	83.6297	11.3713	6	69.20	88.89
180	2250	18	0.08	83.6297	11.3713	22	65.92	66.67
181	2250	20	0.04	70.1200	7.5203	22	62.45	80.00
182	2250	20	0.04	70.1200	7.5203	52	50.88	30.00
183	2250	20	0.04	70.1200	7.5203	47	53.63	40.00
184	2250	20	0.04	70.1200	7.5203	26	63.14	60.00
185	2250	20	0.04	70.1200	7.5203	23	62.17	70.00
186	2250	20	0.06	89.6100	10.6819	56	39.55	30.00
187	2250	20	0.06	89.6100	10.6819	9	67.61	70.00
188	2250	20	0.06	89.6100	10.6819	23	67.96	80.00
189	2250	20	0.06	89.6100	10.6819	39	60.66	50.00
190	2250	20	0.08	100.1053	12.0582	33	68.03	60.00
191	2250	20	0.08	100.1053	12.0582	18	67.66	70.00
192	2250	20	0.08	100.1053	12.0582	59	39.60	40.00
193	2250	20	0.08	100.1053	12.0582	50	52.54	50.00
194	2250	20	0.08	100.1053	12.0582	55	40.88	30.00
195	2500	8	0.04	51.5142	4.6071	4	60.85	75.00
196	2500	8	0.06	67.3400	6.7506	9	62.50	75.00
197	2500	10	0.04	56.7600	5.3041	6	62.48	60.00
198	2500	10	0.06	67.8134	7.8414	11	60.20	60.00
199	2500	10	0.06	67.8134	7.8414	9	58.28	80.00
200	2500	10	0.08	88.5500	10.0541	0	81.70	100.00
201	2500	10	0.08	88.5500	10.0541	13	46.83	60.00
202	2500	12	0.04	57.8300	5.6261	20	55.75	50.00
203	2500	12	0.04	57.8300	5.6261	15	68.80	83.33
204	2500	12	0.06	79.3700	7.8064	12	68.10	83.33
205	2500	12	0.06	79.3700	7.8064	22	59.50	66.67
206	2500	12	0.06	79.3700	7.8064	24	57.36	50.00
207	2500	12	0.08	79.4745	10.5584	27	64.86	50.00
208	2500	12	0.08	79.4745	10.5584	8	66.50	83.33

209	2500	12	0.08	79.4745	10.5584	14	61.55	66.67
210	2500	14	0.04	43.0569	5.8349	21	59.82	42.86
211	2500	14	0.04	43.0569	5.8349	17	52.45	57.14
212	2500	14	0.04	43.0569	5.8349	1	95.04	85.71
213	2500	14	0.06	60.5712	8.1205	33	45.04	57.14
214	2500	14	0.06	60.5712	8.1205	35	44.81	42.86
215	2500	14	0.08	96.6450	11.5089	50	52.83	42.86
216	2500	14	0.08	96.6450	11.5089	31	69.83	71.43
217	2500	16	0.04	55.1031	6.1842	26	48.40	62.50
218	2500	16	0.04	55.1031	6.1842	27	48.68	50.00
219	2500	16	0.04	55.1031	6.1842	9	69.80	87.50
220	2500	16	0.06	72.4081	8.6088	2	97.33	87.50
221	2500	16	0.06	72.4081	8.6088	31	50.50	62.50
222	2500	16	0.06	72.4081	8.6088	24	54.72	75.00
223	2500	16	0.06	72.4081	8.6088	41	61.21	50.00
224	2500	16	0.08	91.5365	11.7560	36	68.11	62.50
225	2500	16	0.08	91.5365	11.7560	55	56.00	37.50
226	2500	16	0.08	91.5365	11.7560	3	97.59	87.50
227	2500	16	0.08	91.5365	11.7560	42	61.78	50.00
228	2500	18	0.04	58.2355	6.2086	1	91.40	88.89
229	2500	18	0.04	58.2355	6.2086	30	67.70	55.56
230	2500	18	0.04	58.2355	6.2086	15	82.10	66.67
231	2500	18	0.04	58.2355	6.2086	13	82.94	77.78
232	2500	18	0.04	58.2355	6.2086	35	54.10	33.33
233	2500	18	0.06	80.0349	9.0088	48	48.60	33.33
234	2500	18	0.06	80.0349	9.0088	36	35.49	55.56
235	2500	18	0.06	80.0349	9.0088	6	97.29	88.89
236	2500	18	0.06	80.0349	9.0088	46	65.30	44.44
237	2500	18	0.08	106.2200	11.3570	46	59.30	44.44
238	2500	18	0.08	106.2200	11.3570	2	74.80	88.89
239	2500	18	0.08	106.2200	11.3570	40	75.80	55.56
240	2500	18	0.08	106.2200	11.3570	59	35.91	33.33
241	2500	20	0.04	64.1100	6.6752	18	80.20	70.00
242	2500	20	0.04	64.1100	6.6752	36	51.50	40.00
243	2500	20	0.04	64.1100	6.6752	6	97.12	80.00
244	2500	20	0.04	64.1100	6.6752	35	62.50	50.00
245	2500	20	0.06	85.2428	9.9081	12	66.92	70.00
246	2500	20	0.06	85.2428	9.9081	53	44.60	30.00
247	2500	20	0.06	85.2428	9.9081	34	56.32	60.00
248	2500	20	0.06	85.2428	9.9081	11	66.53	80.00
249	2500	20	0.08	111.2500	12.4934	19	62.79	70.00
250	2500	20	0.08	111.2500	12.4934	52	45.95	50.00
251	2500	20	0.08	111.2500	12.4934	14	60.53	80.00
252	2500	20	0.08	111.2500	12.4934	39	75.08	60.00

Testing Data (84 samples)

#	S^p (RPM)	f^p (in/min)	Depth (in)	F_{ap}^p (N)	F_{az}^p (N)	ΔR_a	Δf^p	Δf
1	1750	8	0.04	61.2800	5.1687	4	85.00	75.00
2	1750	12	0.04	56.7756	5.5821	9	96.46	83.33
3	1750	12	0.08	119.0100	11.0908	38	70.51	50.00
4	1750	14	0.04	69.5485	6.6034	16	58.30	71.43
5	1750	14	0.04	69.5485	6.6034	36	56.38	57.14
6	1750	14	0.08	104.2900	11.5517	67	61.40	42.86
7	1750	16	0.04	71.8200	5.9493	19	51.76	62.50
8	1750	16	0.04	71.8200	5.9493	39	51.69	50.00
9	1750	16	0.06	96.5100	8.8189	57	54.20	37.50
10	1750	16	0.08	93.9825	11.8150	37	68.20	75.00
11	1750	18	0.04	69.9409	6.2215	27	50.74	55.56
12	1750	18	0.06	72.5272	9.5555	41	64.77	66.67
13	1750	18	0.06	72.5272	9.5555	49	60.17	55.56
14	1750	18	0.08	111.0609	12.6109	9	67.98	77.78
15	1750	20	0.08	123.5400	13.4634	85	46.70	30.00
16	1750	20	0.08	123.5400	13.4634	58	53.06	50.00
17	2000	12	0.04	64.5132	6.5808	32	68.40	50.00
18	2000	14	0.08	91.9936	11.2381	41	61.40	42.86
19	2000	16	0.04	51.0175	5.7246	3	69.70	87.50
20	2000	16	0.04	51.0175	5.7246	10	68.52	75.00
21	2000	16	0.06	66.8951	7.8037	41	50.80	37.50
22	2000	16	0.08	82.5480	10.2688	10	66.62	87.50
23	2000	16	0.08	82.5480	10.2688	42	48.46	37.50
24	2000	16	0.08	82.5480	10.2688	4	66.06	75.00
25	2000	18	0.04	66.0202	6.0393	53	46.90	33.33
26	2000	18	0.04	66.0202	6.0393	19	64.30	77.78
27	2000	18	0.04	66.0202	6.0393	49	50.98	44.44
28	2000	18	0.06	73.7309	9.2007	41	58.71	44.44
29	2000	18	0.06	73.7309	9.2007	8	67.89	77.78
30	2000	20	0.04	70.0569	6.1482	21	52.28	70.00
31	2000	20	0.04	70.0569	6.1482	28	51.10	60.00
32	2000	20	0.04	70.0569	6.1482	10	59.13	80.00
33	2000	20	0.06	91.1100	9.9167	46	45.23	40.00
34	2000	20	0.06	91.1100	9.9167	13	68.07	70.00
35	2000	20	0.08	112.8915	12.3742	41	69.21	70.00
36	2000	20	0.08	112.8915	12.3742	35	68.22	60.00
37	2250	10	0.06	57.3311	7.6380	10	51.98	60.00
38	2250	10	0.06	57.3311	7.6380	5	62.20	80.00
39	2250	10	0.08	69.4344	9.3792	3	57.57	60.00
40	2250	12	0.06	71.0565	8.1031	21	69.78	66.67
41	2250	12	0.08	96.1082	11.0414	29	84.20	66.67
42	2250	14	0.04	55.4474	6.0157	7	94.50	85.71
43	2250	14	0.06	80.7202	9.5229	22	87.10	71.43
44	2250	14	0.06	80.7202	9.5229	34	65.40	57.14
45	2250	14	0.08	95.5042	11.5980	42	60.70	42.86
46	2250	16	0.04	53.0544	6.1137	35	58.40	37.50
47	2250	16	0.08	92.4288	11.1076	47	42.04	50.00
48	2250	18	0.04	63.9631	5.7857	47	48.43	33.33
49	2250	18	0.06	85.5838	9.2114	51	45.17	33.33

50	2250	18	0.06	85.5838	9.2114	18	67.00	88.89
51	2250	18	0.08	83.6297	11.3713	48	38.86	44.44
52	2250	20	0.04	70.1200	7.5203	37	61.44	50.00
53	2250	20	0.04	70.1200	7.5203	6	80.20	90.00
54	2250	20	0.06	89.6100	10.6819	34	76.83	60.00
55	2250	20	0.06	89.6100	10.6819	1	77.40	90.00
56	2250	20	0.06	89.6100	10.6819	51	38.74	40.00
57	2250	20	0.08	100.1053	12.0582	12	77.50	90.00
58	2250	20	0.08	100.1053	12.0582	17	67.64	80.00
59	2500	8	0.08	81.8700	9.5688	12	56.60	75.00
60	2500	10	0.04	56.7600	5.3041	2	62.83	80.00
61	2500	12	0.04	57.8300	5.6261	16	53.04	66.67
62	2500	14	0.04	43.0569	5.8349	16	55.40	71.43
63	2500	14	0.06	60.5712	8.1205	23	53.80	71.43
64	2500	14	0.06	60.5712	8.1205	16	64.10	85.71
65	2500	14	0.08	96.6450	11.5089	37	72.04	57.14
66	2500	14	0.08	96.6450	11.5089	18	66.09	85.71
67	2500	16	0.04	55.1031	6.1842	11	47.80	75.00
68	2500	16	0.04	55.1031	6.1842	31	60.48	37.50
69	2500	16	0.06	72.4081	8.6088	43	54.50	37.50
70	2500	16	0.08	91.5365	11.7560	23	75.37	75.00
71	2500	18	0.04	58.2355	6.2086	31	62.80	44.44
72	2500	18	0.06	80.0349	9.0088	7	97.42	77.78
73	2500	18	0.06	80.0349	9.0088	29	53.40	66.67
74	2500	18	0.08	106.2200	11.3570	27	78.10	66.67
75	2500	18	0.08	106.2200	11.3570	7	58.30	77.78
76	2500	20	0.04	64.1100	6.6752	20	71.30	60.00
77	2500	20	0.04	64.1100	6.6752	9	93.77	90.00
78	2500	20	0.04	64.1100	6.6752	40	44.70	30.00
79	2500	20	0.06	85.2428	9.9081	51	51.80	40.00
80	2500	20	0.06	85.2428	9.9081	5	73.70	90.00
81	2500	20	0.06	85.2428	9.9081	41	63.34	50.00
82	2500	20	0.08	111.2500	12.4934	14	70.50	90.00
83	2500	20	0.08	111.2500	12.4934	58	38.74	40.00
84	2500	20	0.08	111.2500	12.4934	71	38.57	30.00

APPENDIX H - THE PROGRAM OF THE NN-IASRC SYSTEM

```
/* ---------------------------------------*/
/* The NN-IASRC System Program */
/* ---------------------------------------*/

#include "stdio.h"
#include "conio.h"
#include "dos.h"
#include "cb.h"
#include "time.h"
#define MAX(i,j) (i>j)?i:j
#define ABS(i)(i<0)?-i:i
#define number 2000
#define e 2.718282
typedef unsigned int WORD;                    /* 16-bit unsigned int */
clock_t begin,end;

void ClearScreen (void);                      /* Prototypes */
void GetTextCursor (int *x, int *y);
void MoveCursor (int x, int y);

void main ()
   {
   float data[number][4],combxy[number],Max[80];
   int point[4];
   int i,j,k,pmax,per_tooth,range,length,peak1;
   float h_peak,avg1,avg_z,sumf_z,g,t;
   float S,f,ra,pra,dra,df;
   float h11,h12,h13,h14,h15,h21,h22,h23,h24,h25;
   float ah11,ah12a,h13,ah14,ah15,ah16,ah17,ah18,ah21,ah22,ah23,ah24,ah25,ah26,ah27;

   int Row,Col,Row2,Col2;
   int BoardNum = 0;
   int UDStat = 0;
   int Chan0=0,Chan1=1,Chan2=2,Chan3=3, I=0;
   int Gain0 = BIP10VOLTS;                    /*Proximity data channel*/
   int Gain1 = BIP10VOLTS;                    /*X channel*/
   int Gain2 = BIP10VOLTS;                    /*Y channel*/
   int Gain3 = BIP10VOLTS;                    /*Z channel*/
   float data[2000][4], EngUnits,RevLevel = (float)CURRENTREVNUM;
   WORD DataValue0 = 0;
   WORD DataValue1 = 0;
   WORD DataValue2 = 0;
   WORD DataValue3 = 0;

    UDStat = cbDeclareRevision(&RevLevel);    /* Declare UL Revision Level */

   cbErrHandling (PRINTALL, STOPALL);
```

```
/************************************************/
/* set up the screen  & input the machining parameters */
/************************************************/

 ClearScreen();
    printf("input the spindle speed : ");
    scanf("%f", &S);
    printf("input the feed rate : ");
    scanf("%f", &f);
    printf("input the feed rate : ");
    scanf("%f", &ra);
    getchar();

  printf ("Demonstration of cbAIn()\n");
  printf("Press any key to start A/D converting.\n");
  getchar();
  begin=clock();                    /* clock starts       */

 /* collect the sample from the channel until a key is pressed */
  for (I=0;I<number;I++)
         {
         UDStat =cbAIn (BoardNum, Chan0, Gain0, &DataValue0);
         UDStat =cbToEngUnits (BoardNum, Gain0, DataValue0, &EngUnits);
         data[I][0]=EngUnits;

         UDStat =cbAIn (BoardNum, Chan1, Gain1, &DataValue1);
          UDStat =cbToEngUnits (BoardNum, Gain1, DataValue1, &EngUnits);
         data[I][1]=EngUnits;

          UDStat =cbAIn (BoardNum, Chan2, Gain2, &DataValue2);
         UDStat =cbToEngUnits (BoardNum, Gain2, DataValue2, &EngUnits);
         data[I][2]=EngUnits;

         UDStat =cbAIn (BoardNum, Chan3, Gain3, &DataValue3);
         UDStat =cbToEngUnits (BoardNum, Gain3, DataValue3, &EngUnits);
         data[I][3]=EngUnits;
         }

  end=clock();
  printf(" A/D Convert is finished and the converted time is %7.4f\n seconds",(end-begin)/CLK_TCK);

   for (I=0; I<number; I++)
   {
    data[I][1]=(data[I][1]+data[I+1][1])/2;
    data[I][2]=(data[I][2]+data[I+1][2])/2;
    data[I][3]=(data[I][3]+data[I+1][3])/2;
   }

 /* obtain the resultant force in XY plant and absolute force in Z direction */
  for(i=0; i<number; i++)
  {
   combxy[i]=sqrt( pow(data[i][1],2) + pow(data[i][2],2));
   data[i][3]=ABS(data[i][3]);
  }
```

```
for(h_peak=combxy[50], i=50; i<number; ++i)      /* find the max. value of voltage */
  if (h_peak<combxy[i])
  {
       h_peak=combxy[i];
       pmax=i;
  }

j=0;
for(i=50; i<number; i++)                         /* find the value of range and per tooth */
  if (data[i-1][0]<1 && data[i][0]>1)
  {
   point[j] = i;
   j++;
  }

range=point[2]-point[0];
per_tooth=(point[2]-point[0])/4;

length=pmax-per_tooth;                           /* find the first peak value */
while (length>50)
{
  pmax=pmax-per_tooth;
  length=pmax-per_tooth;
}
peak1=pmax;

/* find all peak of the data */
i=peak1;
k=0;

while (k<68)
{
 g=0;
   for (i=peak1; i<peak1+5; i++)
   g=MAX(combxy[i-2],g);
 Max[k]=g;
 peak1=peak1+per_tooth;
 k=k+1;
}


/*****************************************/
/* Calculate the average peak force for 17 rev. */
/*****************************************/
  avg1=0;
  for (i=0; i<67; i++)
     avg1=Max[i]+avg1;
  avg1=50*avg1/68;

  printf("Average peak force for 17 rev. = %7.4f\n", avg1);
```

```
/************************************/
/* Calculate the average force for 17 rev. */
/************************************/
   sumf_z=0;
   for (i=point[0]; i<point[0]+range*17; i++)
      sumf_z=data[i][3]+sumf_z;
   avg_z=50*sumf_z/(range*17);
   printf("average force in Z for 17 Rev.= %7.4f\n", avg_z);


/***************************************/
/* Calculate the predicted surface roughness */
/***************************************/

  /* neurons in hidden layer 1 */
   h11=1/(1+pow(e,-((S*(-0.4581)+f*2.649+avg1*(-6.3270)+avg_z*(-0.5697))-1.7790)));
   h12=1/(1+pow(e,-((S*(-2.391)+f*4.342+avg1*1.279+avg_z*(-2.355))-2.247)));
   h13=1/(1+pow(e,-((S*(-0.8417)+f*8.572+avg1*(-1.31)+avg_z*(-0.2232))-0.8322)));
   h14=1/(1+pow(e,-((S*(-9.444)+f*6.33+avg1*(-0.332)+avg_z*3.401)-6.775)));
   h15=1/(1+pow(e,-((S*(-0.6358)+f*1.114+avg1*(-2.5)+avg_z*(-7.686))+9.427)));

  /* neurons in hidden layer 2 */
   h21=1/(1+pow(e,-((h11*0.6004+h12*(-1.724)+h13*3.817+h14*9.769+h15*(-4.371))-2.072)));
   h22=1/(1+pow(e,-((h11*(-1.003)+h12*0.3169+h13*(-0.8317)+h14*(-2.959)+h15*(-0.7604))+0.0563)));
   h23=1/(1+pow(e,-((h11*1.342+h12*(-0.5514)+h13*(-1.698)+h14*0.0233+h15*0.5712)+0.0774)));
   h24=1/(1+pow(e,-((h11*(-3.063)+h12*1.778+h13*(-3.281)+h14*(-3.504)+h15*0.2006)+0.8216)));
   h25=1/(1+pow(e,-((h11*2.238+h12*(-1.119)+h13*(-4.204)+h14*3.15+h15*3.327)-0.2851)));

   /* output layer */
   pra=1/(1+pow(e,-((h21*4.183+h22*2.21+h23*(-0.4757)+h24*4.236+h25*(-5.034))-0.0021)));
   pra=pra*110+21;

   printf("The predicted surface roughness =  %4.0f\n", pra);


/***************************************/
/* Calculate the adaptive degree of feed rate  */
/***************************************/

   dra=pra-ra;
   if (dra>0)
   {
      /* neurons in hidden layer 1 */
      ah11=1/(1+pow(e,-((S*0.956+f*(-6.845)+avg1*4.977+avg_z*0.901+dra*3.622)-5.096)));
      ah12=1/(1+pow(e,-((S*13.94+f*(-12.72)+avg1*(-3.587)+avg_z*(-3.852)+dra*1.216)+0.9653)));
      ah13=1/(1+pow(e,-((S*12.45+f*(-16.27)+avg1*(-1.763)+avg_z*6.361+dra*12.7)-6.856)));
      ah14=1/(1+pow(e,-((S*(-1.902)+f*(-14.63)+avg1*(-6.668)+avg_z*11.47+dra*(-13.45))+4.465)));
      ah15=1/(1+pow(e,-((S*1.991+f*(-6.303)+avg1*2.087+avg_z*15.17+dra*(-23.8))+1.697)));
      ah16=1/(1+pow(e,-((S*7.351+f*(-10.56)+avg1*(-1.44)+avg_z*3.087+dra*(-4.257))+2.729)));
      ah17=1/(1+pow(e,-((S*(-4.407)+f*(-9.066)+avg1*(-0.302)+avg_z*1.678+dra*(-9.934))+6.046)));
      ah18=1/(1+pow(e,-((S*(-4.232)+f*3.032+avg1*(-5.964)+avg_z*(-15.14)+dra*10.62)+2.392)));

      /* neurons in hidden layer 2 */
```

```
    ah21=1/(1+pow(e,-((ah11*(-7.441)+ah12*(-8.904)+ah13*7.5+ah14*(-2.54)+ah15*(-12.13)
          +ah16*0.932+ah17*(-3.764)+ah18*(-6.534))+1.26)));
    ah22=1/(1+pow(e,-((ah11*10.88+ah12*(-1.626)+ah13*(-15.25)+ah14*(-0.868)+ah15*(-4.868)
          +ah16*8.598+ah17*6.914+ah18*2.597)-4.854)));
    ah23=1/(1+pow(e,-((ah11*3.89+ah12*(-7.147)+ah13*(-4.278)+ah14*1.734+ah15*1.296
          +ah16*0.142+ah17*(-12.16)+ah18*0.101)+2.337)));
    ah24=1/(1+pow(e,-((ah11*(-3.914)+ah12*(-0.887)+ah13*(-4.484)+ah14*(-9.715)+ah15*(-5.116)
          +ah16*6.762+ah17*13.1+ah18*(-6.608))-2.277)));
    ah25=1/(1+pow(e,-((ah11*3.643+ah12*(-1.074)+ah13*1.353+ah14*(-4.294)+ah15*(-0.118)
          +ah16*2.916+ah17*1.613+ah18*(-4.493))-5.393)));
    ah26=1/(1+pow(e,-((ah11*(-8.477)+ah12*(-11.41)+ah13*5.95+ah14*(-3.269)+ah15*(-17.2)
          +ah16*4.194+ah17*(-0.923)+ah18*(-5.893))+0.681)));
    ah27=1/(1+pow(e,-((ah11*11.14+ah12*(-3.871)+ah13*(-4.443)+ah14*(-5.152)+ah15*2.843
          +ah16*(0.13)+ah17*(-15.28)+ah18*(-3.189))+3.06)));

    /* output layer */
    df=1/(1+pow(e,-((ah21*7.701+ah22*18.88+ah23*(-5.973)+ah24*(-15.9)+ah25*(-7.395)
          + ah26*(-10.47)+ah27*6.053)-0.008)));
    df=df*70+30;

    printf("The predicted Ra is larger than the actual Ra by   %4.0f\n", dra);
    printf("The adaptive degree of feed rate should be   %6.2f\n", df);
  }

  else
    printf("The quality of the surface roughness is in control.\n");


  exit(0);
  return;
}


/*****************************************************************************
* Name:    ClearScreen
*****************************************************************************/
#define BIOS_VIDEO  0x10

void
ClearScreen (void)
{
  union REGS InRegs,OutRegs;
  InRegs.h.ah = 0;
  InRegs.h.al = 2;
  int86 (BIOS_VIDEO, &InRegs, &OutRegs);

  return;
}
```

```
/*****************************************************************************
* Name:     MoveCursor
*****************************************************************************/
void
MoveCursor (int x, int y)
{
   union REGS InRegs,OutRegs;
   InRegs.h.ah = 2;
   InRegs.h.dl = (char) x;
   InRegs.h.dh = (char) y;
   InRegs.h.bh = 0;
   int86 (BIOS_VIDEO, &InRegs, &OutRegs);

   return;
}


/*****************************************************************************
* Name:     GetTextCursor
*****************************************************************************/
void
GetTextCursor (int *x, int *y)
{
   union REGS InRegs,OutRegs;
   InRegs.h.ah = 3;
   InRegs.h.bh = 0;
   int86 (BIOS_VIDEO, &InRegs, &OutRegs);
   *x = OutRegs.h.dl;
   *y = OutRegs.h.dh;

   return;
}
```

APPENDIX I - NC PROGRAM FOR THE NN-IASRC SYSTEM

```
%
N5 O9993                          /* Program number */
N10 G90 G80 G40 G17               /* Safety feature */
N20 T16 M6                        /* Change tool to tool #16 */
N30 E7 G0 X-.3 Y.35 Z0.3          /* Set program zero & move to (-.3,.35,.3) */
N40 S215000 M3                    /* Control the spindle speed */
N50 G1 Z-0.005 F15.               /* Control the feed rate and depth of cut */
N60 G1 X2.8
N70 G0 Z0.2
N80 G0 X-.3
N90 G1 Z-0.045                    /* Control the depth of cut */
N100 G1 X1.25
N110 G1 X1.0 Y.35 Z.1
N120 M1                           /* Optional stop the machine */
N130 M3                           /* Turn on the spindle speed */
N140 G1 X1.25 Z-0.045
N150 G1 X2.8
N160 G0 Z0.2
N170 G91 G28 X0.0 Y0.0 Z1.0 M5
N180 M30                          /* End of program */
%
```

REFERENCES

Astrom K. J, & Wittenmark B. (1989). *Adaptive control.* NY: Addison-Wesley.

Baek, D. K., Ko, T. J. & Kim, H. S. (1997). A dynamic surface roughness model for face milling. *Precision Engineering*, Vol. 20, pp. 171-178.

Blessing G. V., Slotwinski, J. A. Eitzen, D. G. & Ryan, H. M. (1993). Ultrasonic measurements of surface roughness. *Applied Optics*, Vol. 32, No. 19, pp. 3433-3437.

Black, J. T. (1991). *The design of the factory with a future.* NY: McGraw-Hill, Inc.

Chang, M. & Lin, P. P. (1999). On-line free form surface measurement via a fuzzy-logic controlled scanning probe. *Int. J. Mach. Tools Manufact.*. Vol. 39, pp. 537-552.

Chen, J. C. (1996). A fuzzy-nets tool breakage detection system for end milling operations. *International Journal of Advanced Manufacturing Technology*, Vol. 12, pp. 153-164.

Chen, J. C. & Black, J. T. (1997). A fuzzy-nets in-process (FNIP) system for tool-breakage monitoring in end-milling operations. *Int. J. Mach. Tools Manufact.*, Vol. 37, No. 6, pp. 783-800.

Chen, J. C. & Lou, M. S. (2000). Fuzzy-nets based approach to using an accelerometer for an in-process surface roughness prediction system in milling operation. *International Journal of Computer Integrated Manufacturing*, Vol. 13, No. 4, pp. 358-368.

Coker, S. A. & Shin, Y. C. (1996). In-process control of surface roughness due to tool wear using a new ultrasonic system. *Int. J. Mach. Tools Manufact.*. Vol. 36, No. 3, pp. 411-422.

Cui, X. & Shin, K. G. (1993). Direct control and coordination using neural networks. *IEEE Trans. System, Man, and Cybernation.* Vol. 23, No. 3, pp. 686-697.

DeGarmo E. P., Black J. T. & Kohser R. A. (1997). *Materials and processes in manufacturing-8th edition.* NJ: Prentice Hall.

Dornfield, D. A. & Fei, R. Y. (1986). In-process surface finish characterization. *Manufacturing Simulation Processes*, Vol. 20, pp. 191-204.

Elanayar, S. & Shin, Y. C. (1995). Robust tool wear estimation with radial basis fusction neural network. *Journal of Dynamic Systems, Measurement, and Control*, Vol. 117, pp. 459-467.

Elbestawi, M. A., Ismail, F. & Yuen, K. M. (1994). Surface topography characterization in finish milling. *Int. J. Mach. Tools Manufact.*. Vol. 34, No. 2, pp. 245-255.

Elbestawi, M. A., Papazafiriou, T. A. & Du, R. X. (1991). In-process monitoring of tool wear in milling using cutting force signature. . *Int. J. Mach. Tools Manufact.*. Vol. 31, No. 1, pp. 55-73.

Fuh, K. H. & Wu, C. F. (1995). A proposed statistical model for surface quality prediction in end-milling of Al alloy. *Int. J. Mach. Tools Manufact.*. Vol. 35, No. 8, pp. 1187-1200.

Gong, W., Obikawa, T. & Shirakashi, T. (1997). Monitoring of tool wear states in turning based on Wavelet analysis. *JSME International Journal,* Vol. 40, No. 3, pp. 447-453.

Hemerly, E. M. & Nascimento, C. L. (1999). An NN-based approach for tuning servocontrollers. *Neural Networks*, Vol. 12, pp. 513-518.

Honeywell Microswitch (1997). *Operation Instructions: Proximity sensors*. CA: Honeywell Microswitch Corp..

Huang, P. T. (1998). A fuzzy logic approach to detect the tool breakage using a dynamometer sensor. *Master Thesis*, IA: Iowa State University

Inasaki I. (1985). In-process measurement of surface roughness during cylindrical grinding process. *Precision Engineering,* Vol. 7, No. 2, pp. 73-76.

Ismail, F., Elbestawi, M. A., Du, R. & Urbasik, K. (1993). Generation of milled surface including tool dynamics and wear. *Journal of Engineering for Industry*, Vol. 115, pp. 245-252.

Jang, J. S., Sun, C. T. & Mizutani, E. (1997). *Neuro-Fuzzy and Soft Computing*. NJ: Prentice Hall.

Jansson, D. G., Rourke, J. M. & Bell, A. C. (1984). High-speed surface roughness measurement. *Journal of Engineering for Industry*, Vol. 106, pp.34-39.

Jung, C. Y. & Oh, J. H. (1991). Improvement of surface waviness by cutting force control in milling. *Int. J. Mach. Tools Manufact.*. Vol. 31, No. 1, pp. 9-21.

Kalpakjian S. (1995). Manufacturing Engineering and Technology, 3rd edition. NY: Addison-Wesley.

Kistler Instrument (1994). *Operating Instructions: Quartz 3-Component Dynamometer Type 9257B*, NY: Kistler Instrument Corp..

Kistler Instrument (1994) *Operating Instructions: Dual Mode Amplifier Type 5010B Preliminary*, NY: Kistler Instrument Corp..

Landau, I. D. & M'Saad M. (1998). *Adaptive control.* NY: Springer

Li, S. & Elbestawi, M. A. (1996). Tool condition monitoring in machining by fuzzy neural networks. *Journal of Dynamic Systems, Measurement, and Control*, Vol. 118, pp. 665-672.

Lin, S.C. (1994). Computer numerical control-from programming to networking. NY: Delmar.

Lou, S. J. (1997). *Development of four in-process surface recognition systems to predict surface roughness in end milling*. Doctoral dissertation, IA: Iowa State University

Lou, M. S. & Chen, J. C. (1999). In-process surface roughness recognition system in end-milling operations. *International Journal of Advanced Manufacturing Technology*, Vol. 15, pp. 200-209.

Mansfield, P. H. (1973). *Electrical Transducers for Industrial Measurement.* London: Butterworth.

Martelloti, M. E. (1941). An analysis of the milling process. *Transactions of the ASME*, Vol. 63, pp. 677-700.

McClave, J. T. & Benson, P. G. (1994). Statistics for Business and Economics-6th Edition. NY: Macmillan.

Melkote, S. N. & Thangaraj, A. R. (1994). An enhanced end milling surface texture model including the effects of radial rake and primary relief angles. *Journal of Engineering for Industry*, Vol. 116, pp. 166-174.

Mendenhall, W. & Sincich, T. (1996). *A second Course in Statistics-Regression Analysis-5th Edition*. New Jersey: Prentice-Hall.

Mou, J. (1997). A method of using neural networks and inverse kinematics for machine tools error estimation and correction. *Journal of Manufacturing Science and Engineering*, Vol. 119, pp. 247-254.

Rumelhart, D. E., Hinton, G. E. & Williams R. J. (1986). *Parallel distributed processing: explorations in the microstructure of cognition*. MA: Cambridge.

Shin, Y. C., Oh, S. J. & Coker, S. A. (1995). Surface roughness measurement by ultrasonic sensing for in-process monitoring. *Journal of Engineering for Industry*, Vol. 117, pp.439-449.

Smith, S. & Tlusty, J. (1991). An overview of modeling and simulation of the milling process. *Journal of Engineering for Industry,* Vol. 113, pp. 169-175.

Stark, G. A. & Moon, K. S. (1999). Modeling surface texture in the peripheral milling process using neural network, spline, and fractal methods with evidence of chaos. *Journal of Engineering for Industry*, Vol. 121, pp. 251-256.

Sugeno, M. & Kang, G. T. (1988). Structure identification of fuzzy model. *Fuzzy Sets and Systems*, Vol. 28, pp. 15-33.

Susic, E. & Grabec, I. (1995). Application of a neural network to the estimation of surface roughness from AE signals generated by friction process. . *Int. J. Mach. Tools Manufact.*. Vol. 35, No. 8, pp. 1077-1086.

Sutherland, J. W. & DeVor, R. E. (1986). An improved method for cutting force and surface error prediction in flexible end milling systems. *Journal of Engineering for Industry*, Vol. 108, pp. 269-279.

Takeyama, H., Sekiguchi, H., Murata, R. & Matsuzaki, H. (1976). In-process detection of surface roughness in machining. *Annals of the CIRP*, Vol. 25, No. 1, pp. 467-471.

Tarng,Y. S. & Lee, B. Y. (1993). A sensor for the detection of tool breakage in NC milling," *Journal of Materials Processing Technology*, Vol. 36, pp.259-272.

Tsai, Y., Chen, J. C., & Lou, M. S. (1999). In-process surface recognition system based on neural networks in end milling operations. *Int. J. Mach. Tools Manufact.*, Vol. 39, pp. 583-605.

You, S. J. & Ehmann, K. F. (1991). Synthesis and generation of surface milled by ball nose end mills under tertiary cutter motion. *Journal of Engineering for Industry*, Vol. 113, pp. 17-24.

Zhang, D., Han, Y. & Chen, D. (1995). On-line detection of tool breakage using telemetering of cutting forces in milling. *Int. J. Mach. Tools Manufact.*, Vol. 35, No. 1, pp. 19-27.

ACKNOWLEDGMENTS

I praise the Lord, that with His spirit inside, I can go this far and finish my degree. It has taken a long time for me to achieve this degree. Throughout the past four years, I have many people to thank that have supported me in many different aspects. First of all, I would like to thank the Department of Industrial Education and Technology and my major professor, Dr. Joseph C. Chen, for their continuous financial support, which was very important for me so that I was able to do the research without any burdens. I am so thankful, especially for my major professor who spent a lot of time guiding me so that my research was able to succeed. I also appreciate his concern in every aspect of my life and my family. He is not just a major professor in my research, but he is also a dear brother in my life.

I also want to give an expression of appreciation to my committee. Dr. Stephenson assisted me in the statistical analysis of my research. Dr. Bradshaw worked with me to understand the theorem of sensing technology. And Dr. Chang and Dr. Smith gave me several suggestions throughout the course of my research. These suggestions expanded my thoughts and allowed me to continue my research. I also want to thank my friend, Wendy Baxter, for her revising of this dissertation to enhance its quality.

To my dear wife, Wen-Uen Chu, I cannot even find words to express my gratitude. She spends all of her time taking care of our family, Angus, Isaac and myself. She tends to our family so that I am able to focus on my research. Finally, I want to give my special thanks to my parents. With their inspiration and support, I have been able to complete my education. I appreciate their love for me while I have been obtaining my knowledge. I am proud of them forever.